

ผลของขนาดอนุภาคและการปรับสภาพด้วยน้ำและความร้อนของวายเป็นไฮโดรไลต์ต่อการแตกตัวเชิงเร่งปฏิกิริยาของ
นอร์มัลออกเทน



นายสุวัชชัย นวลคล้าย

สถาบันวิทยบริการ

จุฬาลงกรณ์มหาวิทยาลัย

วิทยานิพนธ์นี้เป็นส่วนหนึ่งของการศึกษาตามหลักสูตรปริญญาวิศวกรรมศาสตรมหาบัณฑิต

สาขาวิชาวิศวกรรมเคมี ภาควิชาวิศวกรรมเคมี

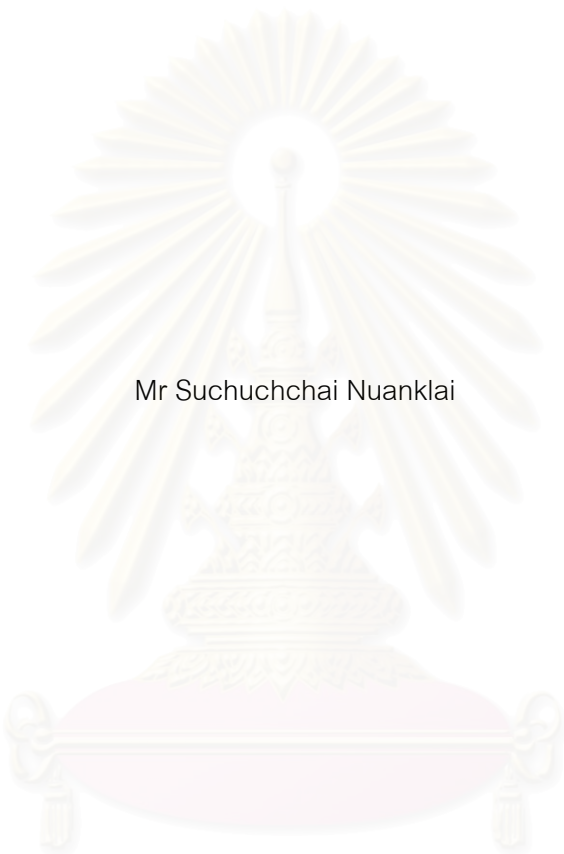
คณะวิศวกรรมศาสตร์ จุฬาลงกรณ์มหาวิทยาลัย

ปีการศึกษา 2547

ISBN 974-53-1462-5

ลิขสิทธิ์ของจุฬาลงกรณ์มหาวิทยาลัย

EFFECTS OF PARTICLE SIZE AND HYDROTHERMAL TREATMENT OF Y-ZEOLITE ON CATALYTIC
CRACKING OF n-OCTANE



Mr Suchuchchai Nuanklai

สถาบันวิทยบริการ
จุฬาลงกรณ์มหาวิทยาลัย

A Thesis Submitted in Partial Fulfillment of the Requirements
for the Degree of Master of Engineering in Chemical Engineering

Department of Chemical Engineering

Faculty of Engineering

Chulalongkorn University

Academic Year 2004

ISBN 974-53-1462-5

Thesis Title EFFECTS OF PARTICLE SIZE AND HYDROTHERMAL
TREATMENT OF Y-ZEOLITE ON CATALYTIC CRACKING OF
n-OCTANE
By Mr Suchuchchai Nuanklai
Field of Study Chemical Engineering
Thesis Advisor Suphot Phatanasri, D.Eng.
Thesis Co-advisor Professor Piyasan Praserthdam, Dr.Ing.

Accepted by the Faculty of Engineering, Chulalongkorn University in Partial
Fulfillment of the Requirements for the Master's Degree

.....Dean of Faculty of Engineering
(Professor Direk Lavansiri, Ph.D.)

THESIS COMMITTEE

..... Chairman
(Assitant Professor Suttichai Assbumrungrat, Ph.D.)

..... Thesis Advisor
(Suphot Phatanasri, D.Eng.)

..... Thesis Co-advisor
(Professor Piyasan Praserthdam, Dr.Ing.)

..... Member
(Joongjai Panpranot, Ph.D.)

..... Member
(Choowong Chaisuk, D.Eng.)

ศุขชัย นวลคล้าย : ผลของขนาดอนุภาคและการปรับสภาพด้วยน้ำและความร้อนของวายซีโอไลต์ต่อการแตกตัวเชิงเร่งปฏิกิริยาของนอร์มัลออกเทน (EFFECTS OF PARTICLE SIZE AND HYDROTHERMAL TREATMENT OF Y-ZEOLITE ON CATALYTIC CRACKING OF n-OCTANE) อ. ที่ปรึกษา : อ.ดร.สุพจน์ พัฒนะศรี, อ. ที่ปรึกษาร่วม : ศ.ดร.ปิยะสาร ประเสริฐธรรม, 98 หน้า. ISBN 974-53-1462-5.

ทำการทดสอบผลของขนาดอนุภาคในช่วง 0.16 ถึง 2.01 ไมโครเมตร และการปรับสภาพด้วยน้ำและความร้อนของวายซีโอไลต์ในการแตกตัวเชิงเร่งปฏิกิริยาของนอร์มัลออกเทนพบว่า เมื่ออุณหภูมิที่ทำการปรับสภาพด้วยน้ำและความร้อนเพิ่มขึ้น ความเป็นอัลตราสเตเบิลวายซีโอไลต์และปริมาณโอเลฟินในผลิตภัณฑ์เพิ่มขึ้น แต่สัดส่วนความว่องไวในการเกิดปฏิกิริยาลดลง ต่อมาพบว่า สำหรับขนาดอนุภาคในช่วง 0.16-0.45 ไมโครเมตร เมื่อขนาดอนุภาคที่ผ่านการปรับสภาพด้วยน้ำและความร้อนแล้วเพิ่มขึ้น ความเป็นอัลตราสเตเบิลวายซีโอไลต์และปริมาณโอเลฟินในผลิตภัณฑ์ลดลง แต่สัดส่วนความว่องไวในการเกิดปฏิกิริยาเพิ่มขึ้น สุดท้ายพบว่าสำหรับขนาดอนุภาคที่ใหญ่กว่า 0.45 ไมโครเมตร เมื่อขนาดอนุภาคที่ผ่านการปรับสภาพด้วยน้ำและความร้อนแล้วเพิ่มขึ้น ความเป็นอัลตราสเตเบิลวายซีโอไลต์และปริมาณโอเลฟินในผลิตภัณฑ์เพิ่มขึ้น แต่สัดส่วนความว่องไวในการเกิดปฏิกิริยาลดลง

สถาบันวิทยบริการ
จุฬาลงกรณ์มหาวิทยาลัย

ภาควิชา.....วิศวกรรมเคมี..... ลายมือชื่อนิสิต.....
สาขาวิชา.....วิศวกรรมเคมี..... ลายมือชื่ออาจารย์ที่ปรึกษา.....
ปีการศึกษา.....2547..... ลายมือชื่ออาจารย์ที่ปรึกษาร่วม.....

##4670559721 : MAJOR CHEMICAL ENGINEERING

KEY WORD: PARTICLE SIZE / Y-ZEOLITE / CATALYTIC CRACKING

SUCHUCHCHAI NUANKLAI: EFFECTS OF PARTICLE SIZE AND HYDROTHERMAL TREATMENT OF Y-ZEOLITE ON CATALYTIC CRACKING OF n-OCTANE. THESIS ADVISOR: SUPHOT PHATANASRI, D.Eng. THESIS CO-ADVISOR: PROF. PIYASAN PRASERTHDAM, Dr.Eng. 98 pp. ISBN 974-53-1462-5.

The effect of particle size in the range of 0.16-2.01 μm and hydrothermal treatment of Y zeolite on the catalytic cracking of n-octane was investigated. For increasing pretreatment temperature, the degree of USY zeolite and the amount of olefins in the product increased but the ratio of the catalytic activity decreased. In addition, for the particle size of treated Y zeolites in a range of 0.16-0.45 μm when the particle size increased, the degree of USY zeolite and the amount of olefins in the product decreased but the ratio of the catalytic activity increased. Finally, for the particle size of treated Y zeolites more than 0.45 μm when the particle size increased, the degree of USY zeolite and the amount of olefins in the product increased but the ratio of the catalytic activity decreased.

สถาบันวิทยบริการ
จุฬาลงกรณ์มหาวิทยาลัย

Department.....Chemical Engineering... Student's signature.....

Field of study... Chemical Engineering... Advisor's signature.....

Academic year...2004..... Co-advisor's signature.....

ACKNOWLEDGEMENTS

The author would like to express his greatest gratitude to his advisor and co-advisor, Dr. Suphot Phatanasri, Professor Piyasan Prasertdam for his invaluable guidance throughout this study. In addition, he is also grateful to, Assitant Professor Suttichai Assbumrungrat as the chairman and Dr. Joongjai Panpranot and Dr. Choowong Chaisuk as the member of the thesis committee.

Special thank to petrochemical laboratory member who has encouragement and guided him over the year of this study

Finally he would also like to manifest his greatest gratitude to his parent and his family for their support and encouragement.



สถาบันวิทยบริการ
จุฬาลงกรณ์มหาวิทยาลัย

CONTENTS

	PAGE
ABSTRACT (IN THAI).....	iv
ABSTRACT (IN ENGLISH).....	v
ACKNOWLEDGEMENTS.....	vi
CONTENTS.....	vii
LIST OF TABLES.....	x
LIST OF FIGURES.....	xi
CHAPTER	
I INTRODUCTION.....	1
1.1 Thesis Objective.....	2
1.2 Thesis Scope.....	3
II LITERATER REVIEWS.....	4
III THEORY.....	16
3.1 Fluid Catalytic Cracking Unit	16
3.2 Catalyst	18
3.3 Hydrocarbon Classification	19
3.4 Gasoline Octane	23
3.5 Zeolite	25
3.6 Application of Zeolite	28
3.7 NaY zeolite	31
3.8 USY Zeolite	32
3.9 Zeolite Properties	32
3.10 Active Site	35
3.11 Mechanism of Catalytic Cracking Reaction	37
IV EXPERIMENTS.....	43
4.1 Preparation of Y-Type Zeolite.....	43
4.2 Hydrothermal Treatment.....	47
4.3 Characterization	48
4.3.1 Scanning Electron Microscopy (SEM).....	48

CONTENTS (Cont.)

	PAGE
4.3.2 X- Ray Diffraction analysis (XRD).....	48
4.3.3 BET surface area measurement.....	48
4.3.3.1 BET apparatus.....	49
4.3.3.2 Measurement.....	49
4.3.4 Temperature programmed desorption of adsorbed ammonia (NH ₃ TPD)	50
4.4 Catalytic cracking of n-octane	51
4.4.1 Chemical and reagent	51
4.4.2 Instruments and apparatus	51
4.4.3 Reaction Method	52
V RESULTS AND DISCUSSION.....	55
5.1 Catalyst Characterization	55
5.1.1 Morphology and Particle size of Y zeolite samples	55
5.1.2 Unit cell size	61
5.1.3 Surface area	75
5.1.4 Acid site	76
5.2 Catalytic reaction	77
5.2.1 Effect of particle size and hydrothermal treatment on the conversion of n-octane	77
5.2.2 Effect of particle size and hydrothermal treatment on the selectivity of olefins	80
VI CONCLUSIONS AND RECOMMENDATIONS.....	81
REFERENCES.....	82
APPENDICES.....	85
Appendix A-1 Calculation of vapor pressure of water.....	86
Appendix A-2 Calculation of unit cell size.....	86
Appendix A-3 Calculation of the specific surface area	88
Appendix A-4 Calculation of Reaction Flow Rate	91

CONTENTS (Cont.)

	PAGE
Appendix B Calibration curve.....	92
Appendix C-1 The particle size and the unit cell size of Y zeolite at various temperature	94
Appendix C-2 The particle size and the unit cell size of Y zeolite at various operating times	94
Appendix C-3 The particle size and the unit cell size of Y zeolite at various operating partial pressures	95
Appendix C-4 The single point BET surface area and the percent relative BET surface area of Y zeolite	95
Appendix C-5 Conversion of n-octane on various particle size of Y zeolites (fresh)...	96
Appendix C-6 Conversion of n-octane on various particle size of Y zeolites (after hydrothermal temperature at 973 K)	96
Appendix C-7 Conversion of n-octane on various particle size of Y zeolites (after hydrothermal temperature at 1023 K)	96
Appendix C-8 Conversion of n-octane on various particle size of Y zeolites (after hydrothermal temperature at 1123 K)	96
Appendix C-9 Olefin selectivity on various particle size of Y zeolites (fresh)	97
Appendix C-10 Olefin selectivity on various particle size of Y zeolites (after hydrothermal temperature at 973 K)	97
Appendix C-11 Olefin selectivity on various particle size of Y zeolites (after hydrothermal temperature at 1023 K)	97
Appendix C-12 Olefin selectivity on various particle size of Y zeolites (after hydrothermal temperature at 1123 K)	97
VITA.....	98

LIST OF TABLES

TABLE	PAGE
4.1 Reagents used for the preparation of Zeolite Y	44
4.2 Operating condition of gas chromatograph (GOW-MAC).....	49
4.3 Operating conditions for gas chromatograph	52
5.1 The BET surface area and the relative BET surface area.....	75
5.2 Conversion ratio of n-octane on various Y zeolites. (reaction temperature at 673 K).....	78



สถาบันวิทยบริการ
จุฬาลงกรณ์มหาวิทยาลัย

LIST OF FIGURES

FIGURE	PAGE
2.1 Diagram of the surface of a zeolite framework	7
2.2 Water molecules co-ordinated to polyvalent cation are dissociated by heat treatment yielding Bronsted acidity.....	8
2.3 Lewis acid site developed by dehydroxylation of Bronsted acid site	8
2.4 Steam dealumination process in zeolite	9
3.1 Conventional fluidized-bed catalytic cracking unit.....	17
3.2 Paraffins	20
3.3 Olefins	20
3.4 Naphthenes	21
3.5 Aromatics	21
3.6 Hybrid molecules	22
3.7 Hybrid molecules side chain cracking	23
3.8 Representations of $[\text{SiO}_4]^{4-}$ and $[\text{AlO}_4]^{5-}$ tetrahedral	25
3.9 Tetrahedra linked together to create a three-dimensional structure	26
3.10 Secondary building units (SBU) in zeolites	27
3.11 The sodalite or cage, linked to create the structures of sodalite, zeolite A and Faujasite (zeolite X/Y)	28
3.12 Bridging hydroxyl group in aluminium substituted zeolites	30
3.13 Stereodiagram of framework topology of faujasite	31
3.14 Geometry of USY zeolite	32
3.15 Silica-alumina ratio versus zeolite unit cell size	33
3.16 Formation of Bronsted site	36
3.17 Formation of Lewis site	36
3.18 Formation of 'true' Lewis site	36
3.19 Main reactions in FCC catalysis	39
4.1 The preparation procedure of NaY zeolite catalyst	46
4.2 Scheme of the apparatus for hydrothermal treatment	47
4.3 Schematic diagram of the reaction apparatus for reaction	54
5.1 Scanning electron micrographs of Y zeolite particle size.....	56
5.2 XRD spectra of Y zeolite, fresh and treated with different size	62

FIGURE	PAGE
5.3 Reaction mechanism for hydrothermal dealumination and stabilization of Y zeolite	72
5.4 Relationship between unit cell size and particle size of Y zeolite after hydrothermal treatment at different treated parameters (a) 873-1223 K, 10 %mol steam and 60 s (b) 30-300 s, 10 %mol steam and 1023 K (c) 0.05-1 P/P ₀ , 60 s and 1023 K.....	73
5.5 NH ₃ TPD of Y zeolite at various hydrothermal temperature (0.45 micron) ..	76
5.6 Conversion ratio of n-octane on various Y zeolites	79
5.7 Olefin selectivity on various Y zeolites	79
B1 Calibration curve of n-octane	92
B2 Calibration curve of ethylene	92
B3 Calibration curve of propylene	93

CHAPTER I

INTRODUCTION

The first commercial catalytic cracking process was developed by Eugene Houdry in the 1920s. This process was an outgrowth of his experiments on catalysts for removing sulfur from oil vapors. These catalysts became deactivated due to build up of a carbonaceous deposit from the oils. Houdry discovered that this deposit could be burned off with air, and the catalyst activity restored. This discovery made a commercially viable process possible. The fluid catalytic cracking (FCC) process continues to play an important role as gasoline producing unit in most oil refineries. Several FCC and catalysts are currently being developed to maximize the production of light olefins for petrochemical usage while maintaining high gasoline yield. The objective of the FCC unit is to convert low value, high boiling point feed stocks into more valuable products such as gasoline and diesel.

Particle size of zeolites has been found to affect the performances of zeolites for many catalytic reactions. For example, Rajagopalan et al. [1] studied the effect of particle size of NaY zeolite in the range of 0.06-0.65 μm on the activity and selectivity in FCC reaction. It was found that the catalysts containing smaller-particle zeolites showed higher activity in the cracking of gasoil and higher selectivity to gasoline and light cycle oil than the ones containing large-particle zeolites. Gianetto et al. [2] showed similar results for the ultra stable submicron Y (USSY) zeolites. The changes of zeolite particle size significantly affected the amount of total aromatics, benzene, C_4 olefins, and coke during FCC. Al Khattaf and de Lasa [3] reported that the cracking conversion of 1,3,5-tri-*iso*-propyl-benzene using 0.4 μm Y zeolite was higher than that using 0.9 μm zeolite due to the constrained diffusional transport in the larger Y-zeolite particles. However, smaller-particle zeolites were often found to be less stable than larger particle ones. The optimum size of zeolite crystal is, therefore, required in order to achieve the desired performance [4-5].

The direct synthesis of zeolite Y was restricted to product silica–alumina ratio of less than 6.0. Because of the increased change for low crystallinity or impurity formation when operating under conditions designed to yield silica–alumina values higher than 5.6, commercial production usually is limited to silica–alumina ratios below 5.6. However, in

the early use of zeolite Y in FCC catalysis the hydrothermal stability of zeolite Y was discovered to be highly dependent on zeolite silica–alumina ratios. This conclusion led to methods of secondary synthesis designed to increase the silica–alumina ratio of as synthesized sodium Y zeolite. The recovery by Maher and McDaniel of ultrastable Y (USY) zeolite, the first of the aluminum deficient Y zeolites, led to its inclusion in FCC catalysts as early as 1964 in XZ–15 produced by Davison [6] However, the use of USY aluminum deficient zeolite in FCC catalyst quickly disappeared because of its substantially lower activity compared to fully or partially rare earth exchanged Y zeolite (REY and REHY). The increased olefinicity and gasoline octane obtained by using USY was interesting.

Techniques have been developed for the chemical dealumination of the zeolite. Such dealumination would minimize the presence of nonframework (NFA) generated by the hydrothermal techniques used to produce USY zeolite. Union carbide patented and commercialized dealumination of zeolite by ammonium fluorosilicate (AFS) for use in FCC catalysts [7]. Commercial techniques involving the hydrothermal treatment of the zeolite to form a conventional USY zeolite containing NFA formed during dealumination which were then modified by chemical washing to eliminate the NFA. Because of the superior stability, octane–producing characteristics, and coke selectivity of these various aluminum deficient zeolites, quickly controlled the major portion of the United States and European catalyst markets.

In this study. The effect of particle size and hydrothermal treatment of Y zeolite in the cracking of n-octane on the structural of Y zeolite were investigated by means of X-ray diffraction (XRD), scanning electron microscopy (SEM), BET surface area (BET), temperature programmed desorption (TPD) of NH_3

1.1 Thesis Objective

To evaluate the effect of particle size and hydrothermal treatment of Y zeolite on the catalytic cracking of n-octane.

1.2 Thesis Scope

1.2.1 Characterization of Y zeolite under hydrothermal treatment as follows:

1.2.1.1 Temperature 873, 973, 1073, 1173 and 1273 K

1.2.1.2 Steam partial pressure 5, 10, 20, 50, and 100 mole percent of water

1.2.1.3 Time 0.5, 1, 2, 3, 5 h

by the following methods

(a) Structure and unit cell size of samples by X-ray diffractometer (XRD).

(b) Morphology of sample by Scanning Electron Microscopy (SEM).

(c) Specific surface area by N₂ adsorption based on BET method (BET).

(d) Acid Contents and strength of acid sites in samples by temperature programmed desorption of ammonia (NH₃TPD).

1.2.2 Evaluate the effect of particle size and hydrothermal treatment of Y zeolite on the catalytic cracking of n-octane.

The present thesis is arranged as follows:

Chapter II presents the literature reviews.

Chapter III presents the theoretical consideration on Y zeolite.

Chapter IV presents the experimental systems and operation procedures. The experimental results obtained from the laboratory scale and standard measurements are reported and discussed in chapter V.

The last chapter gives overall conclusion emerged from this work. Finally the calculation of unit cell size and data experiments are included in appendices at the end of this thesis.

CHAPTER II

LITERATURE REVIEWS

In this section, special attention of related papers devoted directly to the effect of particle size and pretreatment condition of Y zeolite in the catalytic cracking of n-octane. However, the other points are also mentioned so that all information can contribute and lead to some interesting subjects concerned in this thesis.

Besides, hydrothermal stability is an important requirement to be fulfilled by the zeolite component of an FCC catalyst since it influences both the activity level of the equilibrium catalyst and the amount of fresh catalyst addition need. It is therefore necessary to get acquainted with the nature of deactivation process [8]. Hydrothermal treatments at different temperatures and for different times have been used long in order to break down the extreme high initial activity of fresh cracking catalyst, to make them suitable for determining and comparing their catalytic properties by means of standard activity tests.

Gardner et al [9] reported to irreversible deactivation kinetics of H-USY and H-ZSM-5 zeolites with a steam aging technique. The effects of steam partial pressure, temperature and time on zeolite hydrothermal stability have been investigated. Catalyst performance was described in a form of kinetic model of zeolite surface area reduction as a function of aforementioned three variables.

Guo Xing et al [10] prepared siliceous Y zeolite ($\text{SiO}_2/\text{Al}_2\text{O}_3 > 150$) through repeated dealumination with SiCl_4 and steam, displays high thermal and hydrothermal stability. After aged at 1473 K for 4 h, siliceous Y zeolite show specific surface area as high as $510 \text{ m}^2/\text{g}$. Even steamed at 1273 K for 4 h, it still keeps its framework perfectly. When palladium is supported on SY-A carrier, in which 12.3% alumina has been loaded on siliceous Y zeolite, the catalyst shows higher oxidation activity than $\text{Pd}/\text{La}-\text{Al}_2\text{O}_3$ even heated or steamed at 1273 K for 4 h. Its excellent resistances to heat and steam make it a promising catalyst for high-temperature catalytic combustion.

Kerr [11] treated NaY zeolite with an acidic solution of ethylenediamine tetraacetic acid (EDTA) to obtain a homogeneously dealuminated zeolite sample. His proposed dealumination mechanism was that each missing aluminum atom was replaced by four

hydrogen bonding to the oxygen atoms of the vacated tetrahedron. The four hydroxyl products each bonded to silicon were believed to condense to yield water and form Si-O-Si bonds upon heating. The new Si-O-Si bond has been found to improve the framework thermal stability. The optimum removal of aluminum for thermal stability was in the range of 25-50%.

Gallezot, Beaumont and Barthomeuf [12] followed the same procedure as in Kerr's work by using EDTA to remove aluminum atoms of NaY zeolite and derived a homogeneously dealuminated zeolite sample. The results obtained from x-ray powder diffraction showed no significant change of the occupancy factor of the zeolite framework atoms. This was interpreted as the vacancies in the framework left by homogeneously removed aluminum atoms were refilled through a local crystallization process so the overall structure was preserved. The process was found to involve the formation of new SiO₄ tetrahedral. Two possible sources of silicon atoms were either from siliceous impurities, which are often present in synthesis zeolites or from the zeolite framework itself.

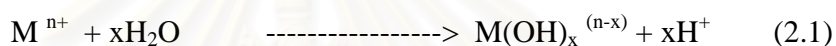
Sulikowski, Karge and Mishin [13] proposed an improved method for dealumination of faujasite-type zeolites with silicon tetrahedral treatment. With this method, in contrast to hydrothermal treatment or acid leaching, the direct substitution of the framework aluminum by silicon atoms was reported. However, the reaction has a limited temperature up to about 773 K. Beyond this point, higher of dealumination cannot be obtained due to the deposition of the reaction product NaAlCl₄ in the pore system. The presence of aluminum extra-framework species was revealed by Al MAS NMR spectroscopy.

The interactions between adsorbed molecules and the framework and cations in the channels of zeolites have been investigated by a wide range of experimental and theoretical techniques. Such information is useful in investigating the catalytic properties of zeolite. For example, to investigate the acid sites in zeolite, a basic probe molecule such as ammonia or pyridine may be introduced, and changes in the vibrational of the guest give information about the nature of the site where the molecule is adsorbed. Hence, infrared studies of pyridine adsorbed in hydrogen-Y zeolite reveal the formation of a pyridinium ion in the latter, indicating that adsorption is at Bronsted and Lewis acid.

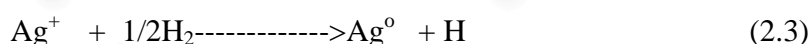
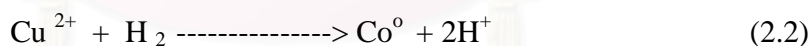
Classical Bronsted and Lewis acid models of acidity have used to classify the active sites on zeolites. Brønsted acidity is proton donor acidity; a tridiagonally coordinated alumina atom is an electron deficient and can accept an electron pair, therefore behaves as a Lewis acid [14].

Protonic acid centers of zeolite are generated in various ways. Figure 2.1 depicts the thermal decomposition of ammonium-exchanged zeolite yielding the hydrogen form [15].

The Bronsted acidity due to water ionization on polyvalent cations, described below, is depicted in Figure 2.2 [16].



The exchange of monovalent ions by polyvalent cations could improve the catalytic property. Those highly charged cations create very centers by hydrolysis phenomena. Brønsted acid sites are also generated by the reduction of transition metal cations. The concentration of OH groups of zeolite containing transition metals was note to increase by hydrogen at 298-723 K to increase with the rise of the reduction temperature [17].



สถาบันวิทยบริการ
จุฬาลงกรณ์มหาวิทยาลัย

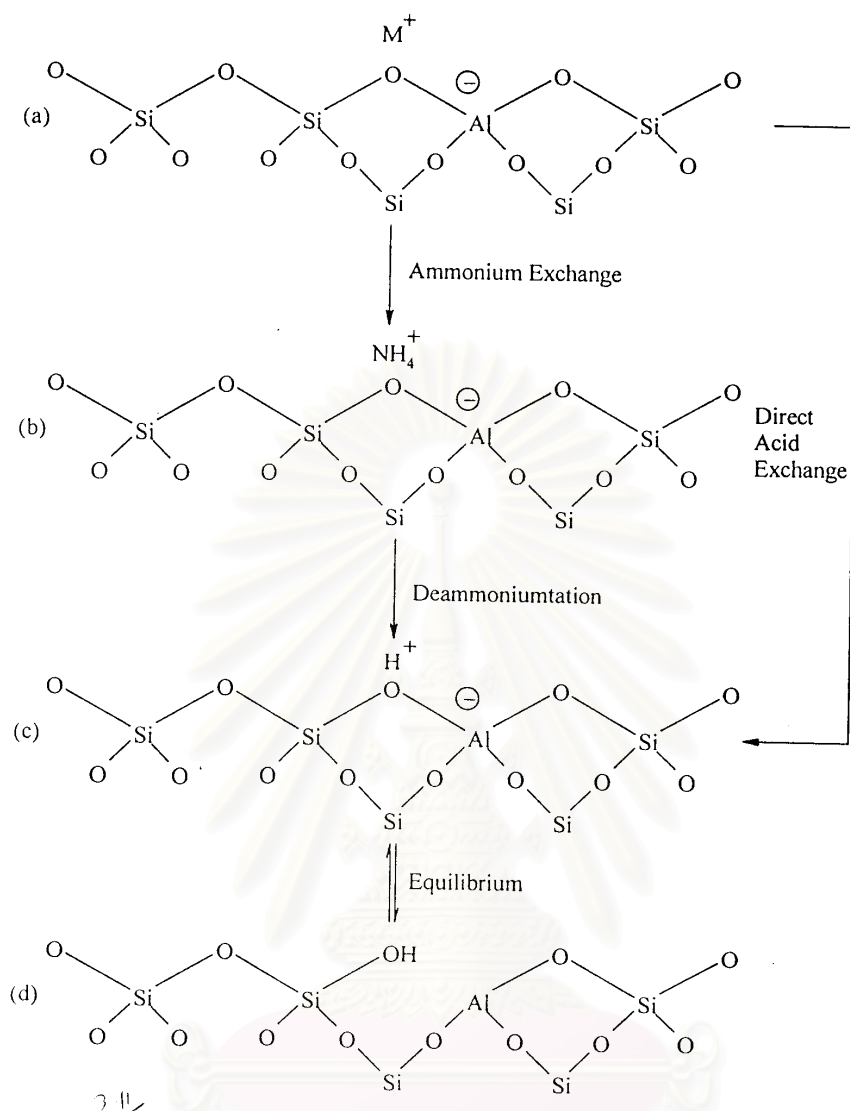


Figure 2.1 Diagram of the surface of a zeolite framework [15].

- In the as-synthesis form M^+ either an organic cation or an alkali metal cation.
- Ammonium in exchange produces the NH_4^+ exchanged form.
- Thermal treatment is used to remove ammonia, producing the H^+ , acid form.
- The acid form in (c) is in equilibrium with the shown in (d), where is a silanol group adjacent to tricoordinate aluminium.

The formation of Lewis acidity from Bronsted acid sites is depicted in Figure 2.3 [23]. The dehydration reaction decreases the number of protons and increases that of Lewis sites. Bronsted (OH) and Lewis (-Al-) sites can be present simultaneously in the structure of zeolite at high temperature. Dehydroxylation is thought to occur in ZSM-5

zeolite above at 773 K and calcination at 1073 K to 1173 K produces irreversible dehydroxylation, which causes defection in crystal structure of zeolite.

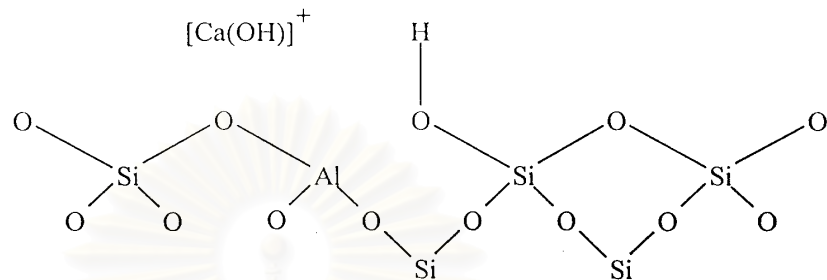


Figure 2.2 Water molecules coordinated to polyvalent cation is dissociated by heat treatment yielding Bronsted acidity [15].

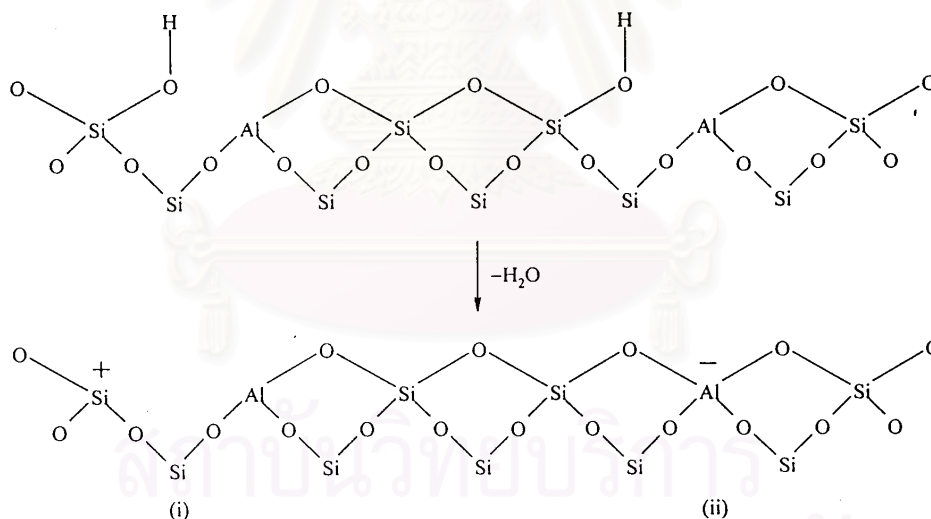


Figure 2.3 Lewis acid sites developed by dehydroxylation of Brønsted acid site [15].

Dealumination is believed to occur during dehydroxylation, which may result from the steam generation within the sample. The dealumination is indicated by an increase in the surface concentration of aluminum on the crystal. The dealumination process is expressed in Figure 2.4 [23]. The extent of dealumination monotonously increases with the partial pressure of steam.

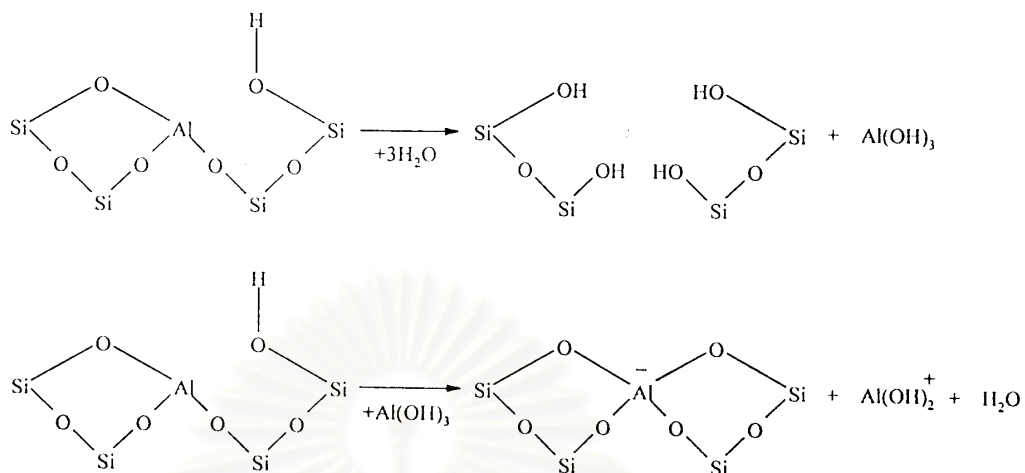


Figure 2.4 Steam dealumination process in zeolite [15]

In general, the increase in Si/Al ratio will increase acidic strength and thermal stability of zeolite [18]. Since the numbers of acidic OH groups depend on the number of aluminium in zeolites framework, decrease in Al content is expected to reduce catalytic activity of zeolite. If the effect of increase in the acidic centers, increase in Al content, shall result in enhancement of catalytic activity.

An improvement in thermal or hydrothermal stability has been ascribed to the lower density of hydroxyl groups, which is parallel to that of Al content [15]. A longer distance between hydroxyl groups decreases the probability of dehydroxylation that generates defects on structure of zeolites.

Y-zeolites have been used extensively in FCC since the 1960s. The commercial FCC catalysts are manufactured with 1–2 μm zeolites dispersed in an amorphous silica–alumina matrix forming the 60 μm particles [19]. In these catalysts, most of the active sites are located within the zeolite pore structure. In order for the reaction to proceed, molecules have to evolve through the large matrix pores into the zeolite crystals. As a result only certain hydrocarbon species with a molecular size smaller than a given dimension can penetrate the zeolite pore structure [20]. For the larger hydrocarbon

molecules, only the active sites situated on the external surface area of the zeolites, representing about 3% of the total surface area, are available [21].

While diffusion in the catalyst matrix belongs to the well-known Knudsen regime, diffusion in zeolites falls into the configurational regime [22]. This kind of diffusion is a process with activation energy substantially larger than the ones for other types of diffusion. Since the size of the molecule in the pore is nearly the size of the passageway, the diffusion of molecules in zeolites is governed by a continuous interaction between the zeolite crystal and diffusing molecules.

The particle size of catalysts for cracking hydrocarbons in fluidized beds reactors (FCC process), which are basically composed of a zeolite component (Y zeolite) in matrix and various additives, are subjected to severe, changing environments in the cyclic operation of commercial units. This is due to the circulation between the reducing atmosphere of the reactor at about 773 K and the oxidizing atmosphere of the regenerator at about 1023 K, where coke is burnt off in air in the presence of steam [23]. A strong dealumination process is induced on the zeolite, as well as profound changes in both the chemical and physical properties of the fresh compound catalyst. It is well known that the loss of aluminum from the zeolite crystal structure translates into unit cell size shrinking concomitantly with the appearance of extra-framework aluminum species; finally, this ends up with the so-called “equilibrium” catalyst (E-CAT). The very different properties of the E-CATs as compared with fresh samples have repercussions on the catalytic performance, stressing the need for proper evaluation procedures [24-26].

The cracking of n-octane, 2,2,4-trimethylpentene and 1-octane was examined over ZSM-5, β zeolite, Y, USY and the composites of any of the two former zeolite as additives to the latter two traditional cracking zeolites, under high-severity conditions, namely relatively high temperature (773 K) and high conversions [27]. The behaviours of these catalysts under the above conditions are very different from those already studied in the literature, which have been at low conversion and lower temperature. While for the latter condition the selectivities for olefins were higher and for aromatics lower over ZSM-5 than over Y faujasite, in the present conditions the above trends are invert. The shifting in the rate of primary cracking, hydrogen transfer, oligomerization

and bimolecular condensation cracking reactions produced by the changes in the zeolite employed and conditions are responsible for this behaviour. For the composite of Y faujasite with either ZSM-5 or β zeolite the C₃ and C₄ paraffin selectivities can be calculated as the weight averages of those for the individual zeolites. In contrast, for the USY zeolite base composites, the additivity rule is not always obeyed and the selectivities for the C₃ and C₄ paraffins can be large than those over the individual zeolites.

Ultrastable Y (USY) zeolites have been treated with sulfuric or phosphoric acids. Aiming at the determination of the interaction of both acids with either framework (FAL) or extraframework (EFAL) aluminas, as well as the effect of such modifications on catalytic properties in ethylbenzene disproportionation [28]. Zeolites have been characterized by means of several physico-chemical techniques (XRD, XRF, FTIR, ²⁹Si, Al and P-MASNMR, nitrogen adsorption and AA). Results revealed that the treatment with H₂SO₄ removed EFAL located in supercavities without attacking the zeolitic framework. Treatment with H₃PO₄ incorporates P in two quite distinct ways: as a monometric phosphate associated to framework aluminum atoms (for low EFAL concentrations) and as a polymeric phosphate originated from the reaction of EFAL with H₃PO₄ (for high EFAL concentrations). Regarding catalytic properties, initial activities are higher for H₂SO₄ leached samples when compared to those which have just been calcined. Nevertheless, initial activities of samples treated with H₃PO₄ depend strongly on the P₂O₅ content incorporated into the zeolite. With respect to isomers (ortho, meta- and para-diethylbenzene) generally formed in this disproportionation reaction, no considerable para-selectivity had been observed.

H₄EDTA and (NH₄)₂SiF₆-liquid phase dealuminated Y zeolites (EDY and FDY) and hydrothermally dealuminated Y zeolite (USY) was obtained by hydrothermal treatment of (80% NH₄⁺) NaY zeolite at 823 K for 18 h under 0.1 MPa pressure, were treated with an aqueous solution of KOH at 313 to 373 K, stirring for 4 h [29]. The products were washed with water and dried in air at 373 K. These products were characterized by using XRD, NMR, FTIR, SEM and fast atom bombardment mass spectroscopy (FABMS) techniques. A decrease of silica to alumina ratio was observed in the basic solution-treated samples. The results clearly show that dissolution of the

surface of EDY and removal of silicon atom from the framework lattice of FDY occurs during basic solution treatment. Realumination of ultrastable Y (USY) zeolite take place through reinsertion of aluminum into the framework vacancies formed during hydrothermal treatment of NH_4NaY or formed during a basic solution treatment of USY.

An ion exchange or an impregnation procedure has prepared Ni/USY catalysts [30]. The modification of support and the effect of sulfidation on the Ni distribution were examined by various techniques (water adsorption, FTIR spectroscopy of chemisorbed NO, XPS, ^{129}Xe NMR and Xe adsorption). In all catalysts the sulfidation of Ni is incomplete and the method of Ni introduction influenced the Ni distribution in Ni/USY zeolites. In unsulfided samples ion exchange technique led to Ni located essentially in hexagonal prisms, whereas in the other samples prepared by impregnation procedure the Ni concentrates were located or near the outer zeolite surface. Some nickel redistribution has been observed during catalyst sulfidation.

The acidic properties and 2-methylpentane cracking turn over frequencies (TOFs) were compared for HY and two dealuminated HY zeolites with similar levels of framework Al : HDY that was dealuminated by ammonium hexafluorosilicate, and a (H, NH_4)-USY zeolite that was dealuminated by steam [31]. Microcalorimetry of NH_3 adsorption, and the types of acid sites dealuminated the acid strength distributions by FTIR spectroscopy. All zeolites possessed Bronsted acid sites with very few Lewis acid sites. The differential heat of adsorption of NH_3 on these zeolites was nearly constant : about 120 kJ / mol for HY and HDY and approximately 7 kJ/mol higher for the (H, NH_4)-USY zeolite. The cracking TOF for HDY was five times large than HY, while the TOF of (H, NH_4)-USY zeolite was 80 times higher. These results suggest that the cracking activity may be affected by other factors in addition to acid strength.

Siliceous Y zeolite (silica to alumina ratio > 150), prepared by treating NaY zeolite with SiCl_4 for 4 h at 773 K, then treating it in 100 % steam at 1073 K for 4 h [32]. Nonframework aluminum was removed from siliceous Y zeolite by leaching with 4 N HCl solution at 353 K for several times displays high thermal and hydrothermal stability. After aged at 1473 K for 4 h, siliceous Y zeolite shows specific surface area as high as $510 \text{ m}^2/\text{g}$. Even steamed at 1273 K for 4 h, it still keeps its framework perfectly.

Ultrastable Y (H-USY) zeolite, prepared by steam treatment of Y zeolite, is a very active hydrocarbon cracking catalyst. However, the extent of enhancement in activity compared to a non-steam sample depends on the reaction condition [33]. A model that has been proposed to explain this behavior is summarized. The model incorporates the three different mechanisms for hydrocarbon pressure, temperature, and conversion, the predominant cracking reaction mechanism may differ. The change in the predominant mechanism may also be a result of the proportionally small increase in external surface area caused by the steaming-induced structural destruction of the zeolite particles. However, these relatively small changes can lead to a much larger overall effect on the cracking rate because of the sensitive dependence of oligometric cracking, and to a lesser extent, bimolecular cracking on the alkene partial pressure.

Steamed HY or ultrastable Y (H-USY) zeolites are active hydrocarbon cracking catalysts [34]. The high activity of H-USY compared to HY zeolite has been previously explained by the generation of unusually strong and active Bronsted acid sites, or an increase in the number of accessible sites in a micropore diffusion controlled reaction. However, neither model explains the accumulated literature observations. A model was proposed that incorporate a change in the predominant cracking reaction mechanism as a function of alkane conversion and the very different rates of these mechanisms. Additionally, an oligometric cracking mechanism is introduced to explicitly account for coking and deactivation of the catalyst. The model is capable of accounting for most literature results. It concludes that the large enhancement in cracking activity by steaming is due to a proportionally smaller increase in external surface area of the zeolite crystals and possibly a small increase in the specific initiation activity of each site. These small changes lead to a much larger overall effect because of the sensitive dependence of oligometric cracking and a lesser extent, bimolecular cracker on the alkene partial pressure.

The present invention relates to a method for preparing novel high silica zeolitic catalyst compositions having a high silica to alumina ratio and a crystallinity of at least about 70% [35]. The method involves cation exchanging an as synthesized faujasite material having a silica to alumina ratio greater than about 4 with a component selected from the group consisting of ammonium ions and mineral acids, then steam calcining

said cation exchanged faujasite in a single steam calcinations step at a temperature from about 755 K to about 1088 K .

n-octane cracking on H-mordenite at 673 K [36]. He reported that the formation of aromatic and coke, associated with hydrogen transfer and cyclization processes could be enhanced by the presence of Lewis acid sites on the catalyst surface. Ratio of branched to linear alkane product could not be correlated with the ratio of Lewis to Bronsted site present. Ratio of alkane to alkane could be correlated with change in the ratio of Bronsted to Lewis site present, at a given reaction temperature.

The effect of the unit cell size of Y zeolite on their performance [37]. The result was concluded that catalytic activity increased with the increasing of unit cell size and the decreasing through a maximum and correlates directly with the number of 0-NNN aluminium atom (strongest acid sites). The increased coke yield with larger unit cell sizes could be attributed to the increased number of 1,2,3,4-NNN aluminium atom .

Vacuum gasoil cracking on USY zeolite (unit cell size 24.5 – 24.25) [38]. It was showed that smaller crystal sizes produced more gasoline and diesel, and less coke and gas. However , smaller crystal was less hydrothermally stable than bigger crystals. But, if NaY zeolite was made with silicon to aluminium ratio ≥ 3.0 , the smaller crystals were hydrothermally stable and showed a higher activity and better selectivity than bigger crystals, even steaming at 1023 K for 5 h.

The ratio of cracking to hydrogen transfer for n-heptane and gasoil increased with increasing dealumination of USHY zeolite [39]. The adsorption of n-butane and 1-butene on USHY samples known that amount of these adsorbed gases decreased with increasing dealumination. A decrease in the effective concentration of the product on the zeolite would favor monomolecular (cracking) over bimolecular (hydrogen transfer) reaction. The ratio of 1-butane to n-butane adsorbed decreased considerably below 10 Al/uc, indicated a less selectivity adsorption of olefins with respect to paraffins where the hydrophobicity (framework silicon-to-aluminium ratio) of the zeolite increased. These adsorption effect had an important influence on the cracking to hydrogen transfer ratio observed, as hydrogen transfer reaction involved olefins, whereas cracking involved mainly paraffinic.

From the above literature reviews, particle size and pretreatment condition of Y zeolite is an important parameter used in various catalytic reactions. However, the effect of particle size and pretreatment condition of Y zeolite in the catalytic cracking of n-octane has not been fully studied. Thus, the effect of particle size and hydrothermal treatment of Y zeolite on the catalytic cracking of n-octane was studied in order to obtain the optimum formula of Y zeolite in the catalytic cracking.



สถาบันวิทยบริการ
จุฬาลงกรณ์มหาวิทยาลัย

CHAPTER III

THEORY

3.1 Fluid Catalytic Cracking Unit

Catalytic cracking is endothermic meaning that heat is absorbed the reactions. The temperature of the reaction mixture declines as the reaction proceed. Heat to drive the process comes from combustion of coke formed in the process. Coke is a necessary product of cracking. It is a solid, black material that is rich in carbon and low in hydrogen ; chemists call this condition “highly unsaturated”. Coke forms on the surface and in the pores of the catalyst during the cracking process, covering active sites and deactivating the catalysts. During regeneration, this coke is burned off the catalyst to restore its activity. Like all combustion process, regeneration is exothermic, liberating heat.

The three main components of a Fluid Catalytic Cracking (FCC) unit are the riser reactor, the stripper and the regenerator. Their process can be described as follows :

1. The riser reactor. The predominately endothermic cracking processes take place, forming products that include coke. In the riser, as the name implies, the catalyst, the feed and product hydrocarbon rise up the reactor pipe. Since the reactions are endothermic, reaction temperature decline from bottom to top. At top, the mixture enter a sold gas separator and the product vapors are led away.

2. The stripper. The steam is added and unreacted–reacted hydrocarbons adsorbed on the catalyst are released. The stripped catalyst is then directed into the regenerator.

3. The regenerator. The air is added and the combustion of coke on the catalyst occurs with the liberation of heat. Regenerator temperature are typically 704- 1,673 K. Heat exchanges and the circulating catalyst capture the heat evolved during regeneration to be used in preheating the reactor feed to appropriate cracking temperatures (510-548 K)

In the FCC process the entire catalyst inventory is continually circulated through the three parts of the FCC unit. A typical plant is shown in figure 3.1. The cracking process is carried out in a ‘fluidised’ bed of catalyst in which pre–heated crude oil (643 K) meets a catalyst bed in a ‘riser’. The reacted slurry is then passed into a reaction zone (753–793 K) and the resulting products pass into a further zone where the catalyst is separated from the products. The catalyst is then steam–treated to recover sorbed hydrocarbons, and then finally regenerated to be re–used as a hot catalyst to pre–heat the crude oil entering the reaction zone. The products then pass on to a fractionator to separate the major products of C1–C3 gas , petrol, light cycle oil, heavy gas oil and recycle (resid) oil. The regeneration stage is designed at 863–1003 K as an air purge to remove coke from the catalyst (coke content is critical, reactors are designed to keep coke content on zeolite to < 0.1 wt %). Catalyst residence time in the riser reactor section is typically 1–3 seconds (with current trends to even shorter residence times). The entire reactor/stripper/regenerator cycle is less than 10 minutes. To achieve cycle time of this order, catalyst circulation rates as high as 1 ton/second in large unit are not uncommon.

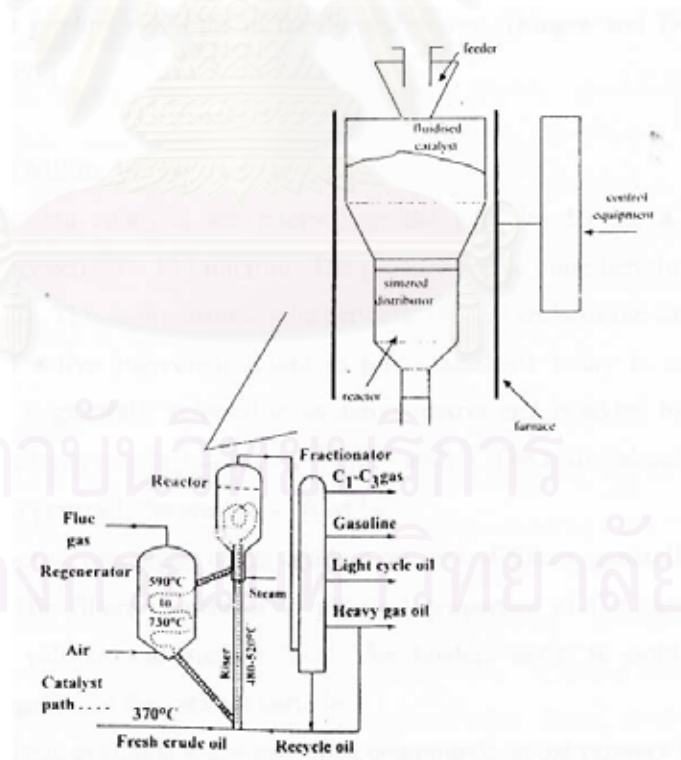


Figure 3.1 Conventional fluidized–bed catalytic cracking unit [40].

One of the truly important properties of FCC catalysts can be intuitively presumed from this brief description of operation the catalyst must be robust to

withstand the obvious stresses of operation. Temperatures are high and fluctuate. Coke is repeatedly deposited and burned off. Furthermore, the tiny catalyst particles are moving at high speed through steel reactors and pipes, where wall contacts and interparticle contacts are impossible to avoid.

All catalyst manufacturers carefully control the “robustness” of the FCC catalyst. The Measurement of FCC particle breakdown with time in special lab sized units puts a semiquantitative evaluation on attrition resistance. This is broadly related to breakdown with time in commercial units.

Catalyst loss from the unit caused by poor attrition resistance can be a serious problem, since the quantities lost must be replaced by fresh catalyst additions to maintain constant unit performance. Catalyst manufacturers work hard to prevent inordinate losses due to attrition, and refineries keep a close watch on catalyst quality to be sure the product conforms to their specifications [40].

3.2 Catalyst [41]

Fluid cracking catalyst are microspheroidal particles having a particle size distribution between 10–150 microns. The primary active ingredient in catalysts is a synthetic zeolite. This component can be between 15–50 wt. % of the catalyst.

A second active ingredient found in many catalysts today is some form of alumina. This is generally referred to as active matrix and is added to improve the heavy oil or bottoms conversation activity of the catalyst. The active alumina content of FCC catalyst is generally between 0–20 wt. %

The non-active remainder of the catalyst consists of fillers, generally kaolin clay and binders. The fillers contribute to physical properties of the catalyst such as density, pore volume and surface area. The binders serve to hold the various constituents together in the catalyst particle.

Most catalysts available today use silica compounds as the primary binder. Other materials used as binders in certain catalyst include various aluminum compounds or clays.

In operation, fresh catalyst must be added to the unit to make up losses and to maintain the catalyst activity. Make-up rates for units processing gas oil feeds are typically 0.15–0.20 pounds of catalyst per barrel of feed. For units processing resid feeds, the make up rate must be higher to control the metals levels on the catalyst. For these units, the make-up rate may be as 1.5 pounds per barrel. When the catalyst make up rate required for activity maintenance or metals control is higher than the catalyst loss rate, equilibrium catalyst must be withdrawn from the unit to balance the fresh catalyst make-up rate.

In addition to the primary cracking catalyst, there are a number of additives which can be added to the unit catalyst inventory. Typical additives are combustion promoter (often referred to as just “promoter”) which is used to accelerate the combustion of CO to CO₂ in the regenerator ; ZSM-5 which is used to increase the gasoline octane and the yield of light olefins and SO_x adsorption additives which are used to reduce the sulfur oxides in the regenerator flue gas.

3.3 Hydrocarbon Classification

The hydrocarbon types in the FCC feed are broadly classified as paraffins, olefins, naphthenes and aromatics (PONA) [42]. Each of these types represents a specific molecular arrangement. When the processed in an FCC unit, each of these types will produce a different slate of products. When mixtures of these types are processed , the net product and their properties will be determined by the composition of mixture [41].

3.3.1 Paraffins

Paraffins are straight or branched chain hydrocarbon having the chemical formula $C_n + H_{2n + 2}$. The name of member end with *-ane* ; example prople propane, isopentane, and normal hexane. Typical paraffins are show in figure 3.2.

In general, FCC feeds are predominantly paraffinic. The paraffin content is typically between 50 wt % and 65 wt % of the total feed. Paraffinic stocks are easy to crack and normally yield the greatest amounts of total liquid products, the most gasoline, the lowest fuel gas, and the least octane number.

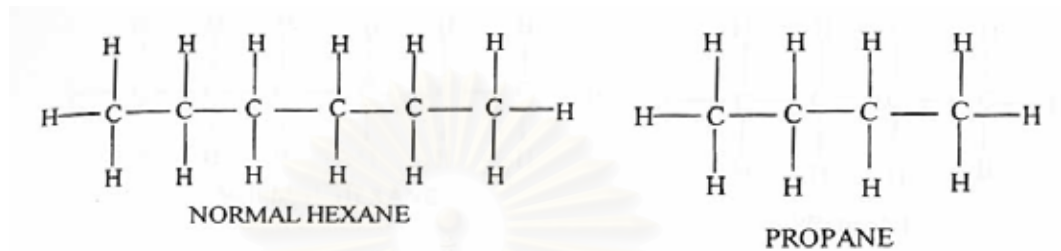


Figure 3.2 Paraffins [42]

3.3.2 Olefins

Olefins are unsaturated compounds with a formula of C_nH_{2n} . The name of these compounds ends with *-ene*, such as ethane (ethylene) and propene (propylene). Typical olefins are shown in figure 3.3.

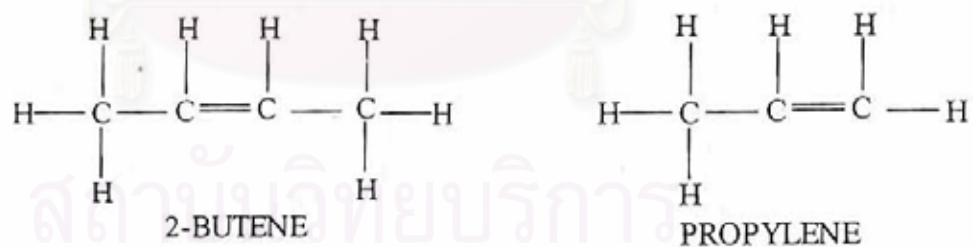


Figure 3.3 Olefins [42]

Compared to paraffins, olefins are unstable and can react with themselves or with other compounds such as oxygen and bromine solution. Olefins do not occur naturally; they show up in the FCC feed as a result of preprocessing the feeds elsewhere. These processes include thermal cracking and other catalytic cracking operations.

Olefins are not the preferred feedstocks to the FCC unit. They usually crack to form undesirable products, such as slurry and coke. Typical olefin content of FCC feed is less than 5 wt % unless charging unhydrotreated thermally-produced gas oils.

3.3.3 Naphthenes

Naphthenes (C_nH_{2n}) have the same formula as olefins, but their characteristics are significantly different. Unlike olefins that are straight-chain compounds, naphthenes are paraffins that have been “bent” into a ring or a cyclic shape. Naphthenes, like paraffins, are saturated compounds. Example of naphthenes are cyclopentane, cyclohexane, and methyl-cyclohexane. Typical naphthenes are shown in figure 3.4.



Figure 3.4 Naphthenes [42]

Naphthenes are desirable FCC feedstocks because they produce high-octane gasoline. The gasoline derived from the cracking of naphthenes has more aromatics and is heavier than the gasoline produced from the cracking of paraffins.

3.3.4 Aromatics

Aromatics (C_nH_{2n-6}) are similar to naphthenes, but they contain a stabilized unsaturated ring core. Example of aromatics are benzene, toluene and aniline. Typical aromatics are shown in figure 3.5.



Figure 3.5 Aromatics [42]

Aromatics are compounds that contain at least one benzene ring. The benzene is very stable and do not crack to smaller componenrs. Aromatics are not preferable as FCC feedstock because most of the molecules will not crack. The cracking of aromatics mainly involves breaking off the side chains, and this can result in excess fuel gas yield. In addition, some of the aromatic compounds contain several rings (polynuclear aromatics) that can “compact” to form what is commonly called “chicken wire”. Some of these compacted aromatics will end up on the catalyst as carbon residue (coke), and some will become slurry product. In comparison to paraffins, the cracking of aromatic stocks results in lower conversion, lower gasoline yield, and less liquid volume gain with higher gasoline octane[42].

3.3.5 Hybrid Molecules [41]

Naphthene and aromatic compounds often contain paraffinic side chains (Figure 3.6). These side chains are subject to the same reaction as paraffinic molecules. Thus, an alkyaromatic molecule, while classified as an aromatic compound, undergo cracking reaction on the alkly side chain. The result of these reactions would be an olefin and an alkyl aromatics with a reduce side chain .

Similarly, an alkyl cycloparaffin could undergo both cracking of the naphthene ring or of the alkyl side chain. This molecules could also be convert to an alkyl aromatic by hydrogen transfer involving the naphthenic ring. Figure 3.7 illustrates some of the possible reaction of these hybrid molecule.

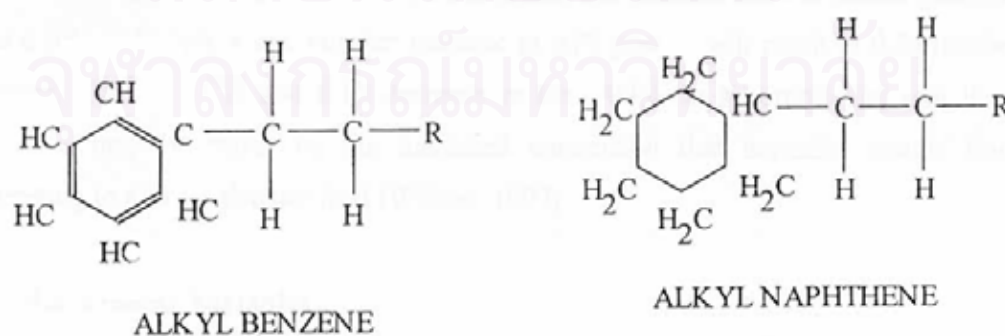


Figure 3.6 Hybrid molecules [41]

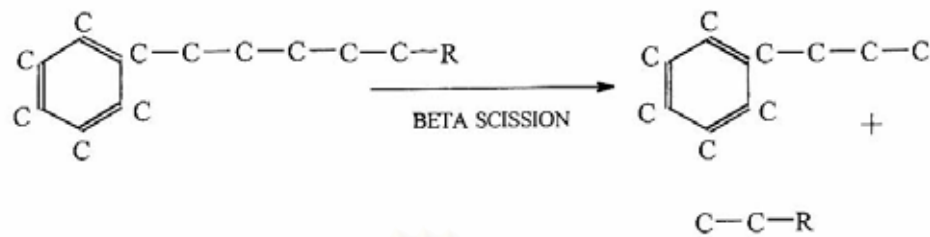


Figure 3.7 Hybrid molecules side chain cracking [41]

3.4 Gasoline Octane

The octane rating of a gasoline blend is primarily a function of the relative concentration of different hydrocarbon in the blend. Aromatic have the highest octane rating and n-paraffins the lowest. Olefins naphthenes and branched paraffins have higher octane rating than the n-paraffins. The octane rating of FCC gasoline is affect by three major factors. 1. Feedstock composition and properties 2. Process variables 3. Ctalyst

3.4.1 Feedstock.

The aromatics have high octane number an increase in aromaticity of the feedstock will result in an increase in gasoline number [43]. Generally feeds with higher API gravities are less aromatic and produce a lower octane gasoline. As a rule of thumb, a one number increase in API gravity will result in 0.25 number decrease in the RON and 0.15 decrease in the MON . In a commercial unit these changes may be offset by the increased conversion that normally results from changing to a lower density feed [41].

3.4.2 Process Variables

Process changes can result in octane gain of up to 3 RON and 1 MON . The following variables have been identified as having an effect on the octane rating of FCC gasoline.

- Conversion

- Reaction temperature
- Regenerator bed temperature
- Carbon on regenerated catalyst
- Oil partial pressure
- Oil residence time (contact time)
- Recycle ratio
- Process steam
- Gasoline boiling range

Among these variables, conversion and reaction temperature have the most significant impact on octane numbers. In general, increased operating severity result in higher octane numbers.

3.4.3 Catalyst

In addition to the of feedstock and operating conditions of the unit, the octane rating of FCC gasoline is also affected by the type of catalyst used in the cracking process. Catalysts designed to boost the octane rating of FCC gasoline are called octane –boosting, octane–enhancing or in short. Octane FCC catalysts. In general, such catalysts can enhance octane by about 3 RON and 1–1.5 MON . depending on the base catalyst and octane level.

Similar to gasoline FCC catalysts, octane FCC catalysts consist of two major components : zeolite and matrix . Some octane catalysts contain a third component : an octane–boosting additive, either incorporated into the catalyst matrix or added as a separate particle. While both the zeolite and matrix components affect the octane rating of FCC gasoline, it is the zeolite component that plays the major role.

According to their composition, most octane FCC catalysts can be classified as follows :

1. Catalysts containing an octane–boosting Y zeolite in a catalytically inert matrix.

2. Catalysts containing an octane–boosting Y zeolite in the catalytically active matrix.

3. Catalysts containing an octane–boosting or a conventional. Rare earth–exchanged Y zeolite and an octane–boosting additive, such as ZSM–5 zeolite.

Catalysts in the first and second category can also contain in addition to the octane–boosting Y zeolite, a conventional, rare earth–exchanged Y zeolite [43].

3.5 Zeolite [44]

In 1756 a Swedish mineralogist, Cronstedt, recognized a new mineral species which he call ‘zeolite’ on the basis of its intumescence. He found zeolites in relatively small cavities in rock of volcanic origin a classical zeolite occurrence.

At present some 39 naturally occurring zeolite species have been recorded and their structures deteemined. In addition more than 100 synthetic species with no know natural counterparts have been confirmed as new zeolite and the majority await full structural determination .

3.5.1 Zeolite Structure

The zeolite have three–dimensional structures arising from a framework of $[\text{SiO}_4]^{4-}$ and $[\text{AlO}_4]^{5-}$ coordination polyhedra (Figure 3.8.)

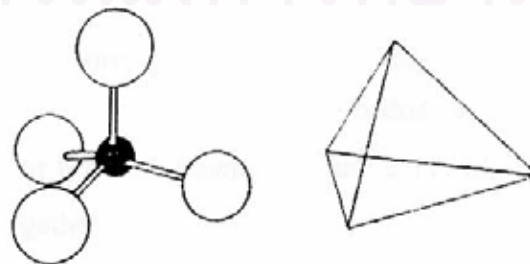


Figure 3.8 Representations of $[\text{SiO}_4]^{4-}$ and $[\text{AlO}_4]^{5-}$ tetrahedral [44]

By definition these tetrahedra are assembled together such that the oxygen at each tetrahedral corner is shared with that in an identical tetrahedron (Si or Al), as shown in figure 3.9. This corner sharing creates infinite lattice comprised of identical building blocks (unit cells) in a manner common to all crystalline materials [44].

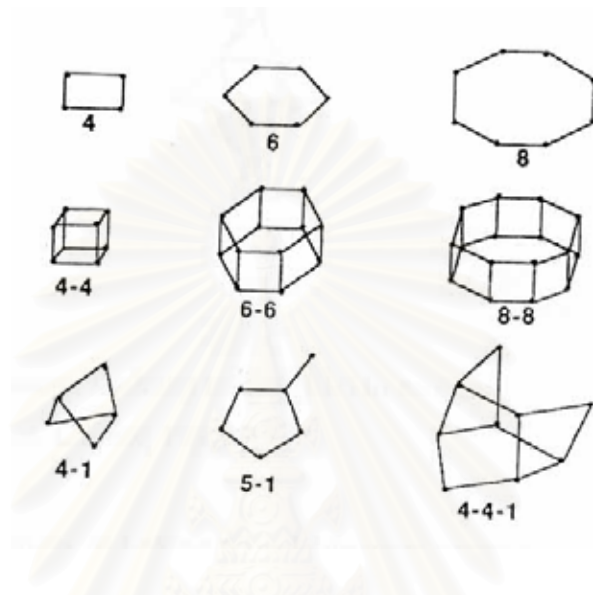


Figure 3.9 Tetrahedra linked together to create a three-dimensional structure [44].

The structures are commonly discussed in terms of levels of organization: the basic tetrahedral units known as secondary building units (SBU), comprising single or double ring structures as shown in Figure 3.10, which in turn are linked together to generate the structure of the zeolite. Higher subsidiary levels of structural organization can be identified in polyhedral building blocks, for example the ‘sodalite unit’ (or β cage) shown in Figure 3.11, which comprises both four and six rings linked together to form a cubo-octahedron; each of the ‘vertices’ of this truncated octahedron has a four-ring of T atoms, while the eight faces are six-rings as shown in the figure. The cage has an internal free diameter of ~ 6 Å assuming a conventional van der Waals radius for oxygen sufficient to encapsulate small molecules.



Figure 3.10 Secondary building units (SBU) in zeolites [45]

Different modes of linking of sodalite units generate some of the commonest zeolite structures. By fusing the unit together via their four-rings generate the structure of sodalite itself, which is both a naturally occurring mineral and a widely synthesized industrial material. One of the most celebrated variants based on the sodalite structure is the beautiful blue dye ultramarine in which S_3^- radicals (which adsorb in the red region of the visible spectrum) are trapped within the sodalite cage.

Bridging (rather than fusing) of sodalite units via four-rings generates the structure of zeolite A also shown in Figure 3.11. The structure, which does not occur naturally, is very extensively synthesized owing to its use in ion exchange, gas separation and drying. An alternative mode of bridging, via six-rings, generates what is probably the single most important zeolite structure, illustrated in Figure 3.11, and referred to as zeolite X or Y depending on the Si/Al ratio, as discussed below. The structure is also adopted by the rare mineral faujasite. The most intriguing feature of this framework is that the mode of linkage of the sodalite units generates very large voids, known as 'supercages', also shown in Figure 3.11. Access to these voids is via large 'window', also evident in the figure, whose molecular diameter is 7.44 Å. This allows organic molecules to diffuse both in and out of the supercages, and the zeolite is indeed

one of the most important catalytic systems, being widely used in the cracking of long to shorter chain molecules is the gasoline range.

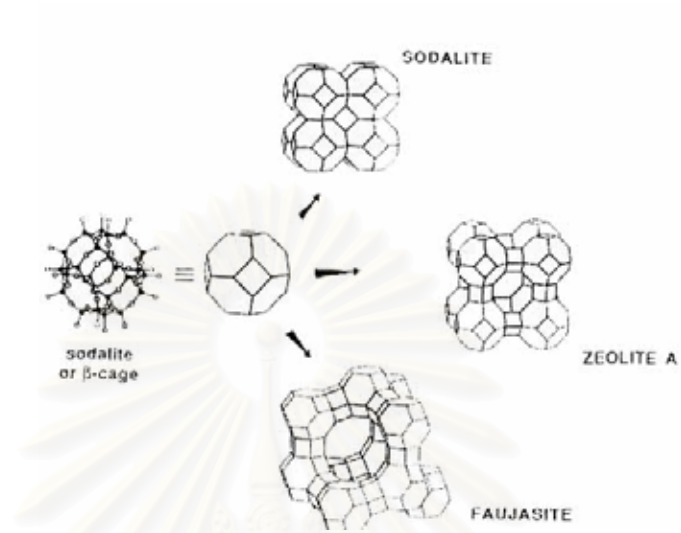
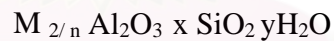
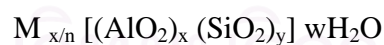


Figure 3.11 The sodalite or cage, linked to create the structures of sodalite, zeolite A and Faujasite (zeolite X/Y) [45].

Zeolites may be represented by the empirical formula:



or by a structural formula:



3.6 Application of Zeolite [45]

Zeolites are routinely used in three main areas of industrial chemistry. The largest is heterogeneous catalysts. Older but important applications are in ion exchange and gas separation.

3.6.1 Catalysis

Zeolites catalyze several types of reaction involving organic molecules. The most important are cracking, isomerization and hydrocarbon synthesis, but there is an increasing application in the field of synthesis of organic fine chemicals. There are two fundamental considerations in zeolite catalysis. The first refers to the basic reaction mechanism and the second to the way in which the products are controlled by the geometry and topology of the microporous crystal structure.

3.6.2 Reaction Mechanisms

Bronsted acid mechanisms are most important in zeolite catalysis. Bridging hydroxyl groups (see Figure 3.12) are, as noted, the commonest type of acid site. As discussed above, these may be considered as protonated oxygens, the protons being present as charge compensators for the negatively charged framework aluminium. The Coulombic interaction between the tetrahedral aluminium and the protons means that Si–OH–Al bridges provide the dominant type of acid species although acid sites associated with defects are thought to contribute to catalytic processes. The variation of acidity with aluminium content is one of the most fascinating aspects of zeolite science and is one where theoretical technique can make an important contribution.

Bronsted acid catalysis within zeolites is essentially conventional. The acidic hydroxyl groups protonate unsaturated organic molecules, or basic groups such as OH and NH₂. The fate of the protonated species may, however, depend strongly on other acid–base properties of the zeolite, including Lewis acidity and basicity of the framework oxygen ions. Moreover, as we have argued, the nature of the product is controlled by the structure of zeolite pores. A simple but important example is the catalytic conversion of metaxylene to paraxylene. The isomers can be interconverted by acid catalysis. However, if the isomerization is undertaken within the pores of the zeolite ZSM–5 the para–isomer has a much higher diffusion coefficient as, unlike metaxylene, it can migrate along the pores of this zeolite. It thus diffuses rapidly out of the catalyst, which therefore effects the required isomerization with high yield.

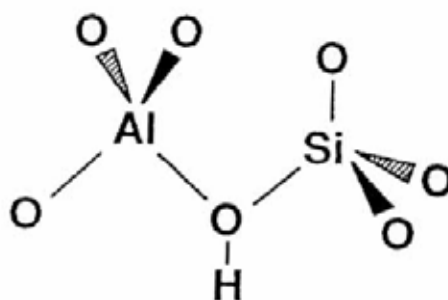


Figure 3.12 Bridging hydroxyl group in aluminium substituted zeolites [45].

Lewis acidity is known to be important in zeolites. Indeed it has been speculated that it plays an important role in hydrocarbon cracking reactions. Fluid bed catalytic cracking which employs zeolite Y and in which the heavy components of crude oil are broken down into hydrocarbons in the gasoline range remains the single most important application of zeolites. Although the technology of this complex process is well developed, our understanding of the reaction pathways is far from complete. The process of coking, whereby the pores of the zeolite become blocked with carbon, is also poorly understood, and there is a clear need for better knowledge at the atomic level of the reaction mechanisms involved.

3.6.3 Ion Exchange

Hydrated cations within zeolite pores are loosely bound and they will readily exchange with other cations in surrounding aqueous media. The study of ion exchange is a mature subject and the thermodynamics of ion exchange equilibria are well understood. The traditional application is in water softening and increasing use of zeolites is made in the detergent industry. Topical recent applications have concerned the removal of radioactive ions from contaminated water.

3.6.4 Gas Separation

The obvious fact that different molecules have different equilibrium constants for sorption and different diffusion coefficients within the pores enables zeolites to be effect gas separation—a phenomenon which has been widely explored. Understanding of the

relative thermodynamics and kinetics of the different sorbed species is crucial for predicting these important technological processes. More specifically, the pore structure of zeolites may be exploited to 'sieve' molecules with the required dimensions to enter the pores. This sieving may be fine tuned by altering the sizes and numbers of the cations present in the pores.

3.7 NaY zeolite

NaY zeolite (faujasite) is produced by digesting a mixture of silica, alumina and caustic for several hours at prescribed temperature until crystallization occurs. A typical NaY Zeolite contains approximately 13% wt Na_2O . To enhance activity, thermal and Hydrothermal stability of NaY, the sodium level must be reduced. This is normally done by the ion exchanging of NaY with a medium containing rare-earth cations or hydrogen ions. Ammonium sulfate solution are frequently employed as a source for hydrogen ion [42].

The structure of Y zeolites consists of a negatively charged, three-dimensional framework of SiO_4 and AlO_4 tetrahedral, joined to form an array of truncated octahedral. These truncated octahedral (β -cages or sodalite cages) are joined at the octahedral faces by hexagonal prisms resulting in tetrahedral stacking. This type of stacking creates large cavities (α -cages or supercages) with a diameter of $\sim 13 \text{ \AA}$. The supercages can be entered through any of four tetrahedral distributed opening (12-membered rings), each having a diameter of 7.4 \AA . The supercages, connected through 12-membered rings, form the large-pore system of the zeolite as shown in Figure 3.13. The structure comprises also a small-pore system, made up of sodalite cages and the connecting hexagonal prisms. The six-member rings of the sodalite cages have a diameter of $\sim 2.4 \text{ \AA}$.

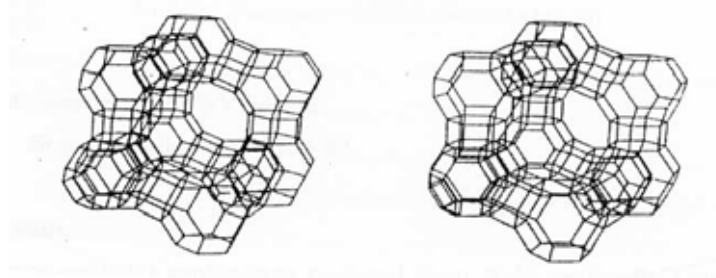


Figure 3.13 Stereodiagram of framework topology of faujasite [42].

3.8 USY Zeolite

USY (ultrastable Y) zeolite was prepared from zeolite NaY zeolite is ammonium exchange with a solution of the ammonium salt in order to reduce the sodium content to 3 or 4 % Na_2O . The partially ammonium exchange zeolite is then calcined at high temperature (about 1033 K) under steam, in order to stabilize the zeolite and move the remaining sodium ions into exchange positions. In commercial operations, the calcinations is usually done in rotary calciners.

Subsequent ammonium exchanges remove most of remaining sodium ions. In its final form, the zeolite contain less than 1 % Na_2O and has unit cell size of about 24.00-24.50 Å , as shown in Figure 3.14. A high framework silica to alumina ratio, low unit cell size and low sodium content are essential in marking these zeolite effective in octane enhancing catalysts.

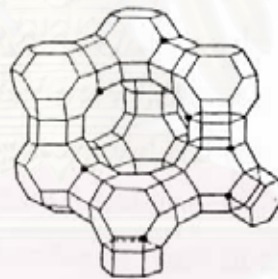


Figure 3.14 Geometry of USY zeolite [42]

3.9 Zeolite Properties

The properties of the zeolite play a significant role in the overall performance of the catalyst, and familiarity with these properties increases our ability to predict catalyst response to continual changes in unit operation. From its inception in the catalyst plant, the zeolite must withstand and retain its catalytic properties under the hostile conditions of the FCC operation. The reactor/regenerator environment can cause significant changes in chemical and structural composition of the zeolite. In the regenerator, for instance, the zeolite is subjected to thermal and hydrothermal treatments. The zeolite must also retain its crystallinity against feedstock contaminants such as vanadium and sodium.

Various analytical tests can be carried out to determine zeolite properties. These tests should supply information about the strength, type, number, and distribution of acid sites. Additional tests can also provide information about surface area and pore size distribution. The three most common parameters governing zeolite behavior are as follow :

1. Unit Cell Size
2. Rare Earth Level
3. Sodium Content

3.9.1 Unit Cell Size

Unit Cell Size (UCS) is a measure of aluminum sites or the total potential acidity per unit cell. The negatively charged aluminum atoms are a source of active site in the zeolite. Silicon atoms do not possess any activity. The UCS is related to the number of aluminum atoms per cell (N_{Al}) by

$$N_{Al} = 111 \times (UCS - 24.215)$$

The number of silicon atoms (N_{Si}) is :

$$N_{Si} = 192 - N_{Al}$$

The SAR (silica–alumina ratio) of the zeolite can be determined either from the above two equations or from a correlation such as one shown in figure 3.15.

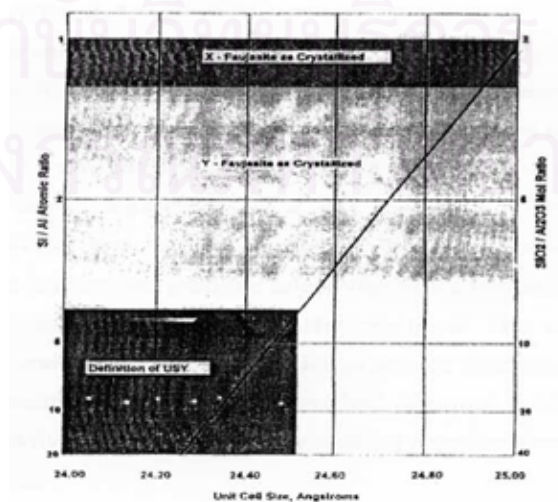


Figure 3.15 Silica–alumina ratio versus zeolite unit cell size [42].

The unit cell size is also an indicator of zeolite acidity, because the aluminum ion was larger than the silicon ion, as the UCS decreases, the acid site become further apart. The strength of the acid site is determined by the extent of their isolation from the neighboring acid sites. The close proximity of these acid sites causes destabilization of zeolite structure. Acid distribution of the zeolite is a fundamental factor affecting zeolite activity and selectivity. Zeolite with lower UCS are initially less active than conventional rare earth exchanged zeolites. However the lower UCS zeolites tend to retain a greater fraction of their activity under severe thermal and hydrothermal treatments, hence the name Ultrastable (USY) .

A freshly manufactured zeolite has a relatively high UCS in the range of 24.50 A to 24.75 A . The thermal and hydrothermal environmental of the regenerator extracts alumina from the zeolite structure and therefore reduces its UCS. The final UCS level depend on the rare earth and sodium level of the zeolite. The lower the sodium and rare earth content of the fresh zeolite, the lower UCS of the equilibrium catalyst.

3.9.2 Rare Earth Level

Rare earth element serve as a 'bridge' to stabilize aluminum atoms in the zeolite structure. They prevent the aluminum atoms from separating from the zeolite lattice when the catalyst is exposed to high temperature steam in the regenerator.

A fully rare earth exchanged zeolite equilibrates at a high UCS , whereas a non rare earth zeolite equilibrates at a very low UCS in the range of 24.25. All intermediate level of rare earth exchanged zeolite can be produced. The rare earth increases zeolite activity and gasoline selectivity with a loss in octane. The octane loss is due to promotion of hydrogen transfer reactions. The insertion of rare earth maintains more and closer acid sites, which promotes hydrogen transfer reactions. In additions, rare earth improves thermal and hydrothermal stability of the zeolite. To improve the activity of a USY zeolite, the catalyst suppliers frequently add some rare earth to the zeolite.

3.9.3 Sodium Content

Sodium content is detrimental to zeolite stability, activity and its octane-enhancing capability. The lower activity and octane-enhancing capacity is attributed to the partial neutralization of strong Bronsted acid sites by sodium ions. In commercial FCC catalysts, the sodium content of the zeolite is minimized, usually below 1 percent Na_2O . This is accomplished by ionic exchange of the zeolite with solutions of small ammonium or rare earth salts. However, there are reports that the presence of small amounts of sodium in the zeolite may have a beneficial effect on stability and selectivity [40]. Sodium decreases the hydrothermal stability of the zeolite. It also reacts with the zeolite acid sites to reduce the catalyst activity. In the regenerator, sodium is mobile. Sodium ions tend to neutralize the strongest acid sites. In a dealuminated zeolite where the UCS is low (24.22°A to 24.25°A), the sodium can have an adverse effect on the gasoline octane. The loss of octane is attributed to the drop in the number of strong acid sites.

Fluid catalytic cracking catalyst vendors are now able to manufacture catalysts with a sodium of less than 0.2 wt %. Sodium is commonly reported as the weight percentage of sodium or soda (Na_2O) on catalyst. The proper way to compare sodium is the weight fraction of sodium in the zeolite. This is because FCC catalysts have different zeolite concentrations [42].

3.10 Active Site

The active sites in cracking catalysts are acid sites, for example they are proton donors (called Bronsted acid sites) or electron pair (two electrons) acceptors (called Lewis acid sites). Both types can initiate the carbenium ion cracking chain described in Figure 3.16. Acid sites in all conventional cracking catalysts are formed by interactions of silica and alumina, SiO_2 and Al_2O_3 . Under appropriate reaction conditions, these two materials (or other materials containing sources of SiO_2 and Al_2O_3) interact to form a solid of the following simplified structure [40].

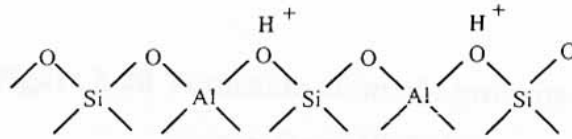


Figure 3.16 Formation of Bronsted site [44].

In high-silica zeolite these ‘protonated’ zeolites can be made by direct exchange with mineral acid. Ideally the ‘protonated’ form contains hydroxyls which are protons associated with negatively charged framework oxygens link into alumina tetrahedral. The protons have great mobility when the temperature is above 473 K, and at 823 K they are lost as water with the consequent formation of Lewis sites, as show in Figure 3.17.

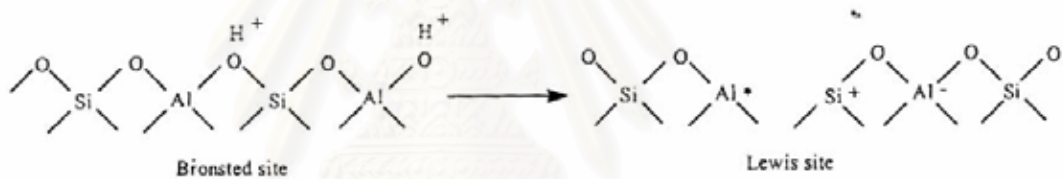


Figure 3.17 Formation of Lewis site [44].

The Lewis sites in turn are unstable, especially in the continued presence of water vapor and an annealing process stabilizes the structure. This produces called ‘true’ Lewis site by ejecting Al species from the framework, as show in Figure 3.18 [44].

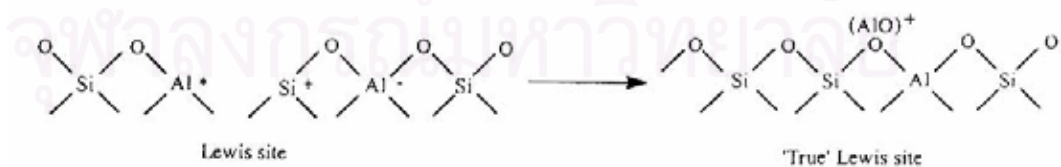
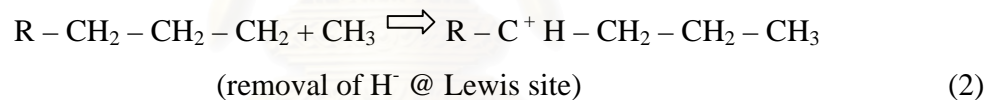
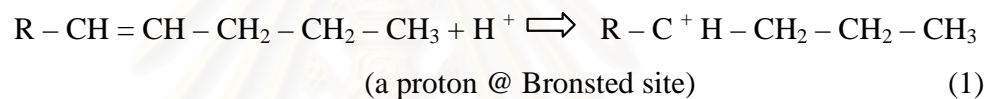


Figure 3.18 Formation of ‘true’ Lewis site [44].

3.11 Mechanism of Catalytic Cracking Reaction

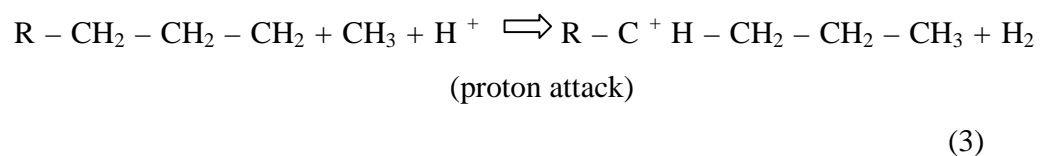
The reaction that occur when a hydrocarbon molecules reacts on the solid surface of a catalyst all involve positively charged organic species, usually carbenium ions. The first step is the vaporization of the feed by the catalyst. The next step is formation of positive-charged carbon atoms called 'carbocations'. Carbocation is a generic term for a positive-charged carbon ion. Carbocation can further be subdivided into carbenium and carbonium ions.

A carbenium ion, $R-CH_2^+$, comes either from adding a positive charge to an olefin or from removing a hydrogen and two electrons from a paraffin molecule (Equations 1 and 2).

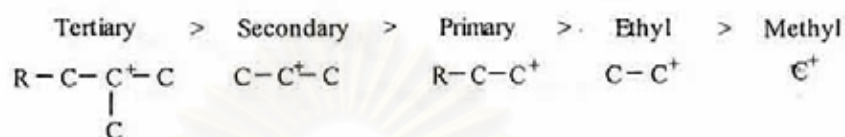


The Bronsted and Lewis acid sites on the catalyst are responsible for generating carbenium ions. The Bronsted site donates a proton to an olefin molecule and the Lewis site removes electrons from a paraffin molecule. In commercial units, olefins are either in the feed or are produced through thermal cracking reactions.

A carbonium ion, CH_5^+ , is formed by adding a hydrogen ion (H^+) to a paraffin molecule (Equation 3). This is accomplished via direct attack of a proton from the catalyst Bronsted site. The resulting molecule will have a positive charge with 5 bonds to it.



The carbonium ion's charge is not stable and the catalyst acid sites are probably not strong enough to form a lot of carbonium ions. Consequently, nearly all the cat cracking chemistry is carbenium ion chemistry. The stability of carbocations depends on the nature of alkyl groups attached to the positive charge. The relative stability of carbenium ions is as follows :



One of the benefits of catalytic cracking is that the primary and secondary ions tend to rearrange to form a tertiary ion (a carbon with three other carbon bonds attached) As will be discussed later, the increased stability of tertiary ions accounts for the high degree of branching associated with cat cracking.

Once formed in the initial step, carbenium ions can form a number of different reactions. The nature and strength of the catalyst acid sites will significantly influence the degree to which these reactions occur. The three dominant reactions of carbenium ions are :

- The cracking of a carbon-carbon bond
- Isomerization
- Hydrogen transfer

3.11.1 Cracking Reactions

The cracking, or beta-scission, is a key feature of ionic cracking. Beta-scission is splitting of the C-C bond at two bonds away from the positive-charge carbon atom. There is a preference for beta-scission because the energy required to break this bond is lower than that needed to break the adjacent C-C bonds. In addition, long-chain hydrocarbons are more reactive than short-chain hydrocarbons ; therefore, the rate of the cracking reactions decreases with decreasing chain length to the point that it is not possible to form stable carbenium ions. The initial products of beta-scission are an olefin and a new carbenium ion (Equation 4). The newly formed carbenium ion will then continue a series of chain reactions. Small ions such as a four-carbon or five-carbon can

then react with another big molecule and transfer the positive charge, and then the big molecule can crack. Cracking does not eliminate the positive charge ; it stays there until two ions run into each other. The smaller ions are more stable and will not crack. They stay longer and finally transfer their charge into a big molecule.



Because beta-scission is monomolecular, cracking is endothermic. Consequently, cracking rate is favored by high temperatures ; cracking is not equilibrium limited. The reactions that occur during gas oil cracking over zeolite catalysts are summarized in Figure 3.19.

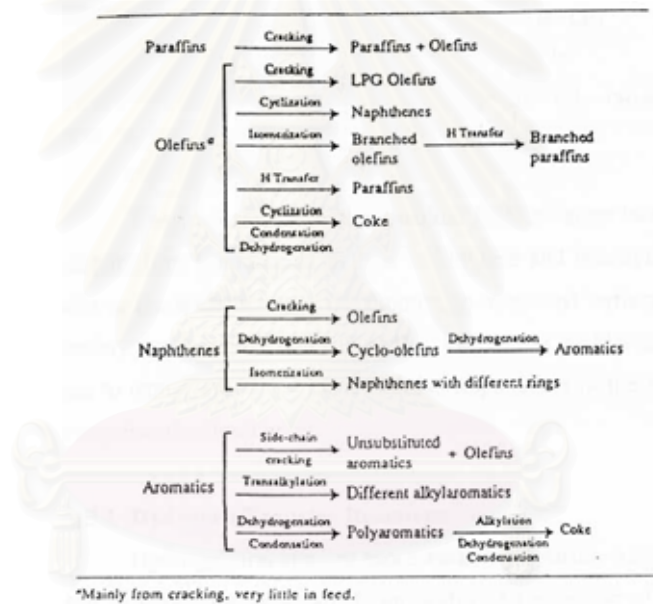


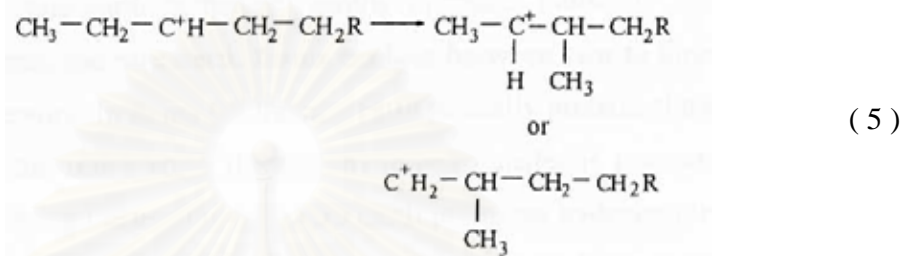
Figure 3.19 Main reactions in FCC catalysis [43].

3.11.2 Isomerization Reactions

Isomerization reactions occur more frequently in catalytic cracking than in thermal cracking. As discussed earlier, thermal cracking is a free-radical mechanism. Breaking of a bond in both thermal and catalytic mechanisms is via beta-scission ; however, in catalytic cracking a number of carbocations tend to rearrange to form tertiary ions. Tertiary ions are more stable than secondary and primary ions ; they shift around and crack to produce branched molecules (Equation 5) . Free radicals do not do

that ; they yield normal or straight compounds. Some of the advantages of isomerization are as follows :

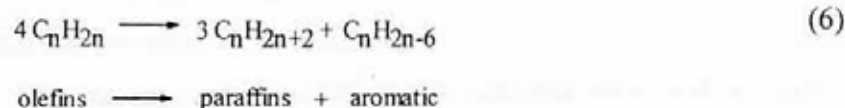
- Higher octane
- Higher-value chemical and oxygenate feedstocks
- Lower cloud point for diesel fuel



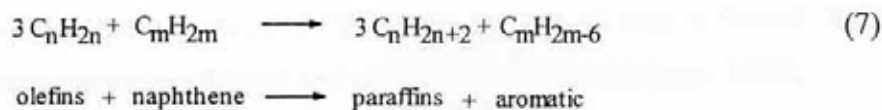
The isoparaffins in the gasoline boiling range have higher octane than normal paraffins. Compounds such as isobutylene and isoamylene will be extremely valuable as the feedstocks for the production of methyl tertiary butyl ether (MTBE) and tertiary amyl methyl ether (TAME). MTBE and TAME can be blended into the gasoline to reduce auto emissions. Finally, isoparaffins in the light cycle oil boiling range improve the cloud point.

3.11.3 Hydrogen Transfer Reactions

Hydrogen transfer, or more correctly hydride transfer, is a bimolecular reaction in which one reactant is an olefin. An example of hydrogen transfer is the reaction of two olefins. Both olefins would have to be adsorbed on the active sites and the sites would have to be close together for these reactions to take place. One of these olefins becomes paraffin and the other becomes cyclo-olefins ; so hydrogen is moved from one to another. Cyclo-olefin is now hydrogen transferred with another olefin to yield cycloidi-olefin. Cycloidi-olefin will then rearrange to form an aromatic, and aromatics are extremely stable. Therefore, hydrogen transfer of olefins converts them to paraffins and aromatics (Equation 6) .



Napthenic compounds are also hydrogen donors and can react with olefins to produce paraffins and aromatics (Equation 7).



A rare-earth-exchanged zeolite increases indirectly hydrogen transfers. In simple terms, the rare earth forms bridges between two to three acid sites in the catalyst framework. In doing so, the rare earth basically protects those acid sites being ejected from the framework. Because hydrogen transfer is promoted from adjacent acid sites, bridging these sites with rare earth promotes hydrogen transfer reactions.

Hydrogen transfer reactions usually increase FCC gasoline yield and its stability. It does so by reducing reactivity of the gasoline being produced. When there is hydrogen transfer, there are fewer olefins. Olefins are the reactive species in gasoline for secondary reactions; therefore, hydrogen transfer reactions reduce indirectly 'overcracking' of the gasoline.

Cracking, isomerization, and hydrogen transfer reactions account for the majority of reactions occurring in cat cracking. There are other associated reactions that do indeed play a role in coking. Under ideal conditions, i.e., a 'clean' feedstock and catalyst with no metals, cat cracking does not yield any appreciable amounts of molecular hydrogen. Therefore, dehydrogenation reactions will only proceed if the catalyst is contaminated with metals such as nickel and vanadium.

Cat cracking of gas oil molecules yields a residue called coke. Chemistry of coke formation is complex and not very well understood. Similar to hydrogen transfer reactions, catalytic coke is a 'bimolecular' reaction product and proceeds via carbenium ions or free radicals. In theory, coke yield should increase as hydrogen transfer rate is increased. It is postulated that reactions producing unsaturates such as olefins, diolefins, and multi-ring polycyclic olefins are very reactive and can polymerize to form coke.

For a given catalyst and feedstock, catalytic coke yield is a direct function of conversion. However, there exists an optimum riser temperature in which the coke yield is minimum. For a typical cat cracker, this temperature is about 783 K. Let's look at two extreme riser temperatures of 454 K and 565 K. At 727 K, a lot of coke is formed mainly because the carbenium ions do not desorb at this low temperature. At 838 K, a large amount of coke is formed largely due to olefin polymerization [42].



สถาบันวิทยบริการ
จุฬาลงกรณ์มหาวิทยาลัย

CHAPTER IV

EXPERIMENT

In this chapter, experimental is divided into three sections. First, preparation of HY-type zeolite is presented in section 4.1. Second, hydrothermal treatment procedure is showed in section 4.2. Third, characterization of Y zeolite under hydrothermal treatment by using SEM, XRD, BET and NH₃TPD is presented in section 4.3. Finally, evaluate the effect of particle size and hydrothermal treatment condition of Y zeolite in the catalytic cracking of n-octane.

In this study, catalysts were prepared and treated by Mr. Somyod Sombatchaisak [46]. The preparation and treatment of Y zeolite are described in section 4.1 and 4.2.

4.1 Preparation of Y-Type Zeolite

The synthesis of Y zeolite was described in parent literature [26]. The stoichiometrical ratio between initial solution of aluminosilicate solution and sodium silicate solution is Na₂O:Al₂O₃:SiO₂:H₂O = 3.68:1:12:148. The preparation procedure of Y zeolite is shown in Figure 4.1, while reagents used are shown in Table 4.1

4.1.1 Materials

Chemical used in this experiment have to be specified as follows:

1. Sodium Aluminate [NaAlO₂] manufactured by Wako Pure Chemical Industries CO.,Ltd., Japan.
2. Sodium Silicate solution [Na₂Si₃O₇] manufactured by Merck Ltd., Germany.
3. Sodium Hydroxide [NaOH] manufactured by Merck Ltd., Germany.

4.1.2 Preparation of uniform slurry

Sodium aluminate and sodium silicate solution were used as Al and Si sources of Al and Si, respectively; while Na source was substantially obtained from sodium hydroxide. The uniform slurry was prepared by the two main steps as follows:

1. S_1 was slowly added into S_2 while vigorous stirring. The mixture was continuously stirred for 2 h. Then the mixture was heated to 333 K and maintained at that temperature for 1 h to form a gel. The gel mixture was separated from the supernatant solution by a centrifuge.

Table 4.1 Reagents used for the preparation of Y zeolite [47].

Reagents	Quantity
First step:	
<u>Solution S_1</u>	
NaAlO ₂	32.81 g
Distilled water	158 ml
<u>Solution S_2</u>	
Na ₂ Si ₃ O ₇	218.6 g
NaOH	95.91 g
Distilled water	534 ml
Second step:	
<u>Solution S_3</u>	
Na ₂ Si ₃ O ₇	216.72 g
NaOH	95.91 g
Distilled water	534 ml

Then it was washed by water and separated from solution by repeating cycles of centrifugation and decantation until the pH of supernatant solution was about 13.5.

2. 181 g of obtained gel from the above step was poured into S_3 . Subsequently, the resultant mixture was stirred to obtain uniform slurry.

4.1.3 Crystallization

1. The uniform slurry was charged into a closed glass vessel and placed at room temperature at different aging time of nucleation (0.5, 2, 4.5, 6.5 days).
2. The glass vessel charged with slurry was heated at various temperatures (363, 373, 383 K) and maintained at such temperature for 24 h.
3. The prepared Y zeolite was left to cool down to ambient temperature, then it was washed with distilled water until the pH of slurry became 7 by repeating cycles of centrifugation and decantation. The obtained crystals were dried overnight at 383 K.

4.1.4 Preparation of the Proton-Type Y (HY)

a) Ammonium Ion-Exchange of NaY Zeolite

1. 2 g portion of the NaY Zeolite was added by 80 ml of 1 N NH_4NO_3 aqueous solution, after that the mixture was heated at 353 K for 1 h.
2. The powder was washed twice by distilled water to remove nitrate ions. Then water was repeated by centrifugation.
3. Steps 1 and 2 were repeated for five times.
4. The sample was dried overnight in an oven at 383 K. The Na-form crystal was thus changed to NH_4 -form catalyst.

b) HY-Type Zeolite

The NH_4Y zeolite was converted to HY Zeolite by removing NH_3 species from the catalyst surface. NH_3 can be removed by thermal treatment of the NH_4Y zeolite. This was done by heating a sample in an air stream at 773 K for 2 h; by heating them from room temperature to 773 K at a heating rate of 280.9 K/min. After the catalyst was cooled down, it was stored in a glass bottle in desiccators for further used.

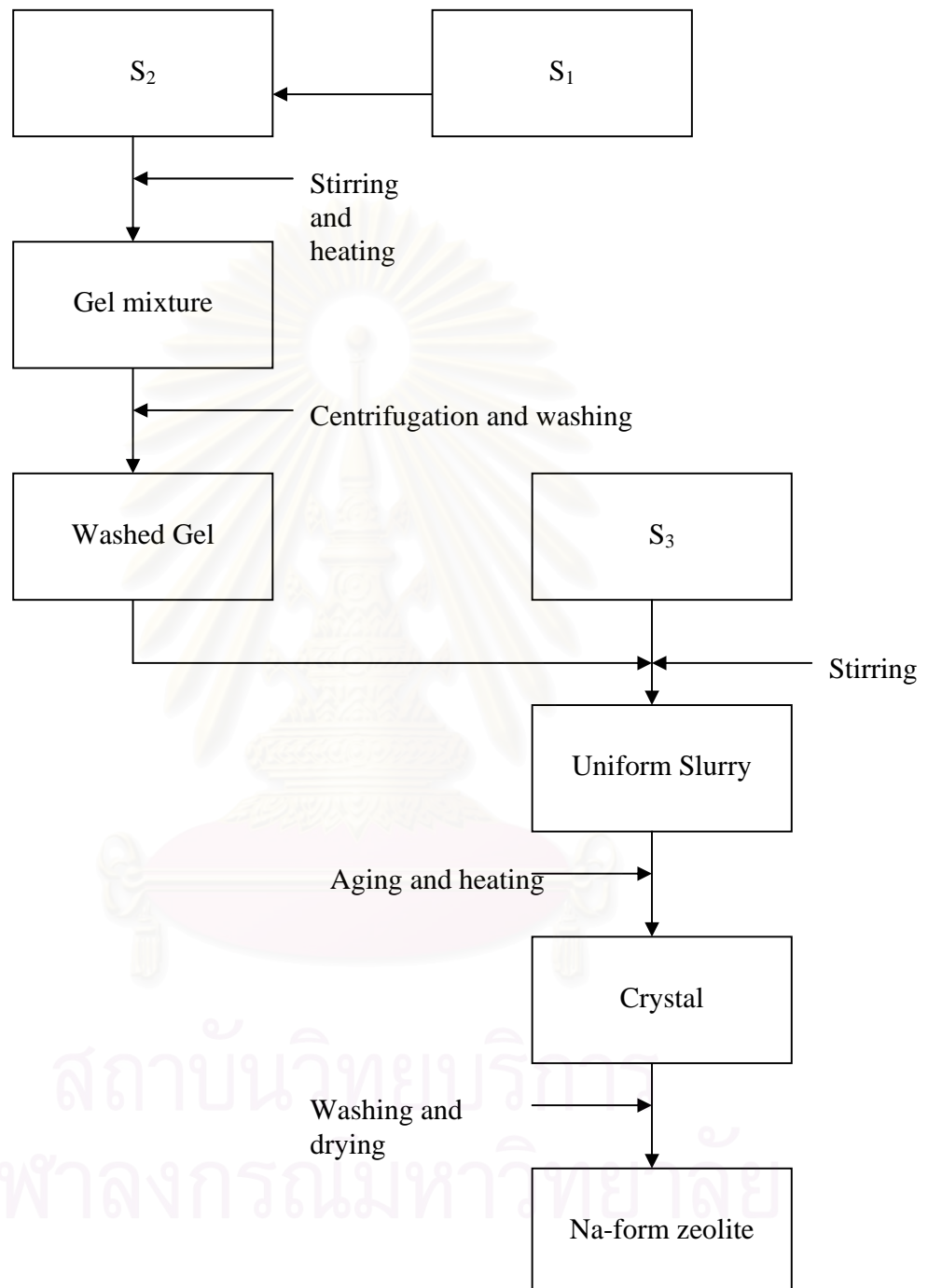


Figure 4.1 The preparation procedure of NaY-zeolite catalyst. [48].

4.2 Hydrothermal Pretreatment

In order to investigate the effect of hydrothermal treatment on the stability of zeolite with different particle size, the hydrothermal treatment is carried out in an apparatus which is schematically represented in Figure 4.2. About 0.5 g of samples is introduced into the reactor at room temperature. Next, the catalyst is heated in a N_2 stream while elevating temperature from room temperature to desired temperature (873, 973, 1073, 1173 and 1273 K) with a constant heating rate of 283 K/min. The catalyst sample is then kept at the desired time (0.5, 1, 2, 3, and 5 h) while steam is added at different partial pressures (0.05, 0.1, 0.2, 0.5, and 1.0). Subsequently, the zeolite is cooled down to room temperature in N_2 stream.

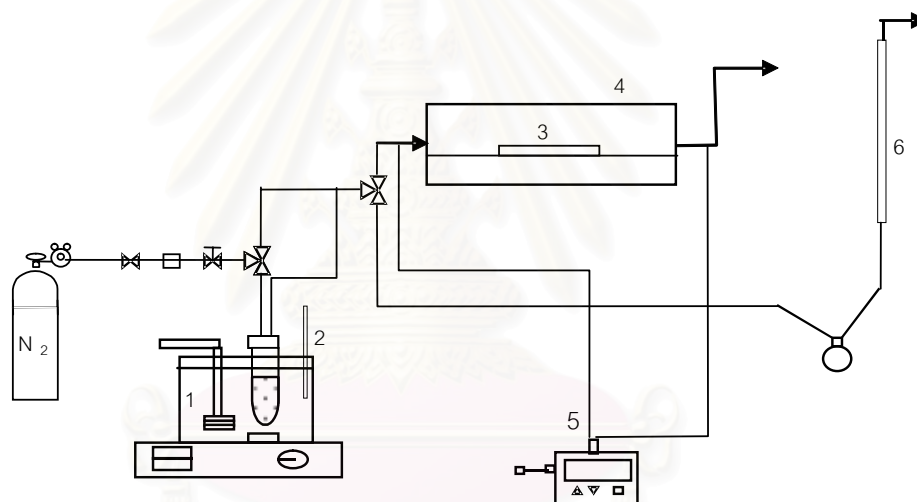


Figure 4.2 Scheme of the apparatus for hydrothermal treatment: 1, steam generating system; 2, thermocouple; 3, sample; 4, carbolite; 5, temperature control; 6, bubble flow meter.

4.3 Characterization

4.3.1 Scanning Electron Microscopy (SEM)

Scanning Electron Microscopy was employed for including the shape and size of the prepared zeolite crystal. The JEOL JSM-35 CF model at the Scientific and Technological Research Equipment Centre, Chulalongkorn University (STREC) was used for this purpose.

4.3.2 X-ray Diffraction Analysis (XRD)

The Unit cell size and X-ray diffraction (XRD) patterns of the catalysts were performed by an X-ray diffractometer SEIMENS D500 connected with a personal computer with Diffract AT version 3.3 programs for fully control of the XRD analyzer. The experiments was carried out by using $\text{CuK}\alpha$ radiation with Ni filter and the operating condition of measurement are 4-40 degree 2θ , with a resolution of 0.04.

The functions of base line subtraction and smoothing were used in order to get the well formed XRD spectra.

4.3.3 Surface area measurement

Physical adsorption isotherms are measured near the boiling point of a gas (e.g., nitrogen, at 77 K). From these isotherms the amount of gas needed to form a monolayer can be determined. If the area occupied by each adsorbed gas molecule is known, the surface area can be determined for all finely divided solids, regardless of their chemical composition.

The specific surface area of samples was calculated using the Brunauer-Emmett-Teller (BET) single point method on the basis of nitrogen uptake measured at liquid-nitrogen boiling point temperature equipped with a gas chromatograph.

4.3.3.1 BET apparatus

The reaction apparatus of BET surface area measurement consisted of two feed lines of helium and nitrogen. The flow rate of the gases was adjusted by means of fine-metering valve on the gas chromatograph. The sample cell made from pyrex glass. The operation condition of gas chromatograph (GOW-MAC) is shown in Table 4.2.

Table 4.2 Operating condition of gas chromatograph (GOW-MAC)

Model	GOW-MAC
Detector	TCD
Helium flow rate	30 ml/min
Detector temperature	80°C
Detector current	80 mA

4.3.3.2 Measurement

The mixture gas of helium and nitrogen was flown through the system at the nitrogen relative pressure of 0.3. The catalyst sample was placed in the sample cell, ca. 0.3-0.5 g, which was then heated up to 433 K and held at that temperature for 2 h. Then the catalyst sample was cooled down to room temperature and the specific surface area was measured. There were three steps to measure the specific surface area.

Adsorption step: The catalyst in the sample cell was dipped into the liquid nitrogen. Nitrogen gas that was introduced into the system was adsorbed on the surface of the catalyst sample until equilibrium was reached.

Desorption step: The sample cell with nitrogen gas-adsorbed catalyst sample was dipped into a water bath at room temperature. The adsorbed nitrogen gas was desorbed from the surface of the catalyst sample. This step was completed when the integrator line was back in the position of the base line.

Calibration step: 1 ml of nitrogen gas at atmospheric pressure was injected through the calibration port of the gas chromatograph and the area was measured. The area was the calibration peak. The calculation method is explained in Appendix A-3.

4.3.4 Temperature programmed desorption of adsorbed ammonia (NH₃TPD)

The acidity measurement was assessed by using the technique of temperature programmed desorption (TPD) of NH₃ at Petrochemical Engineering Research Laboratory, Chulalongkorn University .

NH₃ TPD is carried out in an apparatus to measure the amount of acidic sites on the catalysts. Catalyst (15 mg) was heated from room temperature to 723 K with a constant heating rate of 293 K/min with N₂ gas flowing at 50 ml/min. The temperature was kept at 723 K for 5 min. After the catalyst was dried, the temperature was lowered to 343 K. Adsorption of ammonia (10%NH₃/He) was carried out with flow of 60 ml/min. After the catalyst surface became saturated for a certain period of time, excess ammonia was removed. The temperature-programmed desorption was performed with a linear heating rate of approximate 283 K/min from 353 K to 873 K. The NH₃ that desorbed was measured by a thermal conductivity detector and the electrical signals from the detector.

4.4 Catalytic cracking of n-octane

4.4.1 Chemical and reagent

n-octane hydrocarbon purity 99 % was supplied by Carlo erba.

4.4.2 Instruments and apparatus

4.4.2.1 The reactor is a conventional microreactor made from a quartz tube with 0.6 mm inside diameter, so it can be operated at high temperature. The reaction was carried out under ordinary gas flow and atmospheric pressure.

4.4.2.2 In temperature controller: This consists of a magnetic switch connected to a variable voltage transformer and a RKC temperature controller connected to a thermocouple attached to the catalyst bed in reactor. A dial setting establishes a set point at any temperature within the range between 273 K to 873 K.

4.4.2.3 Electrical furnace : This supplies the required heated to the reactor for the reaction. The reactor can be operated from room temperature to 973 K at maximum voltage.

4.4.2.4 Gas controlling system : nitrogen cylinders each equipped with a pressure regulator (0–120 psig), an on–off valve and a needle valve were used to adjust flow rate of gas.

4.4.2.5 Gas chromatographs : flame ionization detector–type gas chromatographs, Shimudzu GC–14 A and GC–14 B, were used to analyze feed and effluent gas. Operating conditions used are shown in Table 4.3.

Table 4.3 Operating conditions for gas chromatograph

Gas chromatographs	Shimudzu GC-14A	Shimudzu GC-14B
Detector	FID	FID
Column	Silicon OV-1 ϕ 0.25 x 50 m	VZ-10 ϕ 3 x 3 m
Carrier gas	N ₂ (99.99 %)	N ₂ (99.99 %)
Flow rate of carrier gas	25 ml / min	25 ml / min
Column temperature		
- Initial	55 °C	80 °C
- Final	140 °C	80 °C
- Rate	3 °C/min	-
Detector temperature	150 °C	150 °C
Injection temperature	145 °C	100 °C
Analyzed gas	gasoline range hydrocarbon	gaseous hydrocarbon

4.4.3 Reaction Method

The catalytic cracking reaction of n-octane hydrocarbon was carried out by using a conventional flow apparatus shown in Figure 4.3. A 0.1 g portion of the catalyst was packed in a quartz tubular reactor. Nitrogen gas was supplied from a cylinder to control n-octane partial pressure and flow rate of the system (see Appendix A-4). Catalytic cracking reaction of n-octane was carried out under the following conditions : total pressure 1 atm ; n-octane composition 20% balanced with nitrogen ; gas hourly space velocities (GHSV) 6400 h⁻¹ ; reaction temperature 573–773 K.

The procedure used to operate the reactor is as follows :

- (1) Adjust the outlet pressure of N₂ gas to 1 kg/cm², and allow the gas to flow through a rotameter.

(2) Adjust 2 three-way valves to allow gas to pass through the upper line through the reactor and measure the outlet gas flow rate by using a bubble flowmeter.

(3) Heat the reactor from room temperature to 723 K with a heating rate of 293 K/min and maintain at that temperature for 30 min. Then, the reaction temperature controlled by the on-off controller were set and wait until the required reaction temperature was reached.

(4) At the same time switch on the heating line and water-bath.

(5) Set the partial vapor pressure of n-octane to the requirement by adjusting the temperature of the water-bath according to the Antoine equation ,

$$\log p = A - B / (t + C)$$

where :

P	=	vapor pressure of n-octane , mmHg
t	=	temperature, °C
A , B and C	=	constants

The values of these constants for n-octane are $A = 6.92374$, $B = 1355.126$, $C = 209.517$ and range of temperature that applied ability 19–152 °C .

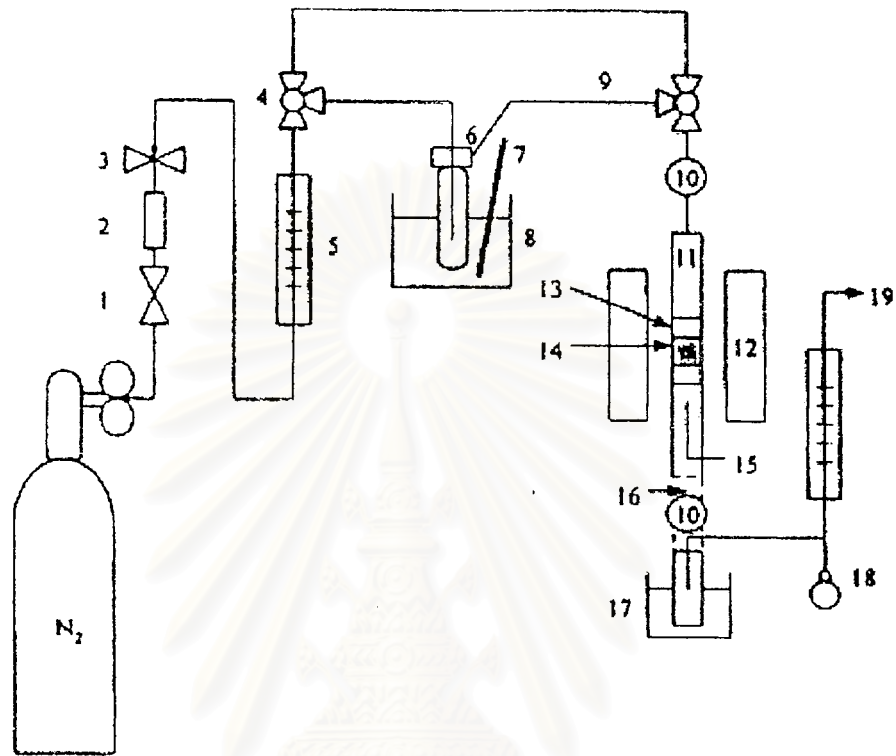
(6) Start to run the reaction by adjusting 2 three-way valves to allow nitrogen gas to pass through n-octane inside the saturator set in the water-bath, and then, carry n-octane into inside of reactor. At that time , the reaction time is taken as zero. The partial pressure of n-octane was controlled by the water-bath temperature .

(7) Take sample to analyze. The reaction product were analyzed by gas chromatographs (for calculation see Appendix B) .

(8) Chromatogram data were changed into weight of reactant and products by calibration curve (in Appendix B) .

$$\% \text{ n-octane conversion} = \frac{\text{weight of n-octane reacted}}{\text{weight of n-octane in feed}} \times 100$$

$$\text{selectivity of product I} = \frac{\text{weight of product I}}{\text{weight of n-octane reacted}} \times 100$$



- | | | | |
|-----------------|-------------------------|---------------------|----------------------|
| 1. On-off valve | 2. Gas filter | 3. Needle valve | 4. Three-way valve |
| 5. Flow meter | 6. Saturator | 7. Thermocouple | 8. Water bath |
| 9. Heating line | 10. Sampling port | 11. Tubular reactor | 12. Electric furnace |
| 13. Quartz wool | 14. Catalyst | 15. Thermocouple | 16. Heating tape |
| 17. Trap | 18. Soap-film flowmeter | | 19. Purge |

Figure 4.3 Schematic diagram of the reaction apparatus for reaction

CHAPTER V

RESULTS AND DISCUSSION

In this chapter, the results and discussion are classified into two parts. Firstly, the effect of particle size on hydrothermal stability of Y zeolite is analyzed by SEM, XRD, BET, and NH₃TPD measurement in section 5.1. Secondly the effect of particle size and hydrothermal treatment of Y zeolite in the catalytic cracking of n-octane is explained in section 5.2.

5.1 Catalyst Characterization

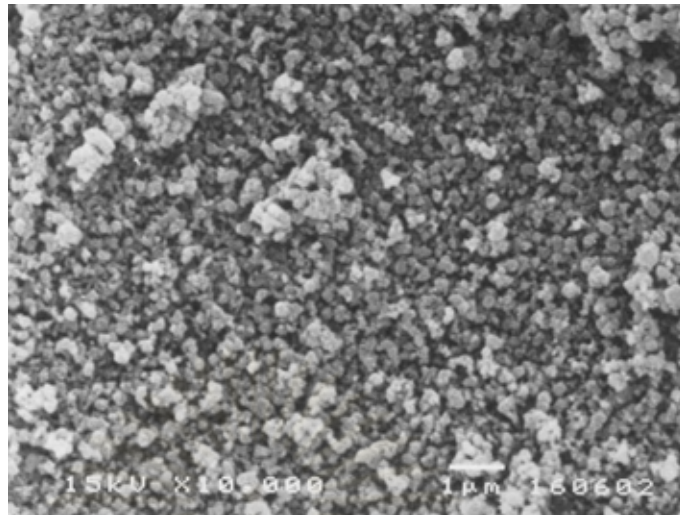
5.1.1 Morphology and Particle size of Y zeolite samples

Y zeolites synthesized by hydrothermal method have different particle size, average 0.16, 0.31, 0.45, 0.82, and 2.01 μm . Average particle size was calculated from

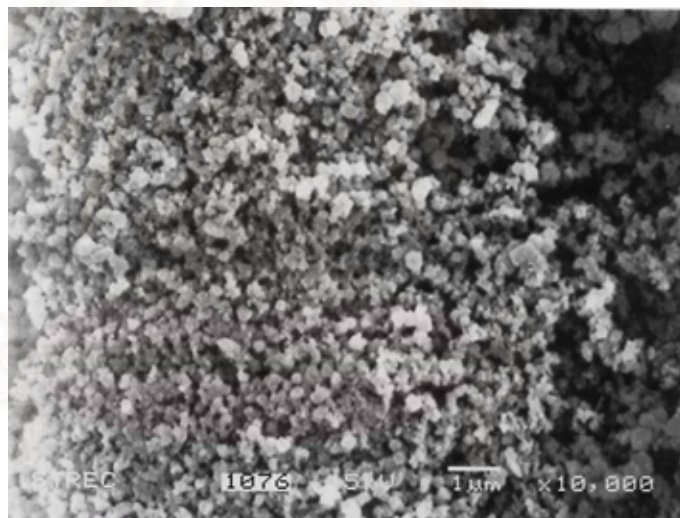
$$\text{Average particle size} = \frac{\sum [(\text{particle size was measured from SEM}) \times (N)]}{\sum N}$$

N = Number of sample

Shape and average size of the particle before hydrothermal treatment can be observed from scanning electron microscopy (SEM) picture [46] as shown in Figures 5.1 (a), (c), (e), (g), (i), and (k), respectively. SEM micrographs of the particle after hydrothermal treatment are illustrated in Figure 5.1 (b), (d), (f), (h), (j), and (l), respectively. Y zeolites prepared with different preparation conditions resulted in spherical particles with average particle sizes varying from 0.16-2.01 μm . The particle sizes and shape remained unaltered after encountered the hydrothermal treatment at 1073 K for 1 h.

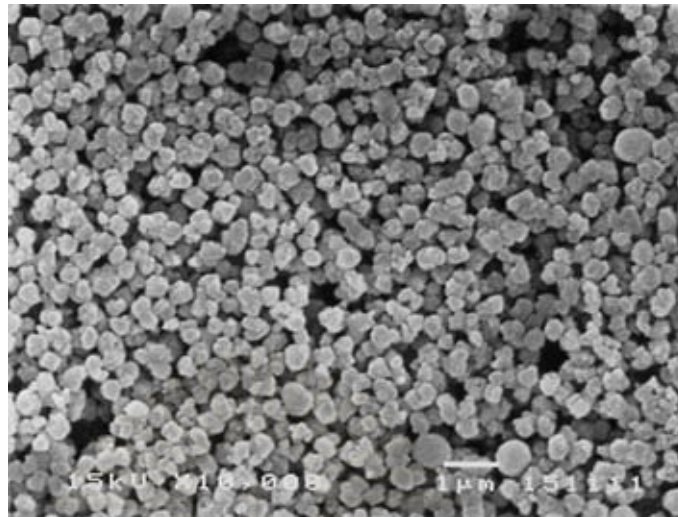


(a)



(b)

Figure 5.1 Scanning electron micrographs of Y zeolite particle size 0.16 μm (a) fresh (b) treated

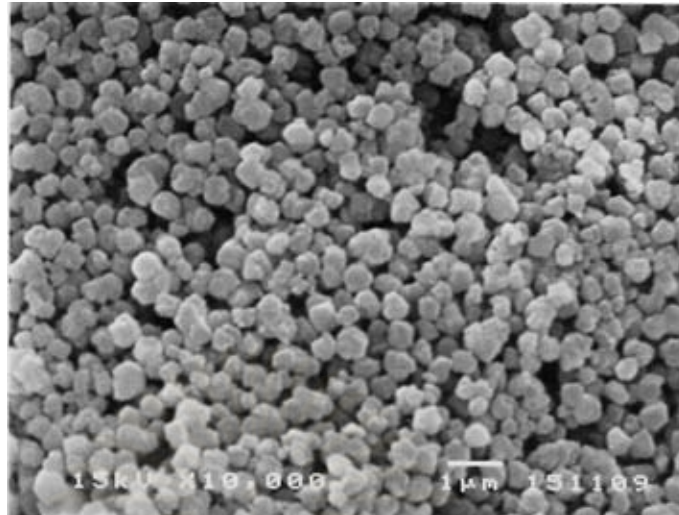


(c)

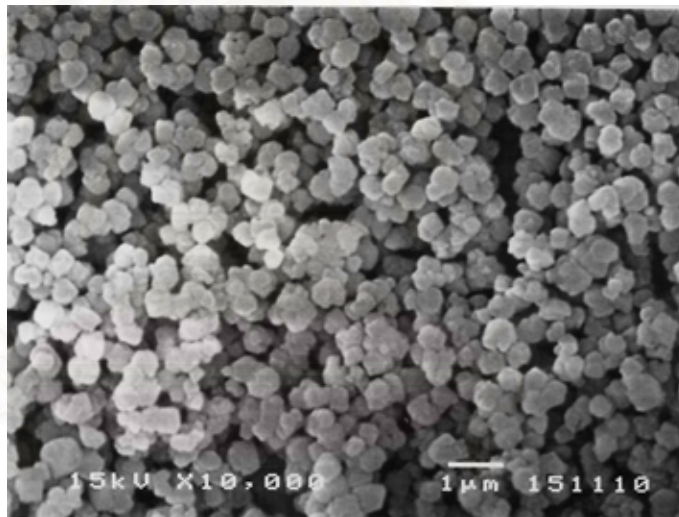


(d)

Figure 5.1 (Cont.) Scanning electron micrographs of zeolite particle size 0.31 μm (c) fresh (d) treated

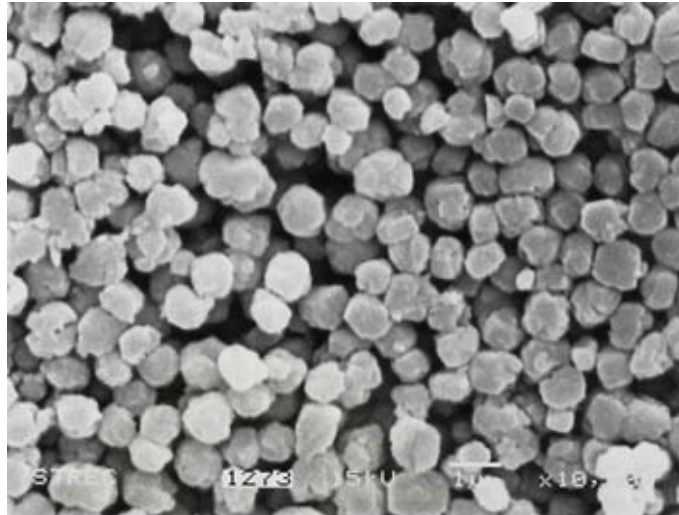


(e)

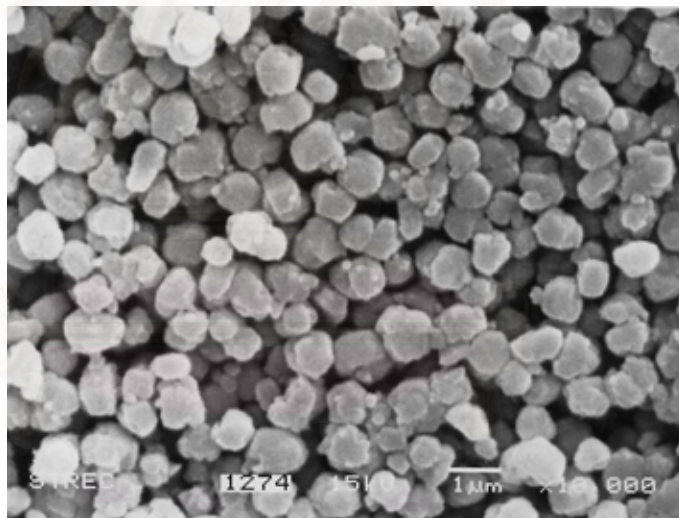


(f)

Figure 5.1 (Cont.) Scanning electron micrographs of zeolite particle size 0.45 μm (e) fresh (f) treated

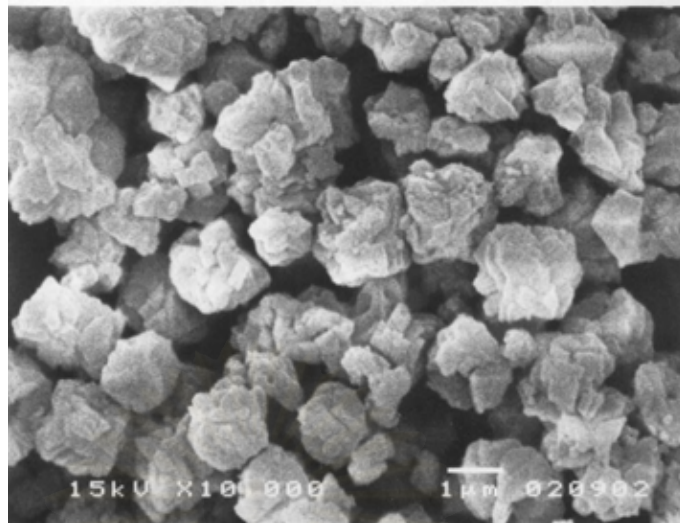


(g)

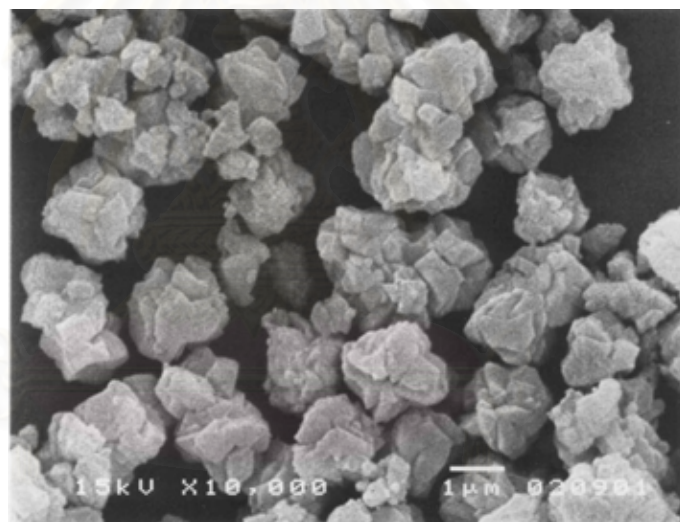


(h)

Figure 5.1 (Cont.) Scanning electron micrographs of zeolite particle size 0.82 μm (g) fresh (h) treated



(i)



(j)

Figure 5.1 (Cont.) Scanning electron micrographs of zeolite particle size 1.81 μm (i) fresh (j) treated

5.1.2 Unit cell size

X-ray diffraction is a technique which can identify the crystal structure. Figure 5.2 shows the comparative XRD patterns of HY zeolite after hydrothermal treatment for each crystallite sizes [46]. The XRD patterns of commercially available Y zeolite “JRC-Z-Y” supplied by Tosoh Corporation were also showed for comparison.

Calculate the unit cell size dimension, a , of zeolite using the equation [49] (see Appendix A-2):

$$a = \{(d_{hkl})^2 (h^2+k^2+l^2)\}^{1/2}$$



สถาบันวิทยบริการ
จุฬาลงกรณ์มหาวิทยาลัย

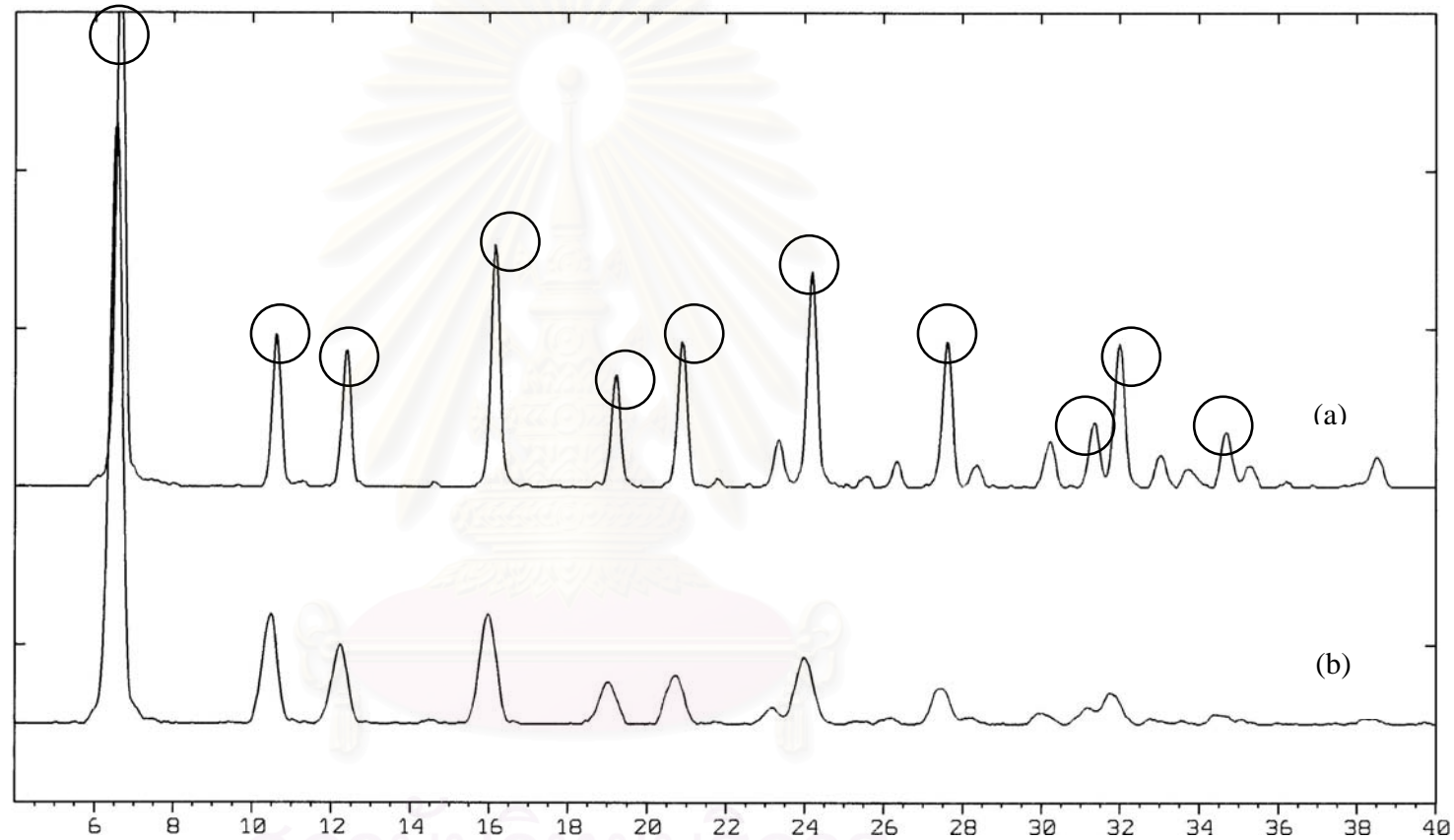


Figure 5.2 XRD spectra of Y zeolite particle size 0.16 μm (a) fresh (b) treated

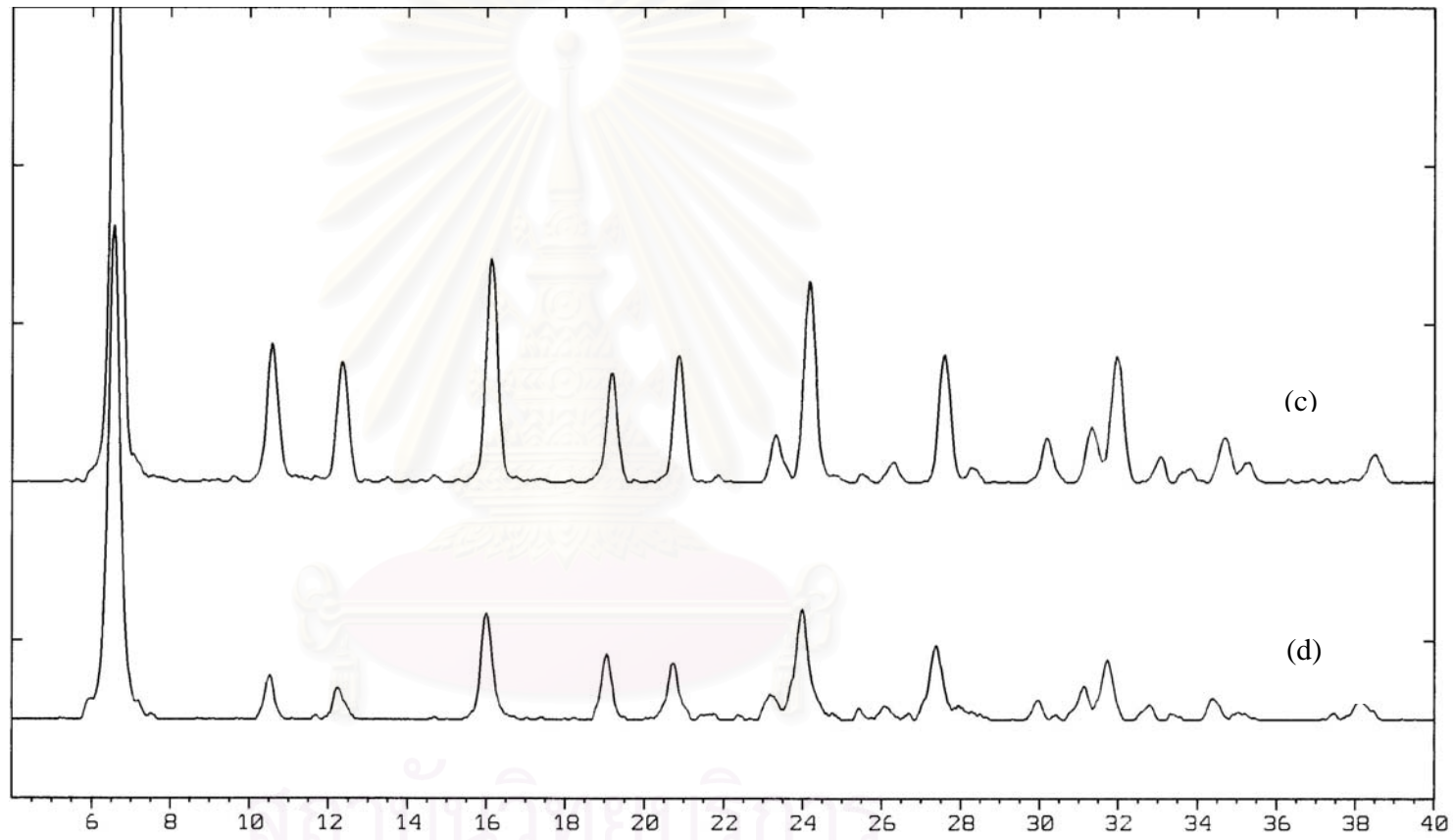


Figure 5.2 (Cont.) XRD spectra of Y zeolite particle size 0.25 μm (c) fresh (d) treated

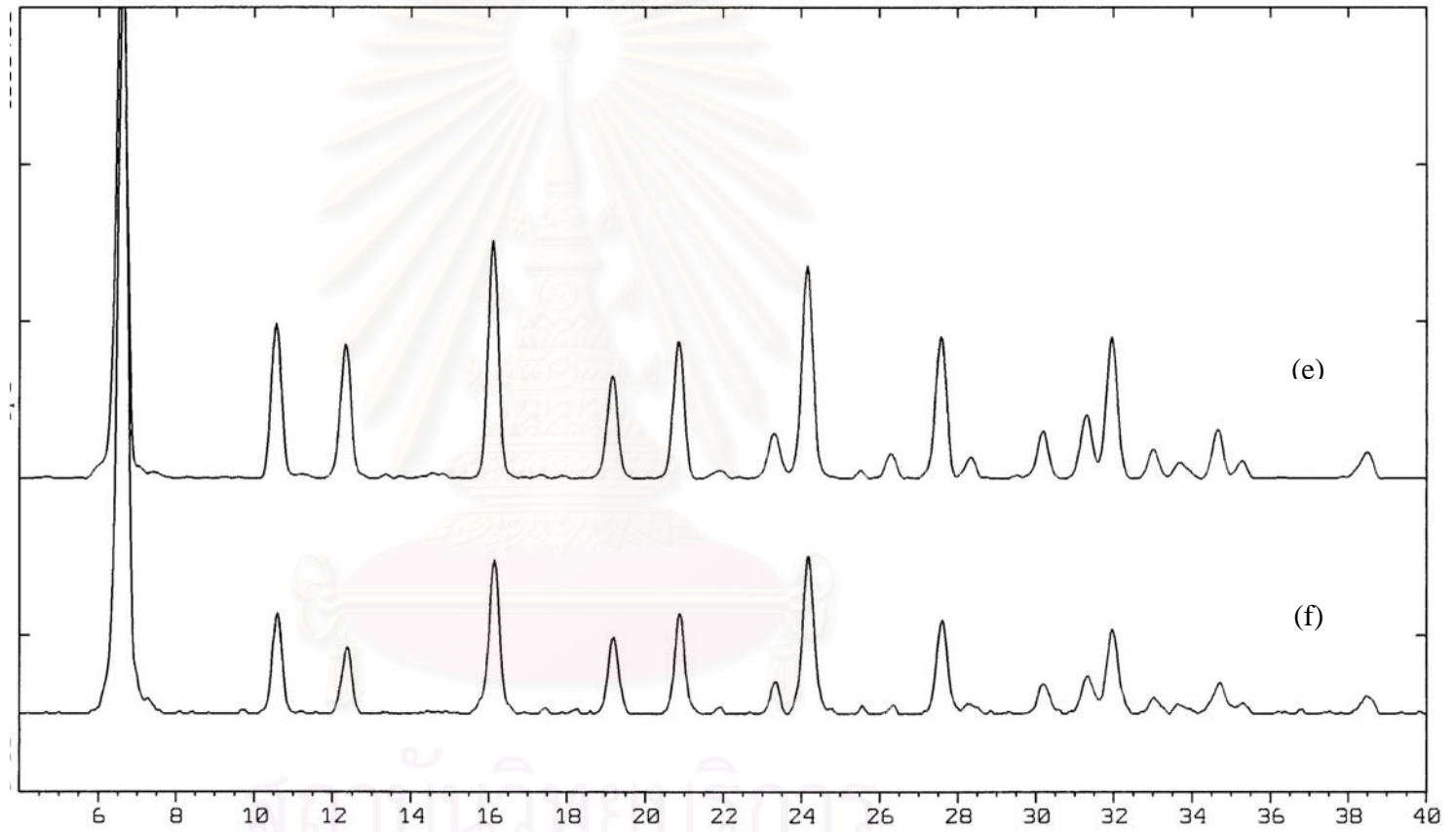


Figure 5.2 (Cont.) XRD spectra of Y zeolite particle size 0.31 μm (e) fresh (f) treated

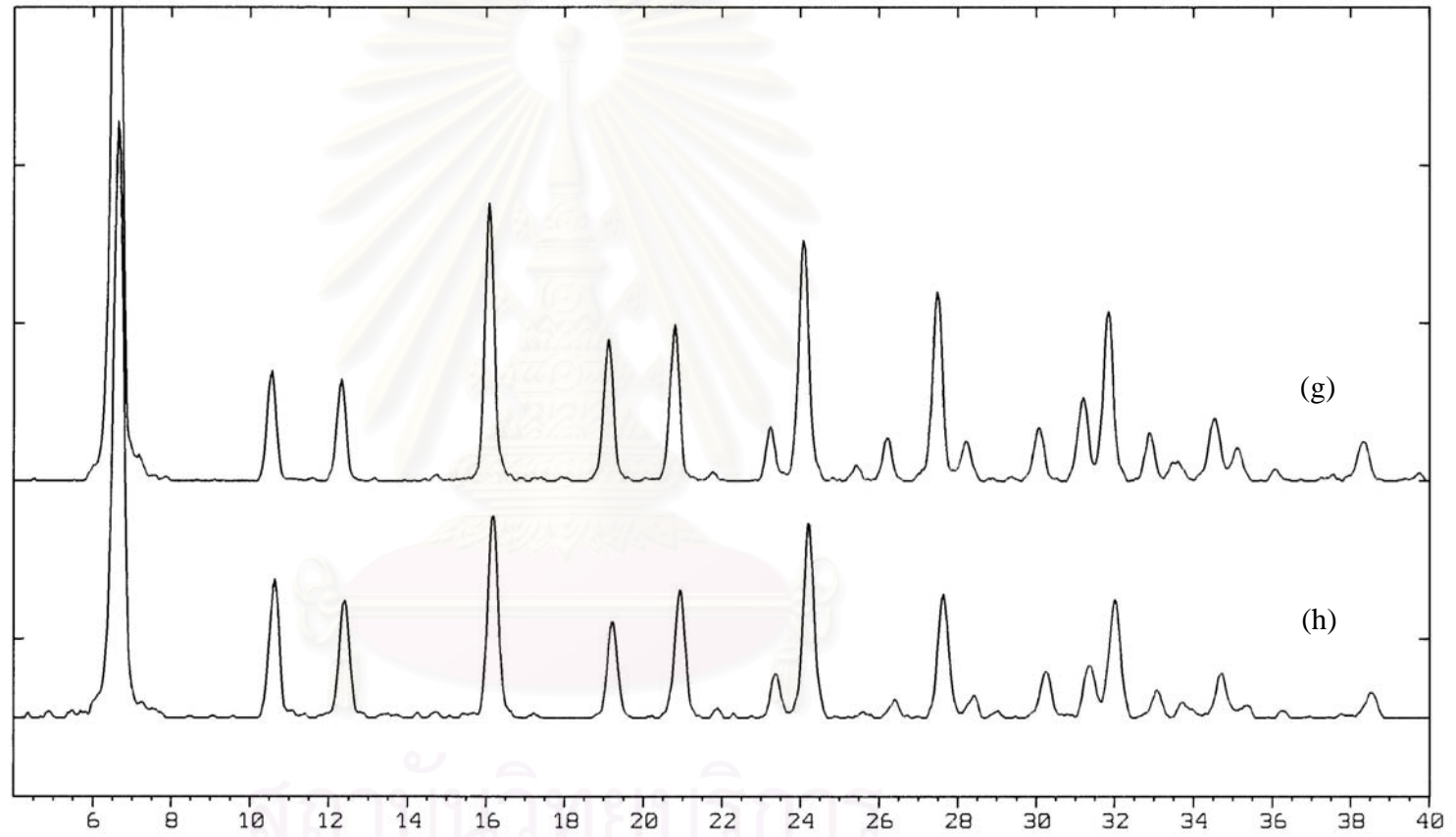


Figure 5.2 (Cont.) XRD spectra of Y zeolite particle size 0.40 μm (g) fresh (h) treated

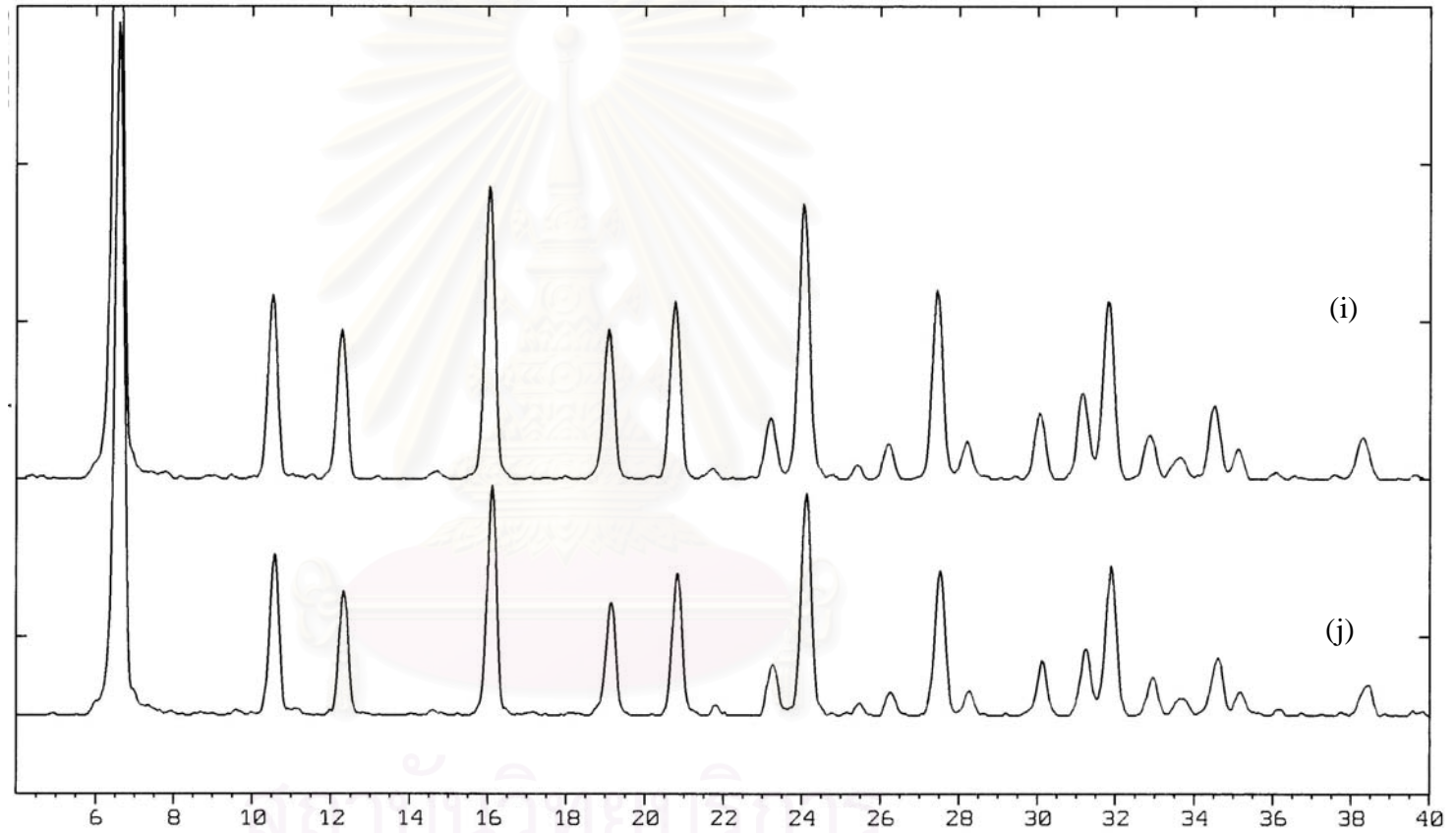


Figure 5.2 (Cont.) XRD spectra of Y zeolite particle size 0.45 μm (i) fresh (j) treated

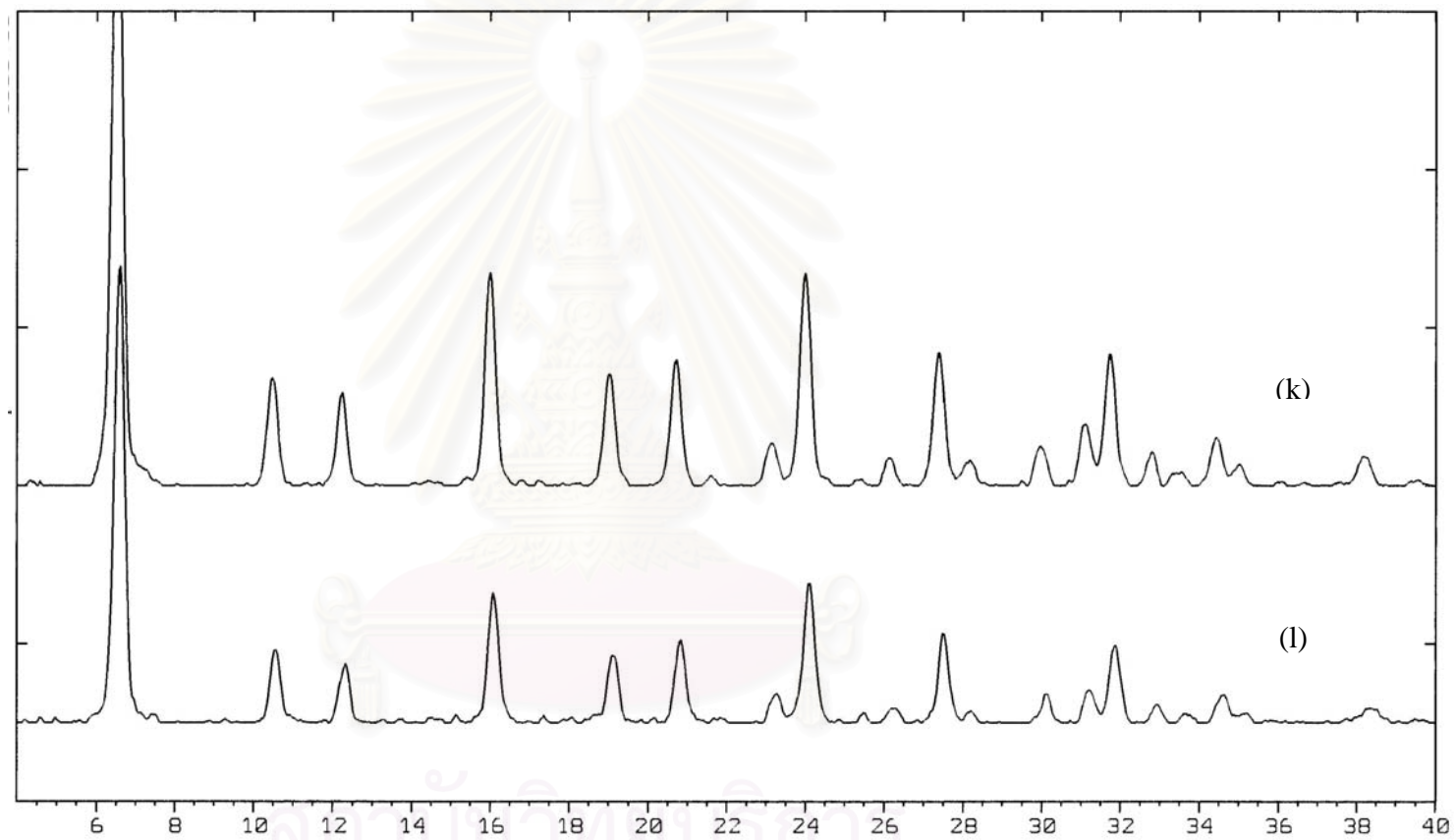


Figure 5.2 (Cont.) XRD spectra of Y zeolite particle size 0.82 μm (k) fresh (l) treated

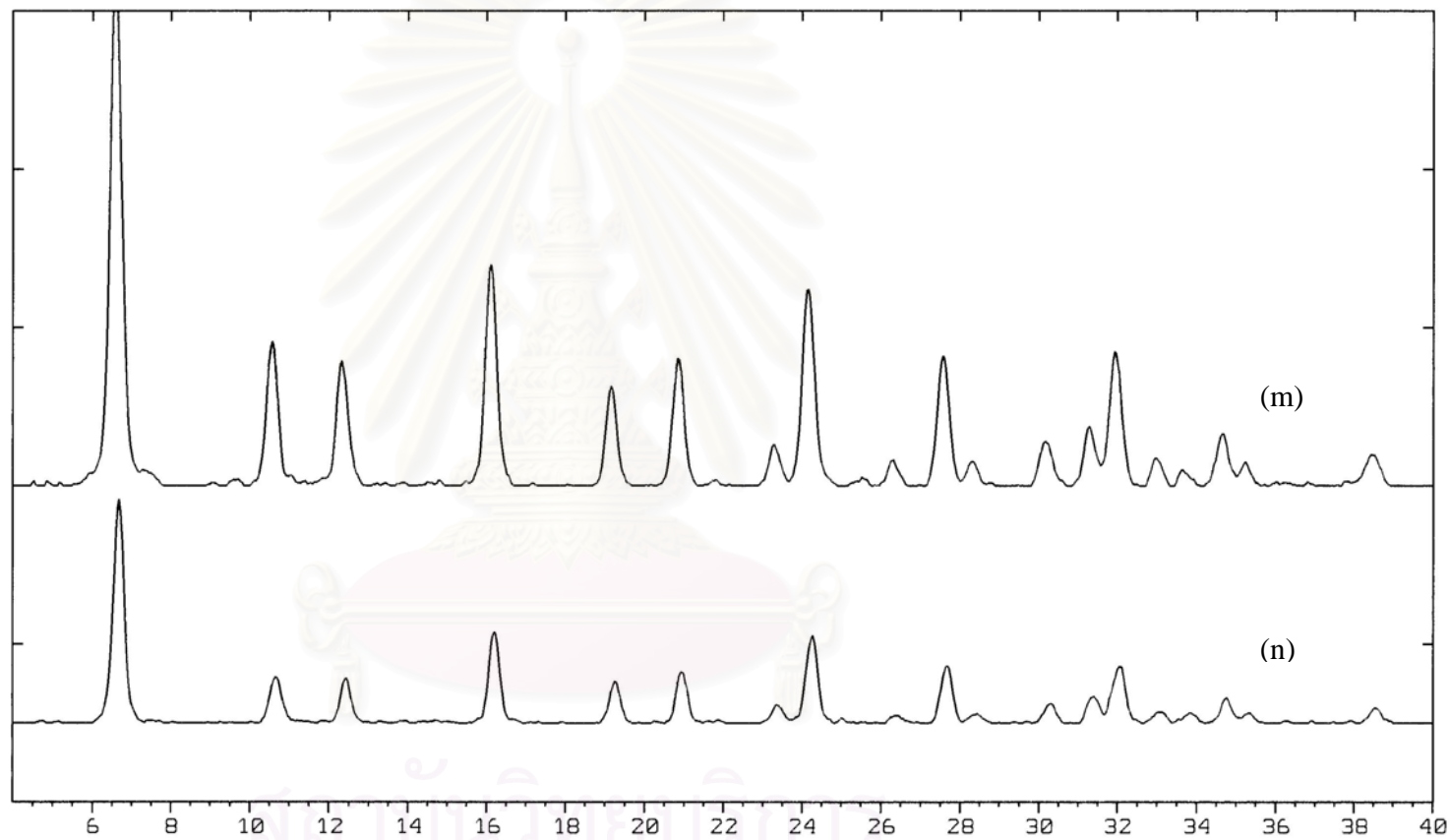


Figure 5.2 (Cont.) XRD spectra of Y zeolite particle size 1.19 μm (m) fresh (n) treated

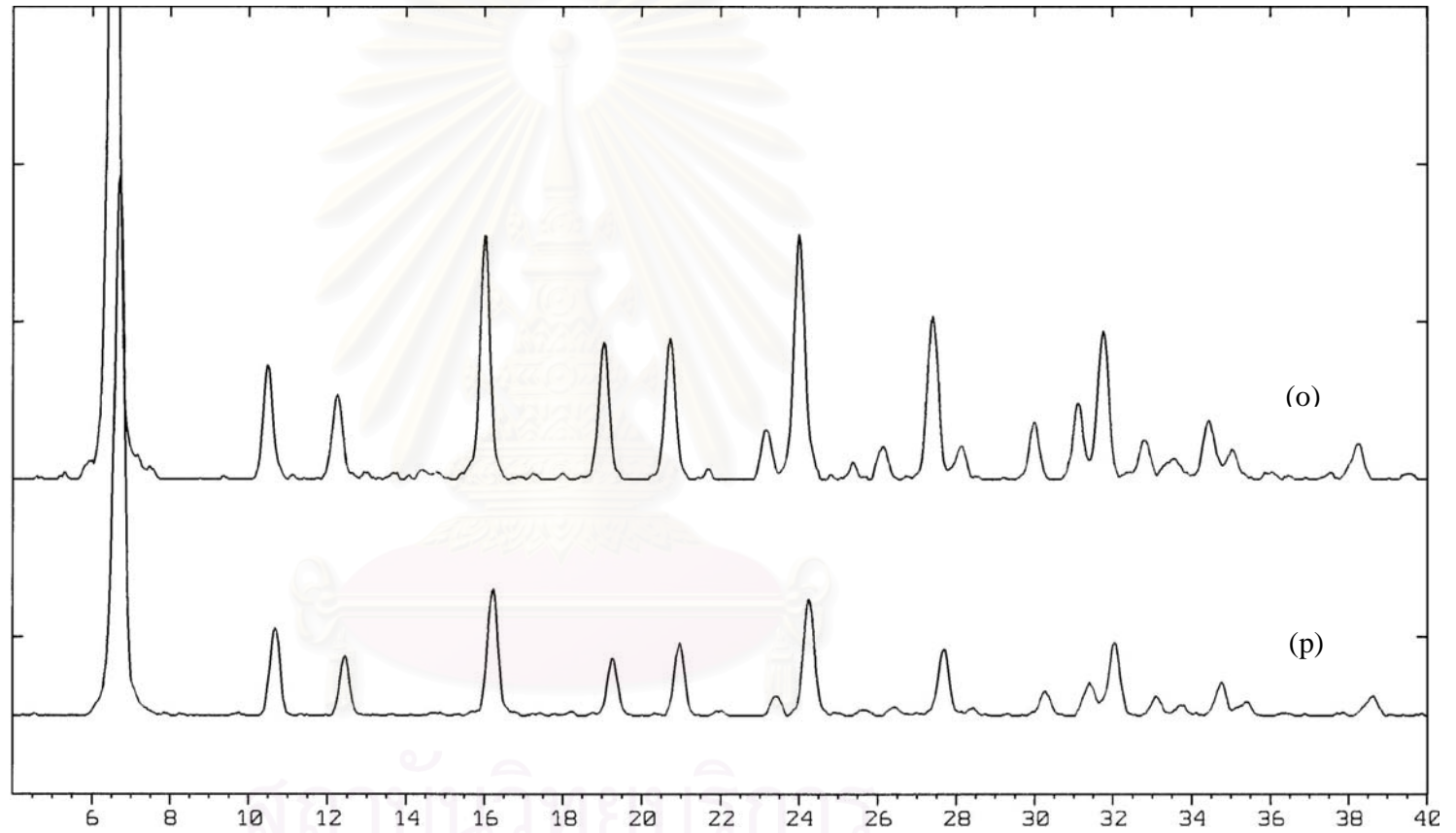


Figure 5.2 (Cont.) XRD spectra of Y zeolite particle size 1.81 μm (o) fresh (p) treated

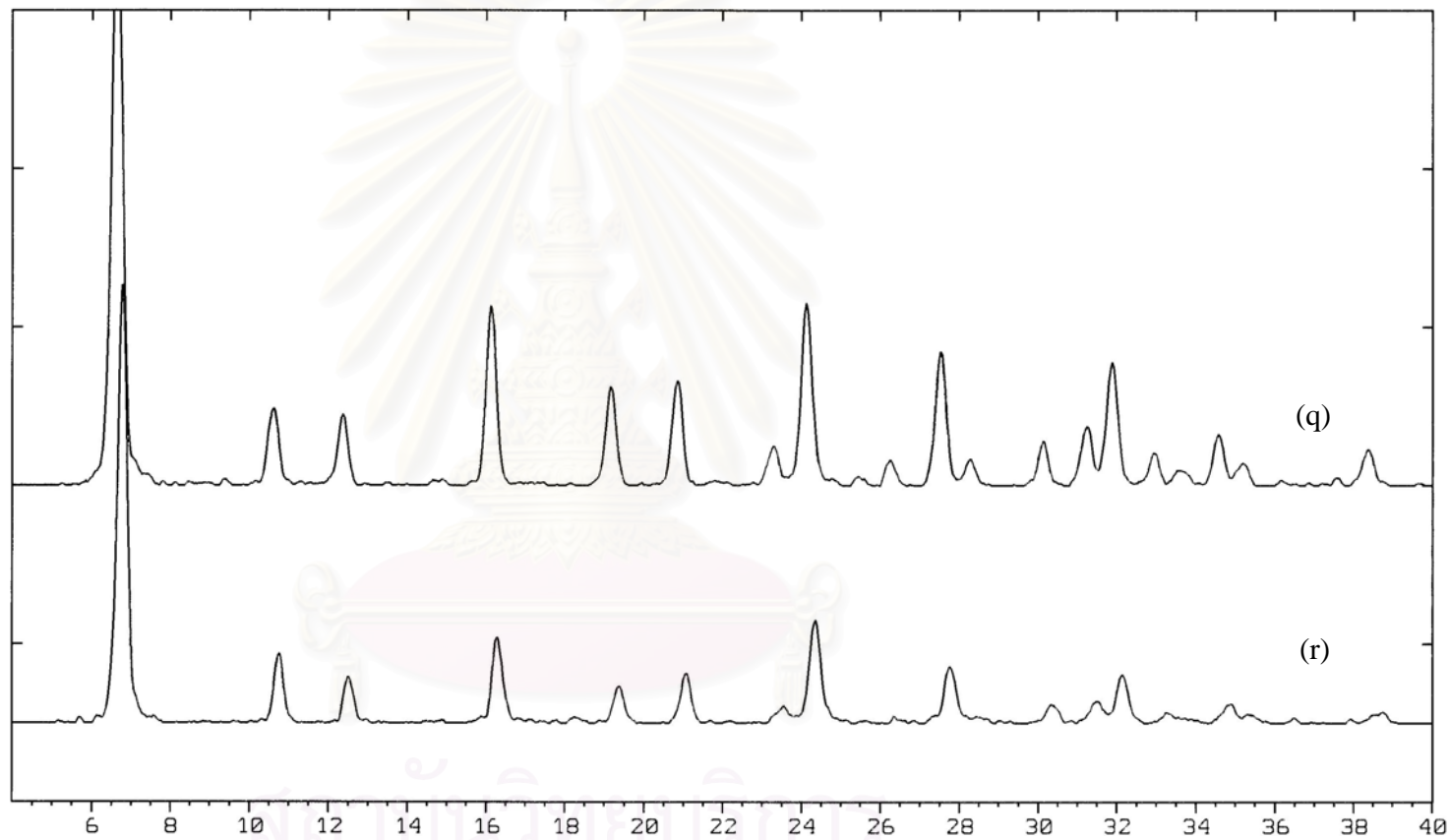


Figure 5.2 (Cont.) XRD spectra of Y zeolite particle size 2.01 μm (q) fresh (r) treated

However, it is known that the unit cell size of Y zeolite was affected during hydrothermal treatment due to aluminum extraction and dehydroxylation [50]. Its property is based on the unit cell size as the structure of the as-synthesized sample was investigated by XRD. Afterwards, effect of particle size between 0.16-2.01 μm on the unit cell size of Y zeolite at different treated parameters is demonstrated in Figure 5.4 show the effect of particle size on the unit cell size of Y zeolite when varying aging parameters is as follows: (a) temperature, (b) aging time, and (c) steam partial pressure, respectively. The relationships between the unit cell size and the particle size of Y zeolite when varying aging parameters follow similar volcano trend. The unit cell size significantly decreased with increasing hydrothermal temperature, steam partial pressure, and aging time, which is typical hydrothermal behavior for zeolite in FCC catalysts [8]. In this study, the lowest unit cell size was observed for the most severe hydrothermal conditions (1273 K, 100% steam partial pressure, and 300 min).

Calcination of an ammonium-exchanged Y zeolite in the presence of steam results in the expulsion of tetrahedral aluminium from the framework into nonframework positions. This process, which consists essentially in a high-temperature hydrolysis of Si-O-Al bonds, leads to the formation of nonframework aluminium species, while increasing the framework silica to alumina ratio and decreasing the zeolite unit cell size (Figure 5.3). In addition to amorphous alumina, amorphous silica-alumina is also formed. The progress of framework dealumination can be observed from the X-ray diffraction scan, since the diffraction peaks are shifted to higher 2θ values (lower d-spacings) with progressive dealumination. It was show that the defect site left by dealumination are filled to a large extent by silica, which leads to a very stable, highly siliceous framework (Figure 5.3) [43].

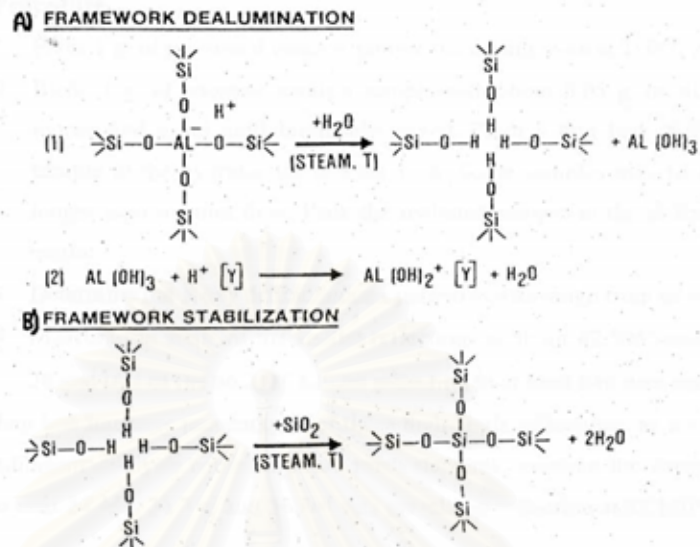
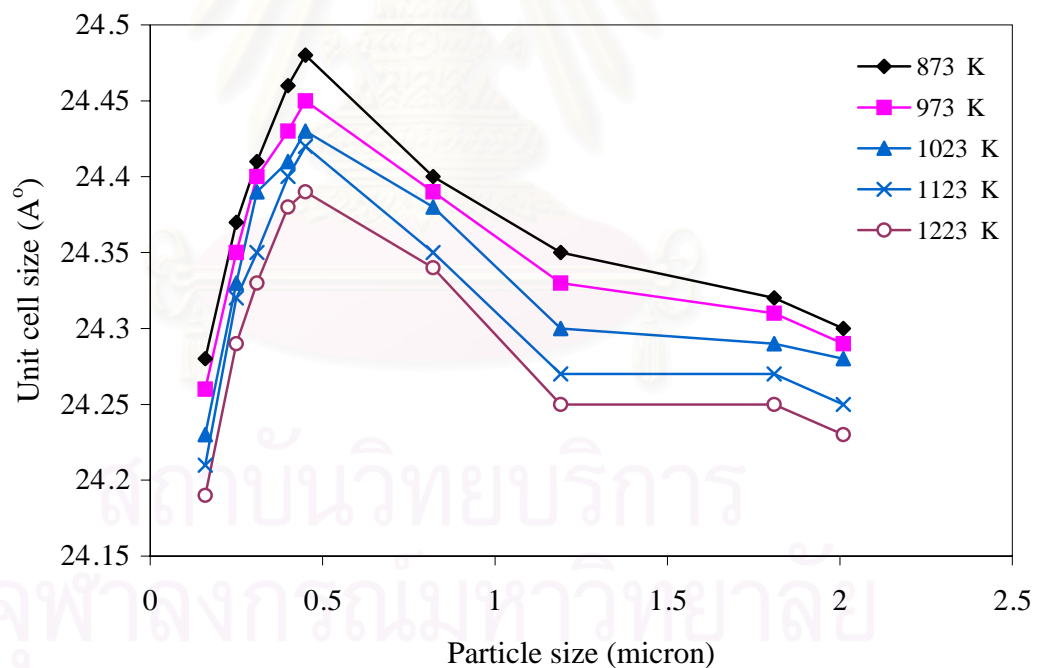


Figure 5.3 Reaction mechanism for hydrothermal dealumination and stabilization of Y zeolite [43].

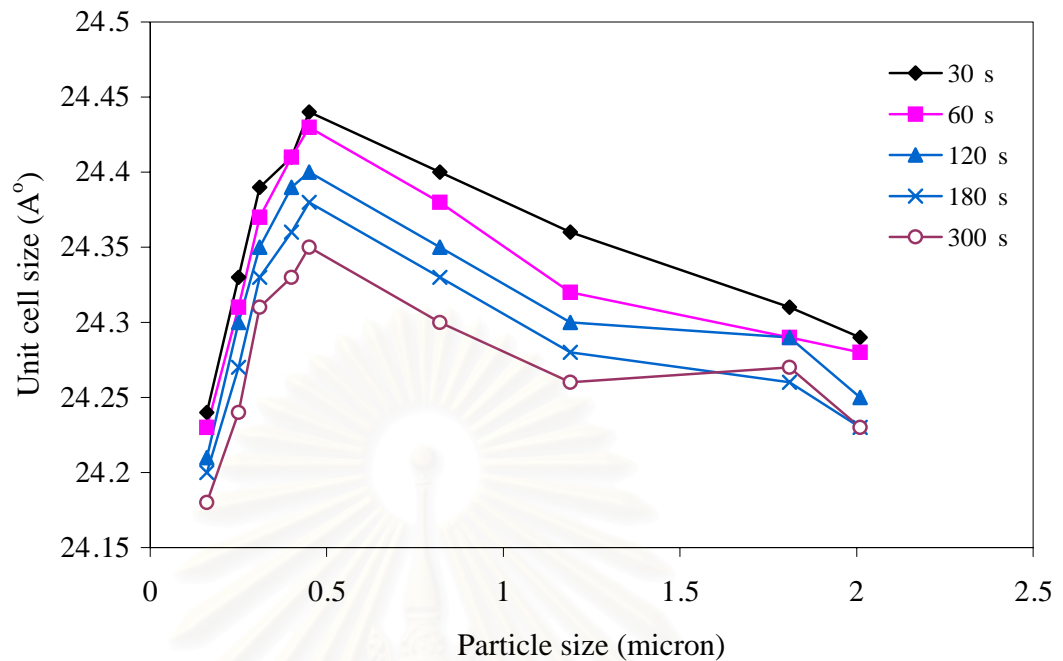
The hydrothermal stability of Y zeolites was also found to be strongly dependent on the particle size of Y zeolites. For the particle sizes ranging from 0.16-0.45 μm , unit cell size increased with increasing particle sizes and the maximum unit cell size was observed for the particle size of 0.45 μm . This trend is in agreement with the literature that smaller crystallite zeolites are more active but less stable than larger ones [48,51]. The increase in unit cell size with increasing particle size in this range is probably due to a structural arrangement in the gel during crystal forming [52]. The unit cell size of Y zeolites, however, gradually decreased when particle sizes were larger than 0.45 μm . The hydrothermal behavior of larger particle Y zeolite is still unclear; however, the decrease in unit cell size is probably due to the large amount of acidic defects in larger particle size Y zeolite. In addition, there may be an influence from the average distance between acidic and metallic sites, [25] or the various pore sizes in large particle shape-selective zeolite.

However, it is known that the unit cell size of USY zeolite is in the range of 24.00–24.50 Å^o [42]. The unit cell size of various particle sizes of Y zeolite were performed by controlled conditions as follows: (a) temperature, (b) aging time, and (c) steam partial pressure, respectively. In the present work, the range of unit cell size of Y zeolite was 24.00–24.50 Å^o. Therefore, all treated Y zeolites were USY zeolites. Following the definition of USY zeolite, it was found that the degree of USY zeolite was low when the unit cell size was high. Vice versa, the degree of USY zeolite was high when the unit cell size was low [42]. In this study, the degree of USY zeolite significantly increased with increasing hydrothermal temperature, steam partial pressure, and aging time. The various particle sizes of Y zeolites were varied across all aging parameters. The particle size ranging from 0.16–0.45 µm, the degree of USY zeolite decreased with increasing particle size and the minimum was observed for the particle size of 0.45 µm. The degree of USY zeolite increased with increasing particle size when the particle size was larger than 0.45 µm.

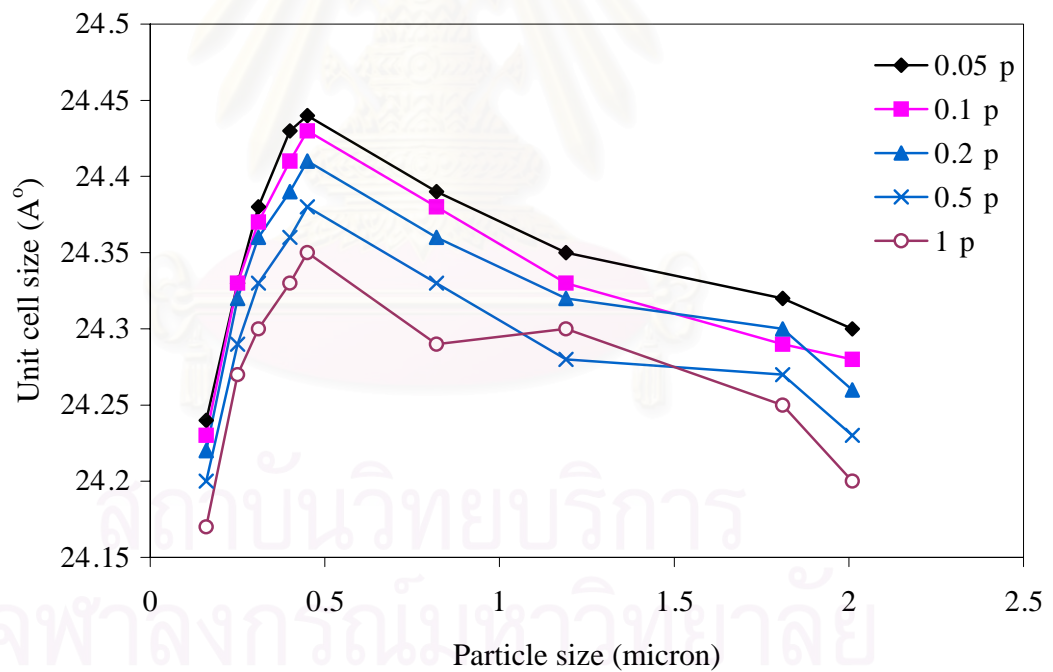


5.4 a

Figure 5.4 Relationship between unit cell size and particle size of Y zeolite after hydrothermal treatment at different treated parameters (a) 873–1223 K, 10 % mol steam and 60 s [46]



5.4 b



5.4 c

Figure 5.4 Relationship between unit cell size and particle size of Y zeolite after hydrothermal treatment at different treated parameters (a) 873-1223 K, 10 %mol steam and 60 s (b) 30-300 s, 10 %mol steam and 1023K (c) 0.05-1 P/P₀, 60 s and 1023 K [46]

5.1.3 Surface area

The single point BET surface area of Y zeolite, both fresh and treated with 10 mol % of water vapor, is shown in Table 5.1. It is clear that the BET surface area for all Y zeolite decrease due to hydrothermal treatment corresponding to literature [53]. However, compared with a smaller and larger particle size, the BET surface area of a medium particle size decreases. This suggests that the structure of Y zeolite for small and large particle size may be easily changed. This is possible due to collapses at surface of zeolite framework [54]. These expectations are confirmed by the comparison of XRD patterns of these samples. The less BET surface area of small and large particle samples correspond to the lower unit cell size.

Table 5.1 The single point BET surface area and the percent relative BET surface area of Y zeolite, fresh and treated samples [46]

Particle size (μm)	BET surface area (m^2/g)		
	fresh catalyst	treated catalyst (1023 K)	Relative BET surface area (%)
0.16	521	322	38
0.25	546	366	33
0.31	498	411	18
0.40	502	432	14
0.45	511	441	14
0.82	531	397	25
1.19	506	384	24
1.81	543	340	37
2.01	550	339	38

5.1.4 Characterization of Acidic Sites

NH_3 temperature programmed desorption (TPD) technique provides information on the amount and the strength of acidic sites. The peak area of a TPD profile represents the amount of desorbed NH_3 while the peak position corresponds to the strength of acidity. The NH_3 TPD profiles of Y zeolites with various hydrothermal temperature (0.45 micron) are shown in Figure 5.5. All catalyst samples exhibited similar TPD profiles. The first desorption peak at ca. 473 K is assigned to the sites of weak acid where the second peak at ca. 653 K correspond to strong acid sites [55]. The amount of weak acid sites was determined to be much higher than that of strong acid ones. Interestingly, higher strength of acid sites were detected on lower hydrothermal temperature of Y zeolite. In last study, unit cell size of Y zeolite significantly decreased with increasing hydrothermal temperature. In this study, unit cell size of Y zeolite significantly decreased with decreasing strength of acidic sites.

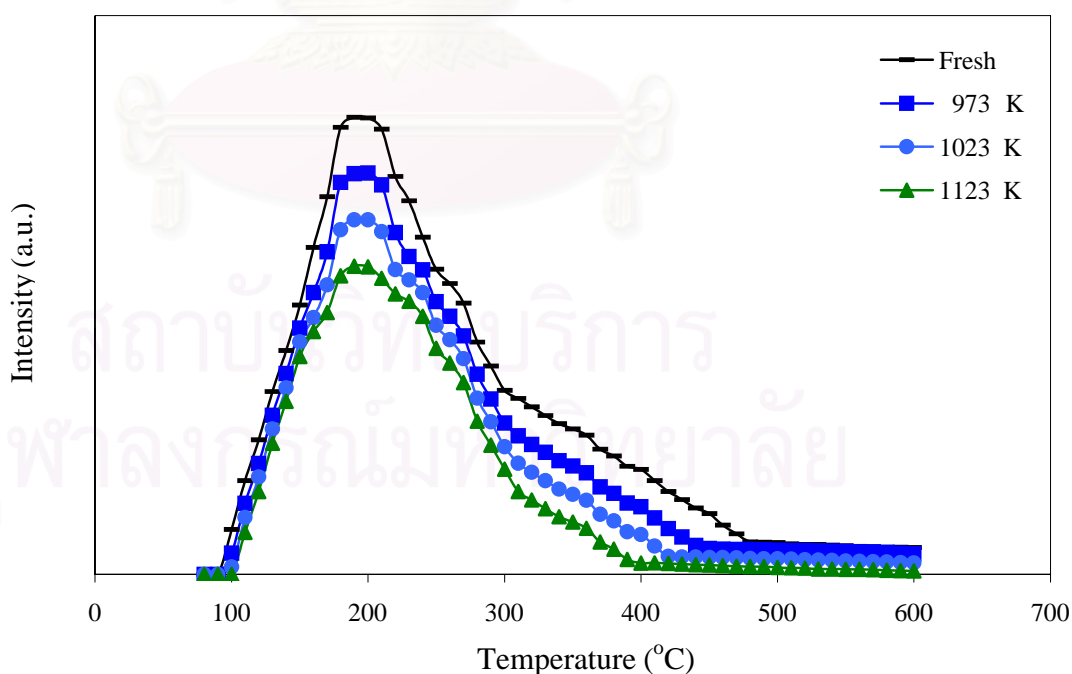


Figure 5.5 NH_3 TPD of Y zeolite at various hydrothermal temperature (0.45 micron).

5.2 Catalytic reaction

In this section, the effect of particle size and hydrothermal treatment of Y zeolite in the catalytic cracking of n-octane was investigated. The catalytic cracking of n-octane was obtained at $6,400 \text{ h}^{-1}$ on stream. The reaction temperatures were varied ranging from 573 to 773 K. The catalytic performance of n-octane cracking on different size of Y zeolite, five sizes of catalysts were used in this study, i.e. 0.16, 0.31, 0.45, 1.19 and $2.01 \mu\text{m}$. These catalysts were treated at different parameters, i.e. 973, 1023 and 1123 K. Conversion of n-octane and selectivity of olefin were shown at 673 K (reaction temperature). Ethylene and propylene are interested product of olefins in this work.

5.2.1 Effect of particle size and hydrothermal treatment on the conversion of n-octane.

The conversion ratio ($\text{conversion treat} \times 100/\text{conversion fresh}$) of n-octane significantly decreased with increasing hydrothermal temperature (Figure 5.6). It was found that the treating of Y zeolites in high temperature, the unit cell size was lower than low temperature because at lower unit cell size, the activity of zeolite is very low due to the low concentrations of active sites[43]. In addition. The treating of Y zeolites in high temperature, the surface area was lower than low temperature. And the treating of Y zeolites in high temperature, the concentration of acid sites were lower than low temperature. The lower acidity made them catalytically less active.

The particle size of Y zeolites, it was ranging from 0.16-0.45 μm . The conversion ratio increased with increasing particle size and the maximum was observed at the particle size of 0.45 μm . The unit cell size significantly increased with increasing particle size and the maximum was observed at the particle size of 0.45 μm . Therefore. Lower unit cell size, the activity of zeolite was very low due to the low concentration of active sites. In addition. the large particle size, the concentration of acid sites were lower than the small particle size. The lower acidity made them catalytically less active.

For the particle size of Y zeolites were larger than 0.45 μm , the conversion ratio decreased with increasing particle size. The unit cell size significantly decreased with increasing particle size. For higher unit cell size, the activity of zeolite was very high due

to the high concentration of active sites. In addition. The large particle size, the concentration of active sites were higher than the small particle size. The higher acidity made them catalytically high active.

Table 5.2 Conversion ratio of n-octane on various Y zeolites. (reaction temperature at 673 K)

Particle size (μm)	Conversion (%)			
	Fresh catalyst	973 K	1023 K	1123 K
		Treated catalyst	Treated catalyst	Treated catalyst
0.16	96.35	79.35	70.01	59.23
0.31	84.06	76.06	65.35	56.03
0.45	79.78	72.78	64.35	54.81
1.19	79.08	69.08	62.05	48.04
2.01	81.98	69.98	61.25	46.88

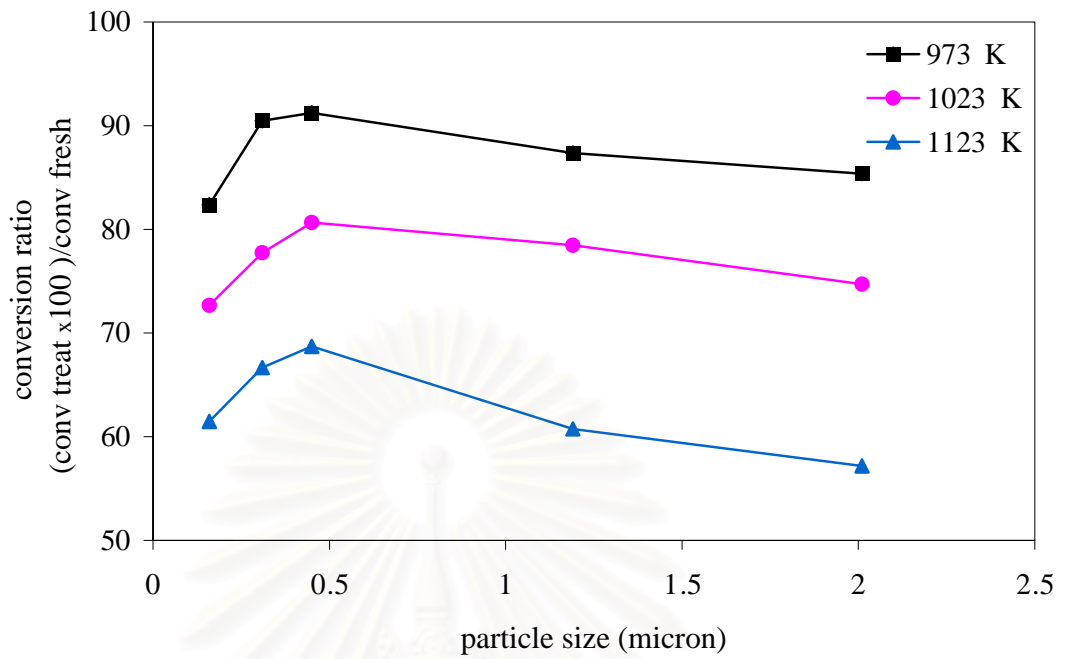


Figure 5.6 Conversion ratio of n-octane on various Y zeolites. (reaction temperature at 673 K)

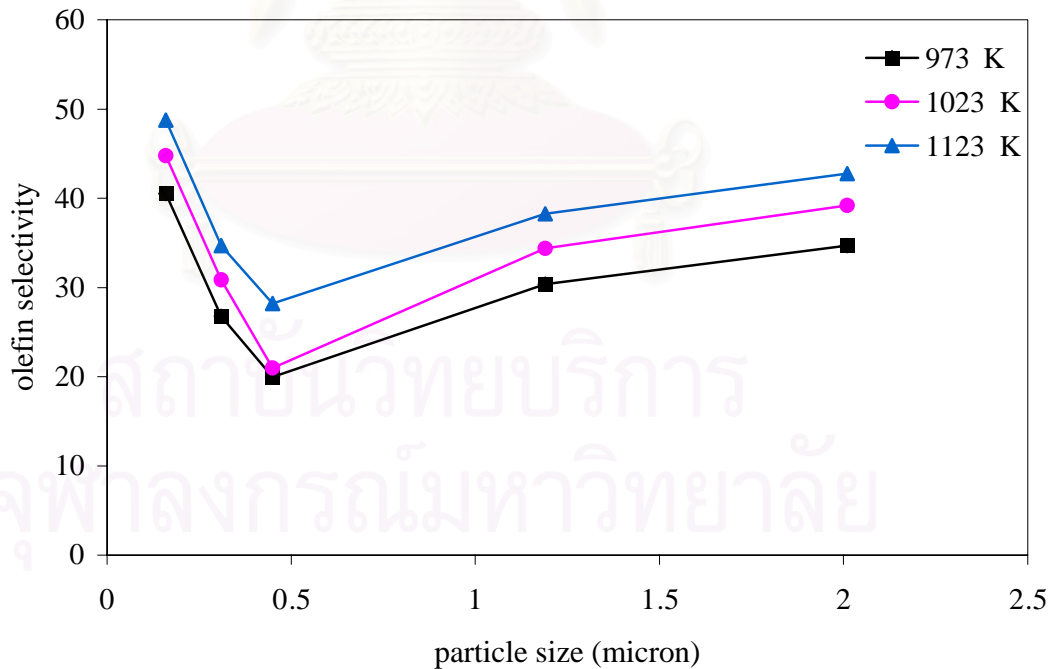


Figure 5.7 Olefin selectivity on various Y zeolites. (reaction temperature at 673 K)

5.2.2 Effect of particle size and hydrothermal treatment on the selectivity of olefins.

The selectivity of olefins increased with increasing hydrothermal temperature (Figure 5.7). The treating of Y zeolites in high temperature, the unit cell size was lower than low temperature. It was revealed that the treated Y zeolites in high temperature were higher degree of USY zeolite than low temperature. Pine et al. [43] was shown that decreasing of unit cell size results in decreasing of acid site density and in the rate of hydrogen transfer reaction, it raised the amount of olefins. For higher unit cell size, hydrogen transfer reaction would be favored, it reduced the amount of olefins.

Hydrogen transfer plays an important role in the gas oil cracking process. It reduces the amount of olefins in the product through bimolecular hydrogen transfer, whereby reactive olefins and naphthenes are converted to more stable paraffins and aromatics. Further hydrogen transfer from aromatics, coupled with condensation and polymerization, can lead to the formation of coke [42].

For the particle size of Y zeolites, it was ranging from 0.16-0.45 μm . The selectivity of olefins decreased with increasing particle size and minimum was observed for the particle size of 0.45 μm . The degree of USY zeolite significantly decreased with increasing particle size and the minimum was observed for the particle size of 0.45 μm . Therefore low degree of USY zeolite, the low amount of olefins were in the product.

For the particle size of Y zeolites were larger than 0.45 μm . The selectivity of olefins increased with increasing particle size. The degree of USY zeolite significantly increased with increasing particle size. Therefore high degree of USY zeolite, the high amount of olefins were in the product.

CHAPTER VI

CONCLUSION AND RECOMMENDATION

The present work was described the effect of particle size and hydrothermal treatment of Y zeolite in the catalytic cracking of n-octane. The conclusions of this research can be summarized as follows:

1. For increasing hydrothermal temperature, the degree of USY zeolite and the amount of olefins in the product increased but the ratio of the catalytic activity (conversion treated \times 100/conversion fresh) decreased.

2. For the particle size of treated Y zeolites was ranging from 0.16-0.45 μm . When the particle size increased, the degree of USY zeolite and the amount of olefins in the product decreased but the ratio of the catalytic activity increased.

3. For the particle size of treated Y zeolites was larger than 0.45 μm . When the particle size increased, the degree of USY zeolite and the amount of olefins in the product increased but the ratio of the catalytic activity decreased.

From this research, the recommendations for further study are as follows:

1. To study the catalytic performance of USY catalyst loaded with rare earth metal.
2. To study the coke characteristic formed on USY catalyst.
3. To study effect and behavior of particle size on the hydrothermal stability at high Si/Al ratio.
4. To study the effect of particle size and hydrothermal treatment of Y zeolite in the catalytic cracking of hydrocarbon and product distribution of paraffin, olefin, aromatic.

REFERENCES

1. Bonetto, L. Clambor, M.A. Corma, A. and Perez-Pariente, J. *Appl. Catal. A.* 1992, 82, 37.
2. Gianetto, A., Farag, H.I., Alberto, P.B., and de Lasa, H.I. *Ind. Eng. Chem. Res.* 1994, 33, 3053.
3. Al-Khattaf, S., and de Lasa, H. *Appl. Catal. A.* 2002, 226, 139.
4. Tatlier, M., and Erdem-Senatalar, A. *Microporous Mesoporous Mater.* 2000, 34, 23.
5. Bonetto, L. Clambor, M.A. Corma, A. and Perez-Pariente, J. *Appl. Catal. A.* 1992, 82, 37.
6. McDaniel, C.V.; Laurel and Maher. *Zeolite Chemistry and Catalysis.* 1974, 314
7. Breck, D.W., et al., *U.S. Patent, No.4,503,023, March 5.* 1985.
8. Halász, I., Horváth, J., Mándy, T., Schmidt, L., and Tasnádi, E. *Zeolites.* 1985, 393.
9. Campbell, S.M., Bibby, D.M., Coddington, J.M., Howe, R.F., and Meinhold, R.H. *J. Catal.* 1996, 161, 383.
10. Niu, G., Huang, Y., Chen, X., He, J., Liu, Y., and He, A. *Appl. Catal. B.* 1999, 21, 63.
11. Kerr, G.T. *J. Phy.Chem.* 1968, 72, 2594.
12. Gallezot, P., Beaumont, R., and Barthomeuf, D. *J. Phy. Chem.* 1974, 78, 1550.
13. Sulikowski, B., Borbely, G., and Beyer, K. *J. Phy. Chem.* 1989, 93, 3240.
14. Barthoment, D. *Zeolites Science and Techonology* (Rebeira, F.H. et al.), Martinus Nijhoff Publishers, The Hange, 1984.
15. Satterfield, C.N. *Heterogeneous Ctalysis in Industrial Practice*, 2nd ed., New York: McGraw-Hill, 1991, 259, 226.
16. Tanake, K., Misona, M., Ona, Y., and Hattori, H. *Stud. Surf. Sci. Catal.* Tokyo: Elsevier. 1989, 51.
17. Sano. T., Fujisawa, K., and Higiwara, H, *Stud. Surf. Sci. Catal.* Amsterdam: Elsevier.1987, 34.
18. Cvetanovic, R.J., and Amenomiya, Y. *Adv. Catal.* 1967, 17, 103.
19. Venuto, P.B., and Habib, E.T. *Fluid Catalytic Cracking with Zeolite Catalysts*, Marcel Dekker, New York, 1979.

20. Karger, J., and Ruthven, D.M. *Diffusion in Zeolites and other Microporous Solids*, Wiley, New York, 1992.
21. Humphries, A., and Wilcox, J. *Oil & Gas J.* 1989, 6, 45.
22. Tsikoyiannis J., and Wei, J. *Chem. Eng. Sci.* 1991, 46(1), 233.
23. Biswas, J., and Maxwell, I.E. *Appl. Catal.* 1990, 63, 197.
24. Wellenstein, D., and Alkemade, U. *Appl. Catal. A.* 1996, 137, 37.
25. di Renzo, F. *Catal. Today.* 1998, 41, 37.
26. Jansen, J.C., and Coker, E.N. *Curr. Opin. Solid State Mater. Sci.* 1996, 1, 65.
27. Smirniotis, P.G. and Ruckenstein, E. *Ind. Eng. Chem. Res.* 1994, 33(4), 813.
28. Gomes, A.C.L., et al. *Appl. Catal. A.* 1997, 148, 373.
29. Liu, D.S.; Bao, S.L. and Xu, Q.H. *Zeolites.* 1997, 18, 162.
30. Pawelec, B., and Fiero, J.L.G., *Zeolites.* 1997, 18, 250.
31. Kuehne, M.A., et al. *Appl. Catal. A.* 1998, 166, 293.
32. Niu, G. et al. *Appl. Catal. B.* 1999, 21, 63.
33. Kung, H.H., et al. *Catalysis Today.* 1999, 52, 92.
34. Williams, B.A. et al. *Appl. Catal. A.* 1999, 177, 161.
35. Vaughan, D.E.W., et al., *U.S. Patent, No. 6,054,113, April 25, 2000.*
36. Abbot, J., and Guerzoni, F.N. *Appl. Catal.* 1992, 85, 173.
37. Ino, T. *Appl. Catal.* 1996, 142, 5.
38. Cambor, M.A., Corma, A., Martinez, A., and Mocholi, F.A. *Appl. Catal.* 1989, 55, 65.
39. Corma, A. *Appl. Catal.* 1989, 47, 125.
40. Tomlinson, A.A.G. *Modern Zeolites.* Trans Tech Publication Ltd, 1998.
41. Wilson, J.W. *Fluid Catalytic Cracking Technology and Operations.* Penn well Publishing Company, Oklahoma, 1997.
42. Sadeghbeigi, R. *Fluid Catalytic Cracking Handbook.* Gulf Publishing Company, 2000.
43. Scherzer, J. *Octane-Enhancing Zeolitic FCC.* New York and Basel : Marcel Dekker. INC., 1990.
44. Dryer, A. *An Introduction to Zeolite Molecular Sieves.* John Wiley & Sons, 1988.
45. Catlow, C.R.A. *Modelling of Structure and Reactivity in Zeolite.* Academic Press Limited, 1992.

46. Sombatchaisak, S. *Correlation between Particle Size and Hydrothermal Stability of Y Zeolite*, A Thesis Submitted in Partial Fulfillment of The Requirements for the Degree of Master of Engineering, Department of Chemical Engineering, Chulalongkorn University, 2003.
47. Jiratthitikan, P. *Catalytic Cracking of n-Octane Over Y Type Zeolite Catalyst*, A Thesis Submitted in Partial Fulfillment of The Requirements for the Degree of Master of Engineering, Department of Chemical Engineering, Chulalongkorn University, 1997.
48. Jacobs, P.A. *Catalysis by zeolites*. Elsevier Science Publishers B.V., 1980.
49. ASTM D-3942-97, Standard Test Method for Determination of the Unit Cell Dimension of Faujasite-Type Zeolite.
50. Kubelkova, L., Beran, S., Malecka, A., and Mastikhin, V.M. *Zeolites*. 1989, 12.
51. Aguiar, E.F.S., Murta Valle, M.L., Silva, M.P., and Débora, F.S. *Zeolites*. 1995, 15, 620.
52. Köroğlu, H.J., Sarioğlu, A., Tather, M., Şenatalar, A.E., and Savaşç, Ö.T. *J. Crystal Growth*. 2002, 241, 481.
53. Ocelli L., Aurox A., baldirghi F., and Leoncini S. *The use of Microcalorimetry and Porosimetry to Investigate the effects of aging on the Acidity of Fluid Cracking Catalysts (FCC)* Fluid Cracking Catalysts Occeeli. and Connor, P., ed. Marcel Dekker: New York, 1997, 203.
54. Gutierrez, L.; Boix, A.; Petunchi, J. *J. Catal.* 1998, 179, 179.
55. Karge, H.G., Dondur, V., and Weitkamp, J. *J. Phys.Chem.* 1991, 95, 283.



APPENDICES

สถาบันวิทยบริการ
จุฬาลงกรณ์มหาวิทยาลัย

APPENDIX A

SAMPLE OF CALCULATIONS

A-1 Calculation of vapor pressure of water

Set the partial vapor pressure of water to the requirement by adjusting the temperature of saturator according to the antoine equation

$$\log P = A - \frac{B}{(T + C)}$$

When P = vapor pressure of water, mbar

T = temperature, °C

A, B and C is constants

Range of temperature that applied ability –20 –126 °C

The values of constants.

Reactant	A	B	C
Water	8.19625	1730.630	233.426

A-2 Calculation of unit cell size

Calculation

1. Correct the measured reflection angles for the zeolite by adding the correction factor to each the quantity.
2. Convert the corrected angles of reflection to d-spacing values using the Equation :

$$d_{hkl} = \lambda / (2 \sin \theta)$$

Where :

d_{hkl} = distance between reflecting planes having the Miller indices hkl (nm x 10) , and

λ = wave length of X-ray radiation which is 1.54060 Å for CuK α . Note that the angle used in this calculation is only θ

3. Calculated the unit cell dimension, of the zeolite in catalyst

using the equation

$$a = \{ (d_{hkl})^2 (h^2 + k^2 + l^2) \}^{1/2}$$

4. Average the valued of a calculated from more than one reflection.



สถาบันวิทยบริการ
จุฬาลงกรณ์มหาวิทยาลัย

An Example of Unit Cell Size Determination

Calculation

2θ	θ	d_{hkl}	$h^2+k^2+l^2$	a
6.36	3.18	13.88604	3	24.05133
10.28	5.14	8.598092	8	24.31908
12.04	6.02	7.344892	11	24.36025
15.92	7.96	5.562467	19	24.24623
18.88	9.44	4.696531	27	24.40389
20.56	10.28	4.316403	32	24.41726
23.96	11.98	3.711033	43	24.33487
27.28	13.64	3.266466	56	24.44399
30.96	15.48	2.886078	72	24.48919
31.68	15.84	2.822109	75	24.44018
34.4	17.2	2.604934	88	24.43645

average 24.35843

A-3 Calculation of the specific surface area

From Brunauer-Emmett-Teller (BET) equation

$$\frac{p}{n(1-p)} = \frac{1}{n_m C} + \frac{(C-1)p}{n_m C} \quad (\text{A-3-1})$$

Where, p = Relative partial pressure of adsorbed gas, P/P_0

P_0 = Saturated vapor pressure of adsorbed gas in the condensed state at the experimental temperature, atm

P = Equilibrium vapor pressure of adsorbed gas, atm

n = Gas adsorbed at pressure P , ml. At the NTP/g of sample

n_m = Gas adsorbed at monolayer, ml. At the NTP/g of sample

$C = \text{Exp} [(H_c - H_l)/RT]$

H_c = Heat of condensation of adsorbed gas on all other layers

H_1 = Heat of adsorption into the first layer

Assume $C \rightarrow \infty$, then

$$\frac{p}{n(1-p)} = \frac{p}{n_m}$$

$$n_m = n(1-p) \quad (\text{A-3-2})$$

The surface area, S , of the catalyst is given by

$$S = S_b \times n_m \quad (\text{A-3-3})$$

From the gas law

$$\frac{P_b V}{T_b} = \frac{P_t V}{T_t} \quad (\text{A-3-4})$$

Where, P_b = Pressure at 0 °C

P_t = Pressure at t °C

T_b = Temperature at 0 °C = 273.15 K

T_t = Temperature at t °C = 273.15 + t K

V = Constant volume

Then, $P_b = (273.15/T_t) P_t = 1 \text{ atm}$

Partial pressure

$$p = \frac{[\text{Flow of (He + N}_2) - \text{Flow of He}]}{\text{Flow of (He + N}_2)}$$

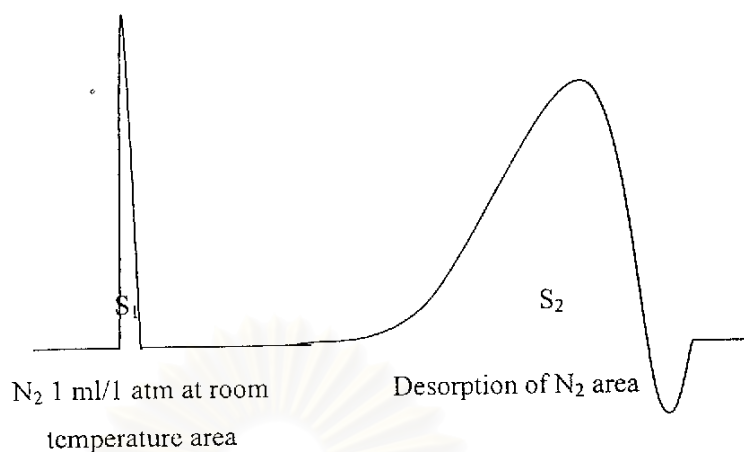
$$= 0.3 \text{ atm}$$

For nitrogen gas, the saturated vapor pressure equals to

$$P_o = 1.1 \text{ atm}$$

Then, $p = P/P_o = 0.3 / 1.1 = 0.2727$

To measure the volume of nitrogen adsorbed, n



$$n = \frac{S_2}{S_1} \times \frac{1}{W} \times \frac{273.15}{T} \text{ ml. / g of catalyst} \quad (\text{A-3-5})$$

Where, S_1 = N_2 1 ml/ 1 atm at room temperature area

S_2 = Desorption of N_2 area

W = Sample weight, g

T = Room temperature, K

Therefore,

$$n_m = \frac{S_2}{S_1} \times \frac{1}{W} \times \frac{273.15}{T} \times (1 - p)$$

$$n_m = \frac{S_2}{S_1} \times \frac{1}{W} \times \frac{273.15}{T} \times 0.7273 \quad (\text{A-3-6})$$

Whereas, the surface area of nitrogen gas from literature equal to

$$S_b = 4.373 \text{ m}^2 / \text{ml of nitrogen gas}$$

Then,

$$S = n_m = \frac{S_2}{S_1} \times \frac{1}{W} \times \frac{273.15}{T} \times 0.7273 \times 4.343$$

$$S = n_m = \frac{S_2}{S_1} \times \frac{1}{W} \times \frac{273.15}{T} \times 3.1582 \text{ m}^2 / \text{g} \quad (\text{A-3-7})$$

A-4 Calculation of Reaction Flow Rate

The catalyst used = 0.1000 g

Packed catalyst into quart reactor (inside diameter = 0.6 cm)

Determine the average high of catalyst bed = H cm.

So that,

$$\text{Volume of bed} = \pi \times (0.3)^2 \times H \text{ cc-cat.}$$

Used gas hourly space velocity (GHSV) = 6,400 h⁻¹

$$\text{GHSV} = \frac{\text{Volumetric flow rate}^1}{\text{Volume of bed}}$$

$$\begin{aligned} \text{Volumetric flow rate}^1 &= 6,400 \times \text{Volume of bed} \\ &= 6,400 \times \pi \times (0.3)^2 \times H \text{ cc/hr} \\ &= (6,400 \times \pi \times (0.3)^2 \times H)/60 \text{ cc/min} \end{aligned}$$

at STP condition :

$$\text{Volumetric flow rate} = \text{Volumetric flow rate}^1 \times (273.15 + T)/273.15$$

Where T = room temperature °C

สถาบันวิทยบริการ
จุฬาลงกรณ์มหาวิทยาลัย

APPENDIX B

CALIBRATION CURVE

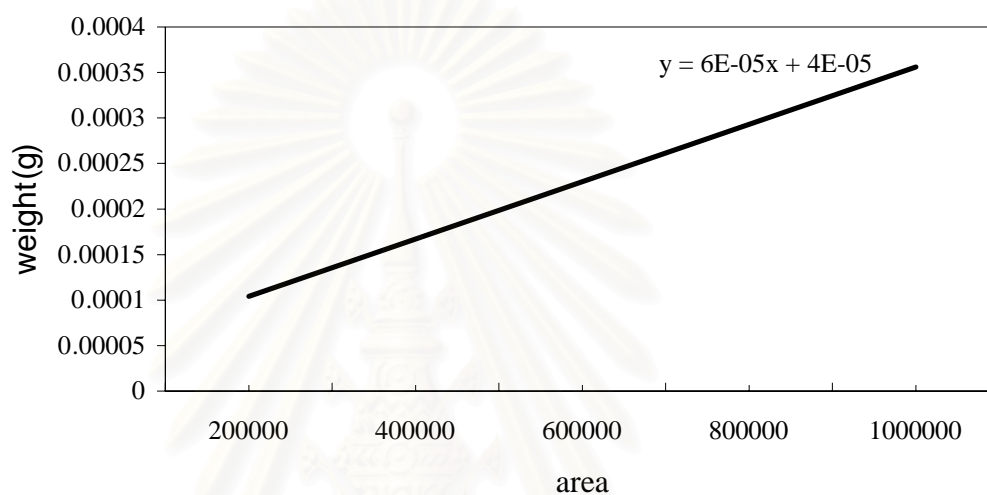


Figure B1 Calibration curve of n-octane (OV-1 column)

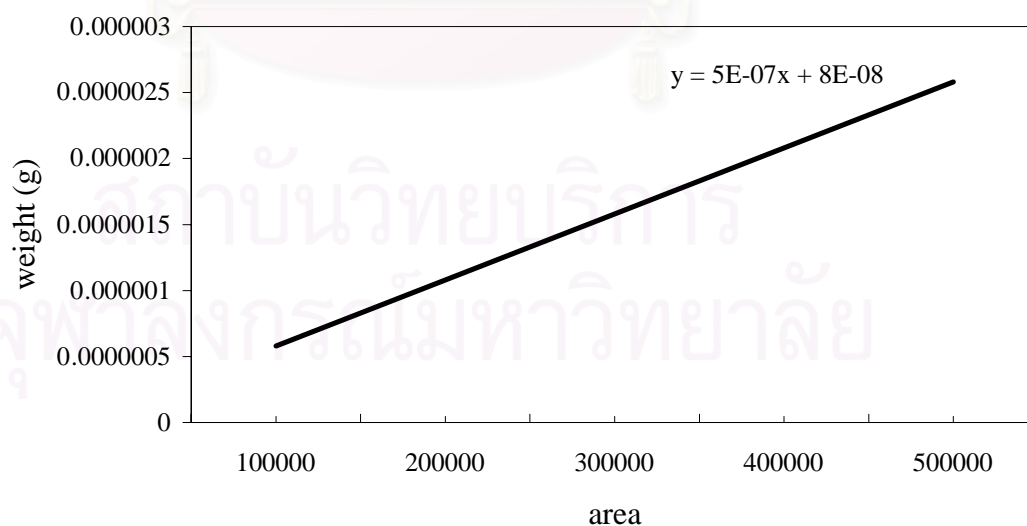


Figure B2 Calibration curve of ethylene (VZ-10 column)

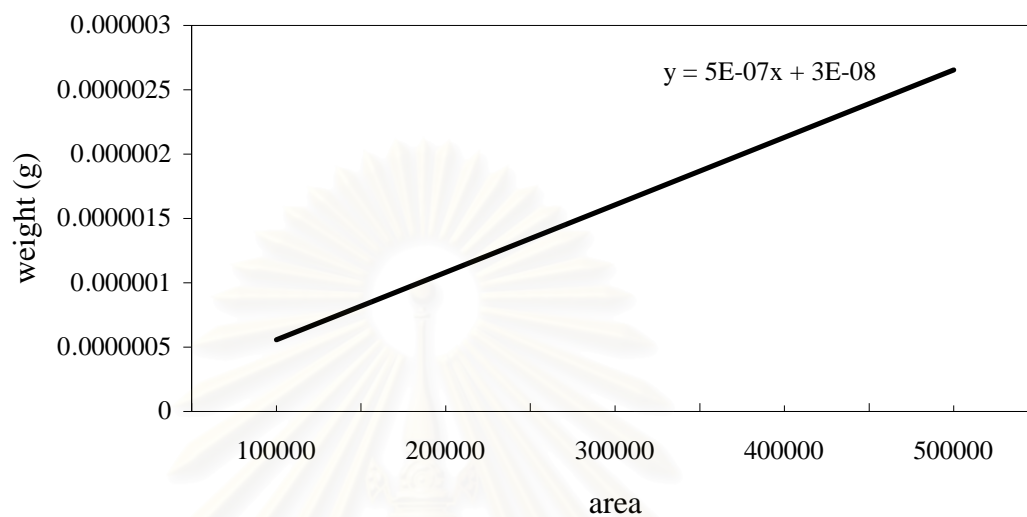


Figure B3 Calibration curve of propylene (VZ-10 column)

สถาบันวิทยบริการ
จุฬาลงกรณ์มหาวิทยาลัย

APPENDIX C

C-1 The Particle size and the unit cell size of Y zeolite at various operating temperatures

Particle Size (μm)	Unit cell size at Various Temperature (K)				
	873	973	1023	1123	1223
0.16	24.28	24.26	24.23	24.21	24.19
0.25	24.37	24.35	24.33	24.32	24.29
0.31	24.41	24.4	24.39	24.35	24.33
0.4	24.46	24.43	24.41	24.4	24.38
0.45	24.48	24.45	24.43	24.42	24.39
0.82	24.4	24.39	24.38	24.35	24.34
1.19	24.35	24.33	24.3	24.27	24.25
1.81	24.32	24.31	24.29	24.27	24.25
2.01	24.3	24.29	24.28	24.25	24.23

C-2 The Particle size and the unit cell size of Y zeolite at various operating times

Particle Size (μm)	Unit cell size at Various Time (s)				
	30	60	120	180	300
0.16	24.24	24.23	24.21	24.2	24.18
0.25	24.33	24.31	24.3	24.27	24.24
0.31	24.39	24.37	24.35	24.33	24.31
0.4	24.41	24.41	24.39	24.36	24.33
0.45	24.44	24.43	24.4	24.38	24.35
0.82	24.4	24.38	24.35	24.33	24.3
1.19	24.36	24.32	24.3	24.28	24.26
1.81	24.31	24.29	24.29	24.26	24.27
2.01	24.29	24.28	24.25	24.23	24.23

C-3 The Particle size and the unit cell size of Y zeolite at various operating partial pressures

Particle Size (μm)	Unit cell size at Various Partial Pressure (P/P_0)				
	0.05	0.1	0.2	0.5	1
0.16	24.24	24.23	24.22	24.2	24.17
0.25	24.33	24.33	24.32	24.29	24.27
0.31	24.38	24.37	24.36	24.33	24.3
0.4	24.43	24.41	24.39	24.36	24.33
0.45	24.44	24.43	24.41	24.38	24.35
0.82	24.39	24.38	24.36	24.33	24.29
1.19	24.35	24.33	24.32	24.28	24.3
1.81	24.32	24.29	24.3	24.27	24.25
2.01	24.3	24.28	24.26	24.23	24.2

C-4 The single point BET surface area and the percent relative BET surface area of Y zeolite, fresh and treated samples

particle size (μm)	BET surface area (m^2/g)		
	fresh catalyst	treated catalyst	%relative BET surface
0.16	521	322	38
0.25	546	366	33
0.31	498	411	18
0.40	502	432	14
0.45	511	441	14
0.82	531	397	25
1.19	506	384	24
1.81	543	340	37
2.01	550	339	38

C-5 Conversion of n-octane on various particle size of Y zeolites (fresh)

Temperature (K)	Particle size (μm)				
	0.16	0.31	0.45	1.19	2.01
573	72.15578	57.25489	53.97512	52.01547	50.36547
623	80.25479	71.75214	67.15489	67.25487	64.11547
673	96.35154	84.06542	79.78512	79.08451	81.98452
723	97.03454	87.36548	86.35487	86.84215	86.01547
773	99.83457	96.04875	91.88457	91.76548	91.34512

C-6 Conversion of n-octane on various particle size of Y zeolites (after hydrothermal temperature at 973 K)

Temperature (K)	Particle size (μm)				
	0.16	0.31	0.45	1.19	2.01
573	55.15687	48.25128	45.98775	42.01547	38.35784
623	65.25687	62.75125	59.15764	58.24832	53.12487
673	79.35478	76.05755	72.78545	69.08545	69.98754
723	81.04782	78.35877	79.35457	74.84521	73.02578
773	87.85411	87.05781	84.87513	79.75122	77.35484

C-7 Conversion of n-octane on various particle size of Y zeolites (after hydrothermal temperature at 1023 K)

Temperature (K)	Particle size (μm)				
	0.16	0.31	0.45	1.19	2.01
573	47.15789	38.15794	37.98547	36.15784	32.35487
623	58.25476	54.25784	51.15478	49.25487	47.12578
673	70.01577	65.35485	64.35488	62.05484	61.25487
723	76.04875	75.21458	68.35487	66.15487	65.02457
773	78.05484	78.05484	76.87514	65.02547	65.35487

C-8 Conversion of n-octane on various particle size of Y zeolites (after hydrothermal temperature at 1123 K)

Temperature (K)	Particle size (μm)				
	0.16	0.31	0.45	1.19	2.01
573	35.35122	30.28457	27.64851	20.01562	19.55152
623	44.36547	42.58461	42.26589	38.35157	34.15847
673	59.23545	56.03578	54.81541	48.04815	46.88517
723	62.07515	60.46217	58.20214	54.7515	50.12546
773	67.6258	68.32159	61.65215	58.82562	56.02598

C-9 Olefin selectivity on various particle size of Y zeolites (fresh)

Temperature (K)	Particle size (μm)				
	0.16	0.31	0.45	1.19	2.01
573	9.012318	4.875545	4.345777	8.567541	11.60914
623	17.1903	10.82002	8.111233	11.90931	14.01149
673	22.6095	14.69366	10.00934	16.25353	18.83321
723	30.08328	17.70313	12.71136	23.46124	26.20807
773	36.29705	25.78209	23.10221	28.25002	31.20048

C-10 Olefin selectivity on various particle size of Y zeolites (after hydrothermal temperature at 973 K)

Temperature (K)	Particle size (μm)				
	0.16	0.31	0.45	1.19	2.01
573	8.280342	12.38342	10.80935	17.10969	14.70611
623	17.37976	17.90612	20.1712	19.80537	31.16022
673	40.50929	26.77048	19.97965	30.38028	34.69998
723	36.99902	26.03928	29.59869	31.50931	32.139
773	38.20736	34.27675	32.797	41.17846	32.10608

C-11 Olefin selectivity on various particle size of Y zeolites (after hydrothermal temperature at 1023 K)

Temperature (K)	Particle size (μm)				
	0.16	0.31	0.45	1.19	2.01
573	14.28027	16.08277	18.81331	15.64603	20.78336
623	20.38426	22.66767	25.87037	19.94033	36.37958
673	44.77312	30.85198	20.9733	34.38054	39.18004
723	43.5414	40.57578	43.80911	36.13908	39.13996
773	47.30296	40.57028	44.28034	41.81303	36.60028

C-12 Olefin selectivity on various particle size of Y zeolites (after hydrothermal temperature at 1123 K)

Temperature (K)	Particle size (μm)				
	0.16	0.31	0.45	1.19	2.01
573	30.96504	21.11109	18.64688	26.3613	31.48901
623	43.20367	30.66132	26.08302	34.02071	37.6982
673	48.75303	34.71108	28.21111	38.26762	42.76637
723	56.33984	37.73964	30.67842	45.56754	50.38476
773	64.18736	48.69802	42.40907	52.16393	57.08469

VITA

Mr Suchuchchai Nuanklai was born on March 20, 1981 in Suratthani, Thailand. He received the Bachelor Degree of Chemical Engineering from Faculty of Engineering, Prince of Songkla University in 2002.



สถาบันวิทยบริการ
จุฬาลงกรณ์มหาวิทยาลัย